SYNTHESIS AND CHARACTERIZATION OF NANOCOMPOSITE POLYMER FILMS

THESIS SUBMITTED FOR THE AWARD OF DEGREE OF

Doctor of Philosophy
In
Applied Physics

BY
Satyendra Kumar
Enrollment No. 654/11

Supervisor
Dr. R. G. Sonkawade, Professor
&
Co-Supervisor
Dr. Bal Chandra Yadav, Associate Professor

DEPARTMENT OF APPLIED PHYSICS
SCHOOL FOR PHYSICAL SCIENCES
BABASAHEB BHIMRAO AMBEDKAR UNIVERSITY, LUCKNOW
(U.P.) INDIA - 226025

2016

DECLARATION

I declare that the thesis entitled **"Synthesis and Characterization of Nanocomposite Polymer Films"** has been prepared by me under the supervision of **Dr. R. G. Sonkawade**, Professor, Department of Physics, Shivaji University, Kolhapur and **Dr. B. C. Yadav,** Associate Professor, Department of Applied Physics, School for Physical Sciences, Babasaheb Bhimrao Ambedkar University, Lucknow. No part of this thesis has formed the basis for the award of any degree, diploma or fellowship previously. Further, I declare that the material embodied in the present work is based on original research work and the indebtedness to others has been duly acknowledged at relevant places.

(Satyendra Kumar)
Research Scholar
Department of Applied Physics**,** School of Physical Sciences
Babasaheb Bhimrao Ambedkar University, (A Central University Lucknow)
Lucknow, Uttar Pradesh-226025.

Date:
Place: Lucknow

DECLARATION

I declare that the Ph.D Thesis entitled "**Synthesis and Characterization of Nanocomposite Polymer Films"** has been prepared by me. The work has not been submitted elsewhere for the award of any other degree or diploma. Further, I declare that the material embodied in the present work is based on original research work, free from any form of falsification, fabrication and plagiarism, the indebtedness to others have been duly acknowledge at relevant places. I shall be solely responsible for any such dispute arising out of my doctoral work.

(Satyendra Kumar)
Research Scholar
Department of Applied Physics**,** School for Physical Sciences
Babasaheb Bhimrao Ambedkar University, (A Central University Lucknow)
Lucknow, Uttar Pradesh-226025

Date:
Place:

CERTIFICATE

This is to certify that the thesis titled "**Synthesis and Characterization of Nanocomposite Polymer Films"** submitted by **Satyendra Kumar** is an original research work and has not been previously submitted in part or full for the award of any other degree or diploma to this or any other university.

The thesis submitted to Babasaheb Bhimrao Ambedkar University, Lucknow satisfies all the requirements as stipulated in the *Doctor of Philosophy (Ph.D.) regulation -1999 as amended in 2010* and it is fit for submission and evaluation for the award of the degree of Doctor of Philosophy of the University.

Prof. R. G. Sonkawade
(Supervisor)
Department of Physics
Shivaji University Kolhapur
Maharashtra-416004

Countersigned with seal
(Head of the Department)

Dr. B.C. Yadav, Associate Professor
(Co-Supervisor)
Department of Applied Physics**,** School for Physical Sciences,
Babasaheb Bhimrao Ambedkar University, (A Central University Lucknow)
Lucknow, Uttar Pradesh-226025

Date:
Place: Lucknow

ACKNOWLEDGEMENT

The writing of this thesis has been one of the most significant challenges. This work would not have been possible without the guidance and help of several individuals who have contributed and extended their help in the completion of this thesis.

First and foremost, I would like to express my deep sense of gratitude to my supervisors- ***Prof. R.G. Sonkawade*** *and* ***Dr. B.C. Yadav****, Associate Professor, for their invaluable guidance and supervision. They have shown me the path and lightened it for me through their useful suggestions, through discussion and interpretation of results. They inspired me to work with strong determination and dedication under adverse situation. I have been blessed by their kind support, valuable inputs and useful suggestions, when I needed the most.*

I express my deepest gratitude to ***Dr. Rajesh Kumar****, Assistant Professor of Physics, Guru Gobind Singh Indraprastha University, New Delhi for scientific discussion and suggestions. He taught me new concepts and ways to explore the work towards fruitful conclusions and have offered me valuable advice throughout my work.*

I would like to convey my thanks to ***Dr. Kamlendra Awasthi****, Assistant professor, Department of Physics, Malaviya National Institute of Technology, Jaipur for fruitful discussion and suggestion in the entire work.*

I am very thankful to Pelletron Staff of Inter University Accelerator Centre (IUAC), New Delhi for their assistance during beam time experiment.

I am privileged to get the help and kindness from all the esteemed Faculty & Staff Member of Department of Applied Physics, BBAU Lucknow.

I had the pleasure to work with many young Scientists. In Particular, I would like to thanks Dr. Asad Ali, Dr. Paramjit Singh and Mr. Sanjeev Kumar Gupta, Mr. Anil Sharma for their suggestion and constant help.

This work would have not been possible without the constant support and encouragement of

my joint family members, infinite moral support, patience and faith in me to pursue higher studies. I would also like to thank my in –laws for all their profound affection, concern and understanding.

I will fall to short of words to express my affluent felling for my wife, ***Ms Anju Mishra****, Assistant Professor, Amity University Noida, who has been a source of inspiration for me and my lovely daughter* ***Miss. Aaradhya*** *for their support, understanding and caring all the times.*

Last but by no means least; I would like to place my deep regards to my parents for their endless love, support and care in all endeavors. Words would not be sufficed for all the sacrifice they have made for me.

I am also thankful to Council of Scientific and Industrial Research (CSIR), New Delhi for financial help (Travel Grant) during my Ph.D.

Above all, I dedicate everything to the ***Almighty GOD*** *for giving me the strength and hope to complete this work. I would like to acknowledge here my* ***Guru Ji (Ek Tu Sachcha Tera Naam Sacha)*** *for his blessing throughout the entire work.*

(Satyendra Kumar)

ABSTRACT

"Synthesis and Characterization of Nanocomposite Polymer Films"

Introduction

Inexpensive inorganic substances are traditional ingredients in polymer industry. They are widely used as fillers to improve mechanical and thermal properties of polymers and polymer composites, to decrease shrinkage and internal stresses during conductivity, thermal stability, flame resistance, and, not of least importance, to improve cost effectiveness. The last motivation often became the most important one despite some deterioration of properties with immoderate filling of polymer or polymer composite.

The work existing in this field shows the possibility to include magnetic ions impurity (Ni, Co, Mn) at low concentration in GaAs, ZnSe, ZnS etc., offers good prospects of combining magnetic phenomena with high speed electronics. If these materials embedded with the polymer matrixes then their stability is expected to improve and agglomeration of nanocrystals will be negligible.

SHI irradiation effect of embedded nanocrystals in a polymer matrix is also important to know whether SHI fluence alter the size as well as distribution of nanocrystals uniformly. In the interaction of ionizing radiation through a polymer, the incident energy is transferred to the medium as a result of primary ionization and excitation of the target molecules. Charged particles lose their energy to the stopping materials, mainly via two independent processes i.e. elastic collisions (ion atom interaction) and inelastic collisions (ion electron interaction). The former is the dominant mechanism at low energies region (~KeV/nucleon), whereas the inelastic collisions dominant at high energies (>1MeV/nucleon).Thus, for heavy ions the electronic energy loss leads to the deposition of incident energy on the target material, which creates defects and atomic displacement due to the formation of tracks in material.

Objective of Research:

For this proposed work transition metal ions (Ni, Cu, Co, Mn…) doped nanocrystalline semiconductors (ZnS, CdS, ZnSe, CdSe,...) are embedded in a polymer matrix like polystyrene (PS), polyvinyl alcohol (PVA), PMMA etc. The motivation behind this work is to understand the distribution of these semiconductor nanocrystals of different-different particle size in the polymer matrix. It is expected that greater particle size semiconductor nanocrystals will be distributed up to higher depth while smaller particle size nanocrystals will be distributed on the surface of the polymer matrix. So distribution of defects will be different for both sizes of nanocrystals. Apart from this it is also expected that the modifications after irradiation of swift heavy ions (SHIs) will be also different at surface of the semiconductor nanocrystals embedded polymer matrix comparatively to higher depth distributed nanocrystals in the same matrix. Ion-matter interaction is an important issue because of nature of electronic and nuclear energy losses. Due to this grain evaporation and grain fragmentation is expected, so ion impact on embedded nanoparticles system is interesting due to suppression of weak link boundaries which is inherent in case of nanostructure films.

Polymers will provide the stability and protect against the agglomeration of the semiconductor nanocrystals. A typical embedded nanoparticles system is different from nanostructure films in view of the presence of isolated nanoparticles where the grain boundary problem is no obvious, which is otherwise observable in nanostructured materials. Therefore, the embedded structure provides a suitable system where ion matter interaction at the nano scale level can be studied in great detail.

It has been reported in the literature that band gap is engineered by control of the crystal size that leads to tunable band-edge emission. By doping the nanocrystals with luminescent

activators, the excitation can be tuned by quantum size effects, even though the activator-related emission energy is largely unchanged.

Doped semiconductor nanocrystals are extensively investigated to obtain basic information on impurity states in quantum dots and to examine their potential applications in novel light-emitting devices. It was reported that doped semiconductor nanocrystals can yield high luminescence efficiencies. The doping of Mn^{2+} into II–VI semiconducting nanoparticles potentially gives rise to a new class of luminescent materials with a wide range of applications in displays, sensors and lasers. An appreciable enhancement in the PL property of ZnS-coated CdS nanoparticles in a polymer polycetyl-*p*vinylbenzyldimethylammonium chloride (PCVDAC) has also been reported.

Some studies show the effectiveness of various inorganic capping agents having different band gaps on the surface passivation of cadmium sulphide (CdS) nanoparticles. They have reported that it is possible to block the non-radiative channels on the surface of these nanoparticles by capping them with wider band gap inorganic materials like Cd $(OH)_2$ and zinc sulphide (ZnS).

The purpose of this work is synthesis of nanoparticles by chemical route, and these nanocrystals embedded in the polymer matrix for the stabilization to protect them from the agglomeration. The embedding of these nanocrystals was done by using the solution cast method. The nanocomposite polymer matrix irradiated by swift heavy ions (SHIs) with in different doses range and different ions. Their alignment after irradiation is characterized.

In summary, the following work has been carried out:

1. Synthesis the nano particles of CdS/ZnS with varying concentration
2. Doping of CdS/ZnS with transition metals
3. Characterization of formed Nano particles
4. To embed these nano particle in a polymer matrix (PS)
5. To characterize optical, chemical and structural properties of nano composite membranes before and after irradiation

The present work is organized into following five chapters:

Chapter-1 Deals with the basics of polymers and nanocomposites. Importance of irradiation in the field of materials science is explained. An idea about energy loss mechanism of ionizing radiation and swift heavy ions irradiation in polymers are discussed. The significance of swift heavy ion beam, in the field of materials science is explained in detail. A review of literature on present experimental work on the swift heavy ion beam on the properties of polymeric materials is carried out. The objectives and future scope of the present work have been given at the ending of this chapter.

Chapter-2 Gives the information about the material used and experimental technique used in present work. The synthesis of ZnS and CdS nanoparticles is shown in this chapter. This chapter gives the information about the formation of nanocomposites film. The facility of Pelletron accelerator is discussed. 60 MeV Ni ions beam of the fluence from 10^8 to 10^{11} ions/cm^2 used for irradiation of nanocomposites film. Different characterization techniques like UV-Visible, XRD, FTIR and SEM are discussed before and after irradiation.

Chapter-3 This chapter includes the comprehensive studies of optical, chemical and structural properties of the pristine and 60 MeV Ni ion beam irradiated with CdS doped

polystyrene (PS) and metal (Ni, Cu) doped polystyrene (PS) films at different fluences. The effect of doping of metals and ion irradiation was studied for modification in optical, chemical and structural properties of PS/CdS nanocomposites. The optical band gap energy and carbon atom through UV-visible spectroscopy for such nanocomposites films is explained. The diffraction peaks of metal doped polystyrene (PS) at various fluence discussed in this chapter. Further, FTIR spectral analysis was used to investigate the bonding and structural changes induced in the nanocomposites polymer due to Ni^{5+} ions beam irradiations.

Chapter-4 In this chapter the optical, chemical and structural properties of the pristine and 60 MeV Ni ion beam irradiated with ZnS doped polystyrene (PS/ZnS) and metal (Ni, Cu) doped polystyrene (PS) films at different fluences. Conformation of ZnS nanoparticles is done by SEM image. The films of Ni doped PS/ ZnS and Cu doped PS/ ZnS were irradiated with Ni^{5+} ions of energy 60 MeV to different fluences of 10^{10} and 10^{11} ions/cm^2.Modification due to heavy ions in optical, chemical and structural modifications were studied by UV-Visible Spectroscopy (UV- Vis), Fourier Transform Infrared spectroscopy (FTIR) and X-Ray Diffraction Spectroscopy (XRD).

Chapter-5 This chapter concludes the outcomes of this research work and presents a discussion of their implications in the context of present and future effects of nanocomposite materials. The future scope of the present work has also been presented.

LIST OF ABBREVIATION

LET	Linear Energy Transfer
PS	Polystyrene
PMMA	Poly (methylmethacrylate)
PET	Polyethylene Terephthalate
CM	Centimeter
SRIM	Stopping & Range of Ions in Matters
TRIM	Transport of Ions in Matters
MeV	Mega Electron Volt
UV	Ultra-Violet
XRD	X-ray Diffraction
FTIR	Fourier Transform Infrared
SEM	Scanning Electron Microscope
SHI	Swift Heavy Ion
HVC	High Vacuum Chamber
CCTV	Close Circuit Television
GPSC	General Purpose Scattering Chamber
FWHM	Full Width at Half Maxima
HUMO	Highest Occupied Molecular Orbit
LUMO	Lowest Unoccupied Molecular Orbit

LIST OF TABLES

LIST OF FIGURES

LIST OF APPENDICES

TABLES OF CONTENTS

CHAPTER 1

Introduction and Literature Survey

1.1 History of Polymer

The Human are using polymer from ancient times in the form of wood, skin and fibers. Many industries were using the polymers since 19th century. The scientist had given the idea that polymers have been made from the small molecules, and bonding between the molecules by the some hidden force. In 20th century the demands of these polymers increased so researcher needed the understanding of the structure of polymers. In 1930 the scientist developed some synthetic polymer such as Polyvinylchloride (PVC). These polymers were called Plastic. Some chemical researcher then focused on Manufacturing of polymer from hydrocarbons such as ethylene and propylene. Later on, with the help of catalysts and polymerization of these hydrocarbons, allowing great control over the properties of the developed polymers. As a result, the people started to investigate their uses in many areas of industry.

In 1953, Staudinger told that polymers composed of giant molecules. In 1960 the introduction of new thermoplastic polymer came. In 1963, the Novel Prize in chemistry was given to chemist Giulio Natta and Karl Ziegler for the development of synthetic polymer. In 1974 the Teflon, nylon, polyethylene (PE) were discovered. The production of these polymers was on peak because of demand of polymer industry.

Nature also has its own nanocomposites, just like the abalone shell and bone. The inclusion of nanoparticles in materials long predates the understanding of the physical, optical and chemical behavior of these materials investigated the origin of the deepness of colour and

the resistance attributing it to a nano particle mechanism. In the year 1950 nanoscale organo-clays have been used for the formations of gels. In the 1970s polymer/composites were the famous topics (Jose-Yacaman et al. 1996). There is always need of smart materials with different properties for the various fields of science and technology. The scientist and researchers are working in this area with a zeal for the useful applications.

The interaction of radiation with polymer materials is an area of great increasing concern. The radiation authorities of primary substitute are either high energy, ionizing radiation such as from gamma or neutron sources, or ultraviolet radiation from arc lamps, lasers or synchrotron sources. The first motive for studying how SHI modifies the chemical structural, optical properties of polymeric materials was the requirement of understanding the radiation-induced degradation of mechanism of nuclear reactors (Cook, 2006). A small dose of radiation can change the physical or optical properties of a polymer, these changes being dependent upon the chemical configuration and the different parameters of radiation like, fluence, energy, mass and the type of target material itself. A highly focused ion beam can modify the material and its properties (chemical, electronic, electrical, structural, mechanical etc) (Xua et al. 1998; Singh et al. 1999; Mehta 2003). The modified properties of the nanocomposites polymer using irradtion can be used in various field like space craft, high-energy particle accelerator, nuclear power plant, sensor, electromagnetic shielding etc (El-Badry et al. 2008).

1.2 Polymer

The meaning of polymer can be understands from the two Greek words poly, means “many”, and mers, meaning “parts” of units. So, when many monomers combine, they form polymers. In the phenomenon of polymerization the monomers are joined together. Hence, a polymer is consist of thousand of monomers joined together to develop a big molecules of

colloidal dimension, known as macromolecule. A polymer has a single feature like that a molecule is a long chain of monomers which are covalently bonded together. Most of the polymers are molecular materials and generally noncrystalline at normal temperature, but pass through the different phase in way of their configuration when structure is willingly carried out.

The most of the known polymers are those made of compounds of carbon but some polymers can also be prepared from chemical materials such as silicates and silicones. Nature has some polymers include proteins, cellulose, resins. These natural polymers are usually found in leather, fur, wood, cotton, wool and many others. There are also some artificial polymers such as polystyrene, polyethylene etc.

Most of the polymers are organic origin and their main characteristics are as follows:

a) They have long chain structures, the individual molecules are very large, which may have thousands of similar small molecules and these small molecules are bonded together with covalent bond.

b) They all have carbon in common, which further combines with oxygen, hydrogen, halogen and other inorganic organic materials.

c) Even though their structures of polymers may be crystalline in simple materials but usually they are not crystalline solids at ordinary temperatures. Of course, they have gone through a viscous phase in the process of formation.

The unique characteristics of polymers are as follows:

I) Light weight

II) Easy fabrication and shaping

III) Poor conductor of electricity as well as poor thermal conductor

IV) Unaffected by chemical attack and decay.

Polymers are used indefinite number of places, indefinite number of uses such as telephone sets, paints, radio cover and television cabinets, coatings, adhesive and other countless objects. Some extraordinary developments in polymer materials are:

i) Materials become stronger than steel

ii) Materials can be used for medical sciences like repairing damaged kidney or even damaged heart

iii) Spacecraft can bear up very high temperature, particularly during re-entering into earth's atmosphere. Temperature increases very high because of friction when the spacecraft re-enters the earth atmosphere.

iv) Film of silicon stops water to pass but it permits dissolved oxygen, in water, to pass through it .Now underwater tents have become possible in which a man can live and work.

Inherently conductive polymer such as polyacetylene and polypyrrole are now more widely researched and some commercial applications are being considered. Polymers that are rendered conducting by the incorporation of carbon black or metal particles are widely used.

1.3 Classification of Polymer

Polymers are classified as per their molecular structure, chemical structure, physical state, morphological behavior, polymerization process and properties etc. All type of polymers is

obtained by connecting together the large number of chemical units. A molecule of the basic monomer has the capability to react to at least with two other molecules of the same monomer resulting in the monomer linking. So monomers must have functionality of at least two or more functional group

1.3.1 Classification of Polymer on the basis of Geometrical Structure

Polymers are created by connecting monomers in a chain. Monomers may be of same type or different types. Polymer can be grouped in different groups depending upon the numbers of types of monomers.

- **Homopolymer:** The phenomenon of polymerizing a single monomer or monomer pair is termed as homolpolymerization and the polymer obtained is known as homopolymer. For example, polystyrene (PS), poly (ethylene terephthalate) (PET). In this thesis work, homopolymer PS has been used.
- **Co-polymer:** In the process of copolymerization, two or more than two monomers or monomer pairs are polymerized all together and therefore polymer is composed of more than one unit. For example, nitrile rubber, acrylonitrile etc.
- **Terpolymers:** Formation of new polymer from the interaction among three different polymers. ABS (acrylonitrile-butadiene-styrene) is a type of terpolymer.

1.3.2 Classification of Polymer by Chain Structure

According to the shape of the macromolecules, polymers structures may be broadly classified as:

1) Linear and framework structures:

In this type of polymer, atoms are arranged in a long chain (Figure 1.1 a). In Figure 1.1 b, this chain of polymer is called backbone. Some of the atoms in the polymer chain have small chains connected to them. This type of backbone chain usually has approx hundreds of atoms. In Figure 1.1 c, repeating polymer structure is shown. A group of atoms which frame the backbone of polymer chain comes in a particular order and further this order repeated all along the path of polymer chain. In polypropylene, the backbone chain has been made of two carbon atoms repeated over and again. In this chain carbon atom is attached by two hydrogen atoms and other has one hydrogen atom and one pendant methyl group. Two hydrogen with the unit of carbon atoms attached by an atom of carbon with a hydrogen atom and methyl group repeats itself all along the backbone chain. This repeating structure of little chain is known as the repeat composition.

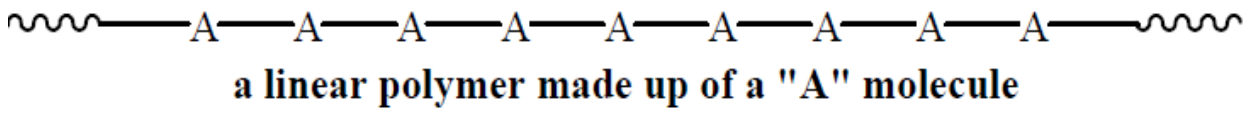

a linear polymer made up of a "A" molecule

(a)

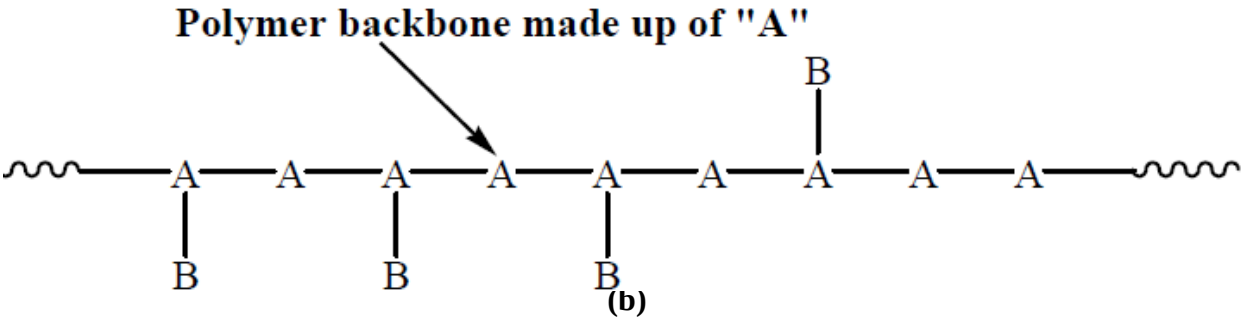

(b)

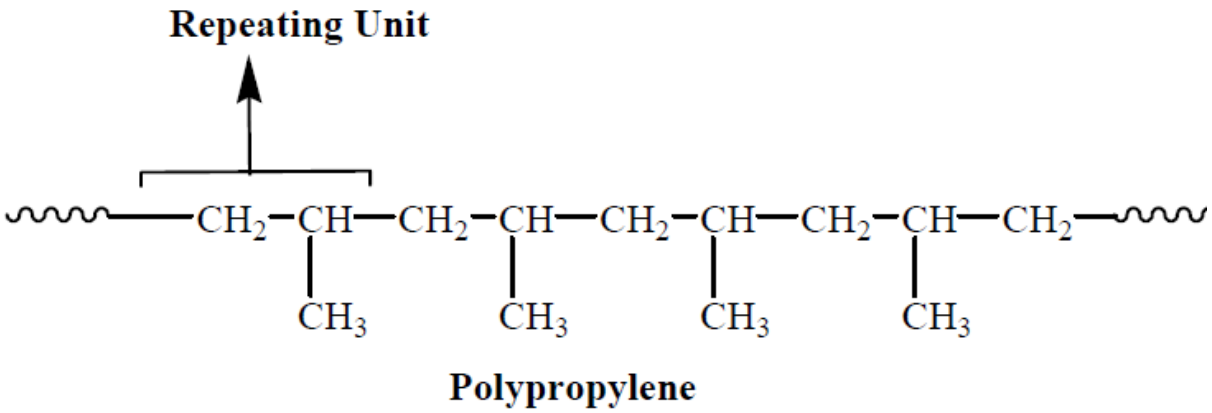

(c)

Figure 1.1: Chemical Structure (a) Linear Polymer (b) Polymer with backbone (c) Repeating Polymer

(2) Branched-chain structures:

In these type of polymers, the chain of polymers has the branches of monomers, which hinders the close packing of polymeric chain and hence, are less tightly packed in comparison to the linear chain polymers. Branched chain polymers have low melting points and less density in comparison to linear chain polymers.

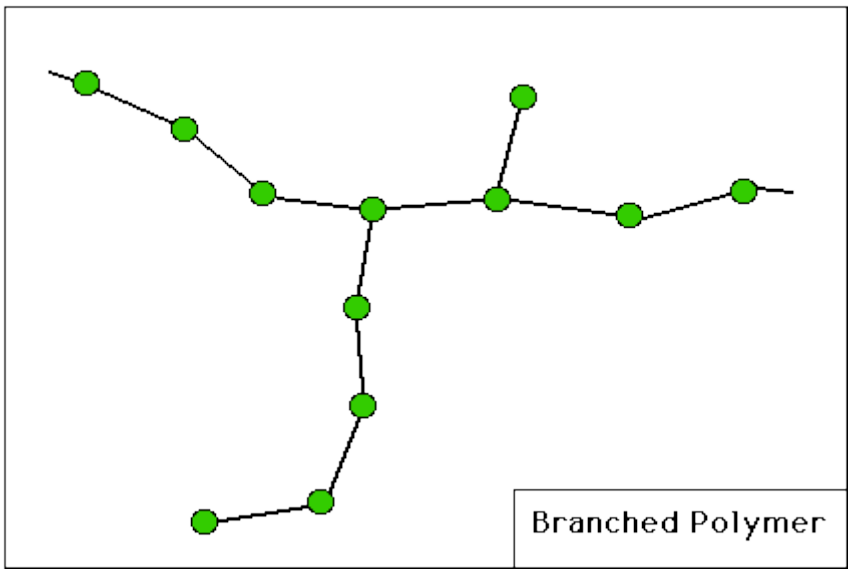

Figure 1.2: Branched Polymer

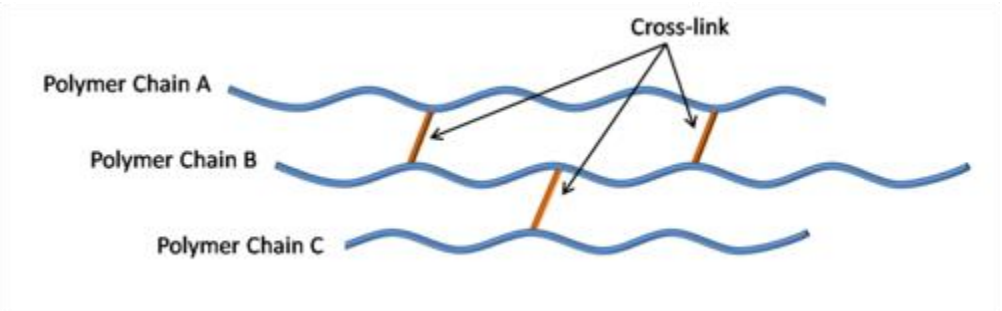

Figure 1.3: Cross-linked Polymers

(3) Cross-linked chain structures:

In the process of polymerization, a large number of branched polymer molecules formed. The side chain from one molecule can interact with those of adjacent ones in the process of polymerization. The molecules present with side chain attached at random positions, the process of inter uniting of side chains of neighboring molecules results in a single molecule with cross network of chain segment in all three dimension. These polymers are called cross-linked

polymers. In cross-linked or network polymer, monomers are crossed linked together in all dimensions. The structure of cross-linked polymer is shown in Figure 1.3.

1.3.3 Classification of Polymer by Thermal Behavior

- **Thermoplastic Polymers:** These types of polymers have branched molecule which have intramolecular covalent bonds very weak intermolecular Van Der Waals bonds. These bonds melt at higher temperature and molecular chains willingly slide fast on one another. These polymers dissolve at higher temperature and turns into different polymers. In cooling process below a temperature called glass transition temperature (T_g), they form a glass just like a frozen liquid. The process of heating, reshaping and retaining the same on cooling can be repeated many times. These types of polymer, that softens on heating and harden on cooling, are called thermoplastic. Polystyrene (PS), Polycarbonate are the examples of these polymers.
- **Thermoset Polymers:** Amorphous polymers which are highly cross-linked networks with no longer range order are termed as thermoset polymers. These polymers are those resins which are polymerized in a reaction resulting in cross linking of the structure into one molecular group. After the polymerization, polymer turns into a rigid, mysterious substances which can not be softened, melted.

1.4 Composite

A material which has been made of two or more components, called composites. This composite material has different properties from the individual components. These new materials are light weighted, less expensive as compare to old material. The physical, chemical and mechanical properties of composites are different that of tradional materials. The filler and a compatible matrix in order to obtain specific properties that were not there before.

1.5 Nanotechnology

Nano science is the study of materials whose at least one dimension should be in nanometer region (1-100 nanometers) and consists of applying the science of the small. It is multi disciplinary field, which involves physics, chemistry and biology in studying, research and engineering over smaller structure of the scale of the size of single atom. Properties are different at the nano scale. Properties such as optical, mechanical, chemical etc not seen on a macroscopic scale now become noticeable and useful.

1.6 Polymer Nanocomposite

In today's time of technology and economical activities, it can be easily understand that the technology has given us the way for modern life and open the window which determines the standards parameters of our lives. These requirements result in nonstop efforts for new, high performance besides low cost materials to meet increasing demands. Polymers are usually doped with a variety of nano particles to improve their properties and performance capabilities. To modify some specific properties of polymers and the nanocomposites, nano fillers are used. Polymer/nanocomposites have properties which are better than those of conventional composites with ordinary particle filler. The nano fillers featuring antibacterial properties, like nano particles of silver, could be appropriate in filtration, applications, or in consumer products. The extraordinary properties of nanoparticles are due to their small size and high surface to volume ratio of atoms. The optical properties of a nano sized particle are better than that of its alike macro-size filler, because the diameter of particles becomes smaller than the wavelengths of light. The nano size filler particles have a bigger specific surface area than its similar traditional macro-size filler particle, so nano particles have more interaction with its surroundings.

A polymer nano composite is generally defined as polymer-nano filler system in which the filler of inorganic material such as metal nano particle is on nano scale. At least one dimension of the nano filler should be in the nano-range. The polymer nanocomposites, are produced when the nanoparticles are doped in polymer matrix. The nanoparticles and the polymers are covalently bonded. The covalent bond can be formed during the *in situ* polymerization (the monomer or the growing polymer chain can react with the filler nano particle), or during the nanocomposite processing. The doping of nano particles in the polymer matrix is desired to be uniform distribution. It can be a challenge to build a favourable interaction between the polymer matrix and the nano particles and thus keep away of nano particles from agglomeration. Metal-polymer nanocomposites are a typical example: using metal nano-particles as filler in polymer matrix. The metals of nano size have different properties from metals of macro size originating from nanocrystals size. Nanocrystals quantify a few nanometers containing few hundred atoms. In this way, nonmaterial shows special properties (electronic, magnetic and structural) depending on structure of nanoparticles. In this way, metal-polymer nanocomposites may be applicated for a number of industrial and technological applications such as optical devices, optical sensors, and light color filters.

Nanocomposite is the area where, researcher and scientist all over the world doing a great amount of work for developing the new devices. A composite is formed as the two-phase or multi phase system in which the size of the one component should be in nanometer range. Nanoparticles itself have great applications but when incorporated in a polymer matrix hint to extraordinary performance, which make them most demanding for uses in different area. For example the nanocomposites made of inorganic nanoparticles, incorporated in polymer such as polyethylene used for automotive applications because of their high tensile strength, light weight,

high stability and low cost. The use of nanocomposites in technology for optical applications has been progressed.Optoelectronic devices such as OLED and photovoltaic cell have latterly attracted expectant attention for the possibility of substitute of inorganic counterpart in several applications. Now a days the production cost of optoelectronic devices is high because of complex processing of conventional semiconductor (silicon, gallium). By using organic material with advantage like simple processing, light weight the production cost of optoelectronics devices can be low. Many organic devices including display, solar cell are already in the market for consumers. But because of weak stability and photo oxidation of organic material, the efficiency of these devices is very poor. The efficiency of optoelectronic devices can be improved by doping of nanoparticles (CdS, ZnS) to the host materials i.e. composites. Optical properties can also be tune by varying the doping of semiconducting nanoparticles. Thus nanocomposites are used as an active material for improving the efficiency of devices (Thien-Phap Nguyen et al 2011). The composites used for optical properties include polymer and inorganic material such as semiconductor. These composites can be prepared by two method, the first include the inorganic nanoparticles incorporated in polymer matrix and second the polymer deposited in an inorganic material. The selection of the size of the nanoparticles is crucial for the coveted optical properties (F. Iskandar et al 2009).The incorporation of metal nanoparticles in the polymer increase the long term stability .The metal ions help for increasing the thermal stability of the legion polymer (Tugba Orhan et al 2014).

Nanocomposites materials with nano scale filler have come out in the past decade as a bright novel class of material which takes reward of higher achievable load, control interfacial interactions. Graphene nano fillers in polymer have been used for the development of multi stacking heterogeneous with 2d structure with extraordinary properties (Kesong Hu et al 2014).

Graphene-polymer nanocomposites introduced different combinations of nanofiller of grapheme and polymer. Device made of polymer-graphene nanocomposites and other ingredients including, metal, semiconductor and organic small molecules. Young et all reported the fabrication and characterization of polymer-graphene nanocomposites (Young et al 2012). Recently Sun et al. provided perceptiveness on the integration of both graphene and carbon nanotubes materials in polymer nanocomposites (Sun et al 2013).

Development of polymer-nanocomposite (PN) is one of the latest evolutionary steps in polymer technology. PCNs are a class of organic-inorganic hybrid composite materials. A nanocomposite is formed when phase mixing occurs on a nanometer length scale. One successful approach to achieve such nanocomposites is the in situ polymerization of metal alkoxides in organic matrices via the sol gel process. Inorganic components, especially silica have been formed by the hydrolysis/condensation of a mononuclear precursor such as tetraethoxysilane (TEOS) in many polymer systems. Another method of synthesis of nanocomposites is direct dispersion of nano particles in polymer matrix. Today technologies are available for synthesis of a wide variety of nonmaterial like silicon whiskers, carbon nanotubes etc. Modern life and industry continuously needs new materials with unique combination of properties. Many efforts have been made in the last decades using novel nanotechnology and nanoscience knowledge in order to get nanomaterials with determined functionality.

1.6.1 Nanocomposites topology

Differing mutual arrangement of small size particles i.e. nano can be observed not only on the stage of nanocomposite but also on the level of individual nanoparticles and polymer chain. The commonly usual assembly is that of nanoparticles encapsulated by polymer matrix. However, in some cases, it has been found that polymers can also be incorporated inside the

nanoparticles. In recent time, it was discovered that a polyacetylene chain can be formed by fusion of close-packed acetylene molecule inside a CNT (Kim G et al 2005). For the sake of completeness, we state that chemical vapour deposition of metals and ceramics is also used to produce 2D nanocomposites of inorganic coating on substrate of polymeric. ZnS hollow sphere were synthesis by coating SiO_2 nanospheres and subsequent dissolution of the silica core with hydrofluoric acid.

1.7 Synthesis of Nanocomposites

A polymer nanocomposite contains a rigid polymer component dispersed within a flexible polymer matrix on a nanoscale level. The rigid polymer, with high modulus and high strengths, usually has high melting temperature. These rigid polymers are insoluble in organic solvents, and combining it with flexible polymer is thermodynamically adverse.

Nanocomposites are prepared mainly by three methods:

1) Sol-gel approach
2) Ex-situ approach
3) In-situ approach

Cheap inorganic materials are tradional ingredients in industry of polymer. They have many applications as filler to modify mechanical and thermal properties' of polymer and its composites. The inclusion of inorganic materials in polymer decreases shrinkage and internal stresses and it also increases thermal stability, thermal conductivity, flame resistance and not of least importance, to make better cost economically. The ultimate inspiration often happened to very crucial one-even though some declination of properties with effusive filling of polymer and polymer composite.

Polymer-inorganic nanocomposite materials are capable for modifying various properties. Nanocomposites have their unique and special optical, electronic and mechanical properties. In all over the world, researchers, scientist and engineers in recent decades are working on nanocomposites because of their improved optical, electronic and mechanical properties. In the last twenty years, polymer technology has achieved great growth in developing fresh methods of synthesis of a vast diversity of polymers with restricted macromolecular architecture and morphology which are well defined (Shvarcz M et al 1968, Ruckenstein E et al 2005). Among these, it is vital to note initially restricted living ionic and radical polymerization and copolymerization (Wang J-S et al 1995, Matyjaszewski K et al 2005). In today's time it seems possible to synthesis block copolymers of various architecture virtually all kinds of vinyl monomers by ionic and free-radical mechanisms by bulk, solution, and suspension or emulsion process.

Many different procedures are used for the synthesis of inorganic nanoparticles. For further manipulations, usually existing as aggregates, are dispersed in a liquid or solid medium. Different mechanochemical approaches including sonication by ultrasound can be used for this purpose. However the scope such approach for dispersing the nanoparticles and the establishment of an equilibrium state under definite condition, which determine the size distribution of the agglomerate of dispersed nanoparticles. Particle coated by a polymer shell are considerably more stable against aggregation because of a large decrease of their surface energy in comparison with bare particles. Such a polymer shell can be obtained by first synthesizing the inorganic nanoparticles in one way or another, and then dispersing them in polymer solution. Finally the polymer coated inorganic nanoparticles are precipated into a non-solvating phase. This is so-called ex-situ approach. The ex-situ approach is the most general one because there are

no limitations on the kinds of nanoparticles and polymer that can be used. The presence of such a shell increases the compatibility of the particles in the polymer matrix and makes it easier to disperse them.

In some cases, the process of protective polymer coating formation and nanoparticles preparation can be combined into one process or performed as a series of consecutive processes in one reactor (the in-situ approach). This approach can be used also for the preparation of nanocomposites. In the in situ methods, nanocomposites are generated inside a polymer matrix by precursor, which are transformed into the desirable nanoparticles by appropriate reaction. The researchers are getting attracted for in situ approaches because of their apparent technological advantage over ex situ approach. These core/shell nanoparticles have characteristic optical properties which suggest promising applications in optical nano devices and in biotechnology

Semiconductor nanocrystals capped with organic molecules can have relatively huge number of unpassivated surface site as it is very difficult to passivate both anion and cationic surface sites concurrently by these capping groups (X.G. Peng et al 1997). These unpassivated surface sites work as non-radiative recombination centers which suppress their luminescence. In addition organic capped nanoparticles have very extended emission lifetime and large stoke's shift (B.S. Zou et al 1999) whereas inorganic capped nanoparticles show improved luminescence efficiencies (Margaret et al 1996) and shorter life times. The epitaxial growth of inorganically caped nanoparticles can remove both the anionic and cationic surface dangling bonds (X.G. Peng et al 1997). Surface defect spots can be removed by the inorganic passivation which is more efficient than organic passivation. It has been stated by the researchers that fluorescence intensity can be enhanced by making a jacket of Cd $(OH)_2$ over the surface of the nanoparticles. It has been stated that effectiveness of the various inorganically capped agents having different energy

band gaps on the surface passivation of cadmium sulphide (CdS) nanoparticles. It has been reported in the literature that these the non-radiative channels can be blocked by doing the capping of surface of nanoparticles with wider energy band gap inorganic material like Cd $(OH)_2$ and zinc sulphide (ZnS).It has been found in surface passivation, zinc sulfide (ZnS) is more efficient than $Cd(OH)_2$ because of its size compatibility with cadmium sulfide (CdS), ensuring in increased optical band edge emission. Growth of a semiconductor (ZnS) with wider band gap on the surface of semiconductor (CdS) with narrower band gap, developing CdS/ZnS core shell nanoparticles, leads to noticeable passivation resulting in improvement of photoluminescence (PL) emission. It has been reported in the literature that quantum efficiencies can be enhanced by the growth of CdS/ZnS graded shell on CdS rods. Making of very luminescent photostable core shell nanocrystals of CdSe/CdS and CdSe/ZnS (B.O. Dabbousi et al 1997) has been reported and these core shell nanocrystals have been used as fluorescent biological levels. Mn^{2+} doped semiconducting nanoparticles potentially gives birth to a smart group of luminescent materials with an extensive variety of applications in optical displays, sensors and lasers etc. A noticeable improvement in the Photo Luminescence property of ZnS-coated CdS nanoparticles in a polymer polycetyl-p-vinylbenzyldimethylamonium chloride (PCVDAC) has also been reported (S.Y. Lu et al 2003). The enhancement in PL intensity with increased ZnS nanoparticles concentration gives additional support for the development of core shell nanoparticles rather than a mixture of CdS and ZnS nanoparticles. Nanostructures have attracted an expectant attention of researchers due to their extraordinary optical, electronic, chemical and structural properties. The most famous approach involves the synthesis of nanoparticles in situ within the block copolymer containg metal precursor. Block copolymers with the ability to form static micelles in solution

and at interfaces are fantabulous nominee for the preparation of various metal nanoparticles with a narrow size dispersion and long-run stability (Tugba Orhan Lekesiza et al 2014).

1.8 Properties of Nanocomposites

1.8.1 Optical Properties of doped nanocrystals

Nanocrystals are the particles of small dimension in nanometer region that are neither tiny molecules nor bulk materials. The nanoparticles of semiconductor, which show properties unique from bulk solids, are smart group of materials that have great potential for broad uses in the electronics and photonics industry (J. Lee et al 2000, H. Mattoussi et al 1998). As the radius of the semiconductor crystal comes close to its exicton Bhor radius, the optical and electronic properties begain to modify and quantum confinement effects comes for playing a vital role. The optical absorption onset of small semiconductor crystals happens at higher energies (blue shift) versus absorption of bulk materials due to quantum confinement.

Most of the studies have been done on undoped rather than doped semiconductor nanocrystals such as CdS, CdSe due to their attractive color tenability as a function of the size of the semiconductor. Though the observation of 18% PL efficiency from Mn-doped ZnS nanoparticles doped semiconductor nanoparticles (Bhargava at al 1994) has been reconigized as a talented form of radiant materials.

Presently, the nanoparticles of semiconducting materials are being studied because of their extraordinary luminescent characteristics and comparatively low cost in combination with the high chemical flexibility, thin film light emitting diodes (LEDs) (Colvin et al 1994), low threshold lasers, optical amplifiers media for telecommunication networks (Harrison et al 2000) and biological levels. A bright scope of ignite research has just came into view on the utilization of special dispersive nanocrystals as basic building blocks for the production of quantum dots

superstructures and the inspection of the combined properties of these novel synthetic materials. There are many nanocrystals for the several semiconductors. But, broadly studied nanocrystals among semiconductor nanoparticles are CdSe. In a very successful synthesis method of CdSe nanocrystals, an excellent control over the size of nanocrystals, its structure and nondispersity is possible.

A big step in the direction of the synthesis of strong highly luminescent nanocrystals was the passivation with wider optical band gap in analogy with the highly sensitive method for the development of 2D quantum wells. Many II-VI semiconductors were explored as the shell material for CdSe nanocrystals. Thus, ZnS (Hines et al 1996) CdS (Peng et al 1997) or ZnSe (Reiss et al 2002) shell grown around CdSe core results in drastic enhancement of PL efficiency and specially, the chemical stability and photostability of the nanocrystals properties. In terms of stability, zinc sulfide (ZnS) shell is superior to the cadmium sulfide (CdS) and ZnSe shells. Moreover, the PL QE OF CdSe/ZnS nanocrystals decrease with growing core size, and the reported values for red emitting CdSe/ZnS nanocrystals are comparatively low (10-40%) (Peng et al 1997, Ebenstein, Y et al 2002, Gerion, D. et al 2001).

The inorganic-polymer nanocomposites provide unique optical properties which can be applied in various electronic and optical devices. The preparation of ZnS doped polymer composites has many future applications. Guo et al reported the synthesis of ZnS –polymer nanocomposites using PMMA as polymer matrix (Guo et al 2007). Thus, metal doped polymer nanocomposites may be implicated for wide industrial applications such as optical devices, LED, sensors and light color filters.

1.8.2 Physical and chemical properties of metal doped nanoparticles

The definite-size dependence of physical properties becomes apparent when they no longer follow classical physics but rather are expressed by quantum physics; are dominated by specific interface effects; shows properties due to a small number of constituents, since the usual term "material refer to an almost large number of constituents (e.g. atoms, molecules) displaying an averaged statistical behavior. In addition, embedded nanoparticles of metals strongly influence polymer typical some of the properties like physical and chemical (glass transition, crystallinity etc.) open a broad range of promising applications. The properties like optical, electronic, mechanical can be modified by the doping of nanoparticles as support elements in polymers. This is an ordinary way to modify the electronic, optical, mechanical and electrical properties of nanocomposites. The mechanical properties can be enhanced by the doping of nanoparticles and this enhancement can be attained when an adequately high-quality interaction between the nanoparticles and the matrix of polymer takes place and with a necessity that the particles are well distributed within the polymer matrix. Nanocomposites lead to achieve excellent bonding between the nanoparticles and the polymer matrix. The strength of polymers can be increased by CNT. Carbon nano tubes (CNTs) are able to making polymers more conductive and thermally more stable already at low volume fractions. Polymer nanocomposites (PNC) doped by relatively small amounts of ultrafine, nano-particles produced materials with extraordinary properties. The extraordinary properties of these smart materials were surprisingly high stiffness, toughness ratio, gas-barrier properties, flame retardance etc.

1.9 Advantage of Nanocomposites

The following are nanocomposites advantages:

1) Improved mechanical properties

2) Decreased thermal expansion coefficients
3) Lower residual stress
4) Increased solvent resistance

1.10 Applications of Nanocomposites

Nanocomposites have potential application in the following industries:

1) Automotive
2) Packaging
3) Aerospace
4) Electronics

1.11 Ionizing Radiation

Ionizing radiation consists of particles that independently can release an electron from an atom or molecule, create ions. Ions are atoms or molecules with a net positive or negative charge. These ions are chemically reactive and can do damage to the material. The level and nature of such ionization depend on the mass, energy and type of the particles composing the radiation. In the interaction of ionizing radiation to a polymer, a result of main ionization and excitation of the target molecules, the incident energy is transported to the medium. These phenomenons of ionization and excitation within the target lead to break of initial bonding, creation of excited and ionized species. There are various processes like chain scission, radical formation, bond rearrangement, etc occurred due to the excitation and ionization. These entire phenomenons are accountable for the change in properties of polymers starring to their uses in diverse areas of science and technology.

The properties of polymers change by the various process such as cross-linking, chain scissoring. The radiation which has low energy density, known as low linear energy transfer

(LET) Radiations, such as X-rays, γ-rays, fast electrons, etc. interact with matter by three different process i.e. photoelectric effect, pair production and Compton effect. Interaction of radiation polymer can produce irreversible changes in their properties. The fundamental phenomenon in polymers is ionization, chain scission and cross linking. When swift heavy ions bombardendent, its lose its energy in the process of exciting electrons and ionizing the atoms. SHI can do noticeable modification in chemical structure of polymer.

1.12 Ion-Solid interactions

Nowadays ion beam modification is only one of its kind tool for improving properties of polymers in a coveted way. Swift Heavy Ion beam induced modifications in solids can be classified into two groups: In group one, SHI induced modification on the surface of the material known as the surface modification and the other is a uniform modification as a function of depth. The surface modification is associated to ion implantation modifications near surface layers and the later is ion beam bombardment through a thin sheet (Davenas and Thevenard, 1993). Ion bombardment admits the modification on the surface of films and ion beam mixing at the port of films and substrate due to radiation effects. In the interactions of energetic ions with the electrons and the nuclei of the target atoms in the solid material gradually loses its energy along its path and eventually comes to rest. The energy loss of charged particles per unit length is known as 'Stopping Power' and is usually written as - S (E) = -dE/d*x*, where E is the energy and *x* is path length. The value of stopping power varies and depends to the type of materials. The energy losses can be represented in terms of LET which is an amount of the energy deposition on the unit length of ion, often represented in SI unit of eV/nm. The extent of ionization will depend upon the amount of energy deposited along the ion track or LET (Lee, et al.1999). The energetic ion loses its energy in solid material by two ways i.e. electronic and nuclear stopping

(Krasheninnikov and Banhart, 2007; Ziegler et al. 1985). These two process i.e. electronic and nuclear stopping occur during ion solid interaction are shown in Figure 1.5.

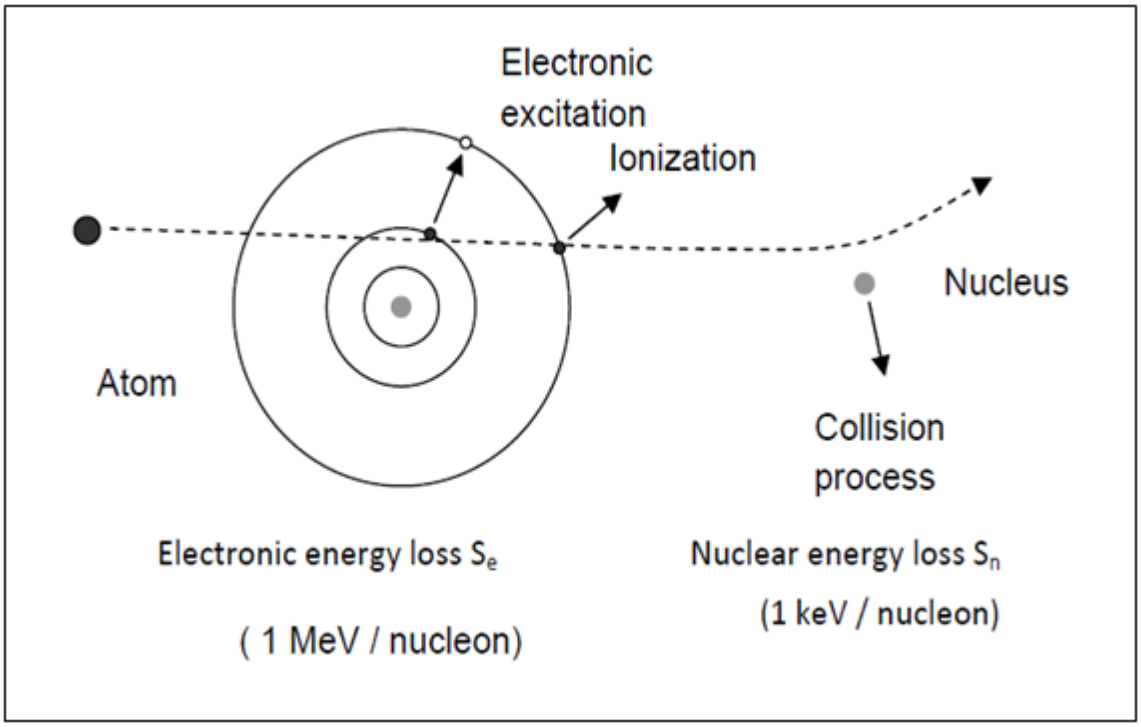

Figure 1.4: Basic Ion-Solid Interaction

The nuclear stopping is a process between the ion and the nuclei of atoms in the target so that the ion's kinetic energy is moderately transferred to a target atom as a whole resulting in its translatory motion. The energy losses are determined by Coulomb interactions. The nuclear stopping is crucial only for very heavy ions. The electronic stopping is regulated by inelastic collisions between the moving ion and the electrons in the target, which can be either free or bound. The compound nature of the electronic energy loss is understandable when one consider

its probable origins: (i) straight transfer of kinetic energy to the electrons of target atoms, mostly due to electron-electron collisions, (ii) excitation of target atoms, (iii) excitation of conduction band electrons and (iv) excitation or electron-capture of the projectile itself.

Electronic stopping dominates at high ion energies. Energetic electrons interact with the nuclei and the electron system in the target (Banhart, 1999). Generally the projectile looses energy with penetration depth x is taken as a sum of nuclear and electronic energy-loss terms, i.e.

$$-\frac{dE}{dx} = \left(\frac{dE}{dx}\right)_{nuclear} + \left(\frac{dE}{dx}\right)_{electronic}$$

The forms of the energy loss over all the energy range are complex. Though, over a constrained energy system, estimated forms for the energy losses can be obtained, which permit the ion penetration and stopping processes to be calculated correctly. At small ion velocities, where the nuclear energy-loss leads, the energy loss process is rather correctly explained by using a Thomas-Fermi potential (Ziegler et al. 1985). At higher ion velocities, the electronic energy losses are better explained by the Bethe-Bloch formalism (Ziegler et al. 1985):

$$-\frac{dE}{dx} = \frac{4\pi n z^2}{m_e c^2 \beta^2} \cdot \left(\frac{e^2}{4\pi\varepsilon_0}\right)^2 \cdot \left[\ln\left(\frac{2m_e c^2 \beta^2}{I \cdot (1-\beta^2)}\right) - \beta^2\right]$$

The symbols are defined as:

E ion energy

x length of the ion path

m_e mass of the electron (9.109×10^{-31}kg)

c speed of light (2.998×10^{8} m/s)

n target electron density

z charge of the ion

$\beta = \frac{v}{c}$

v ion velocity

e elementary charge (1.602×10^{-19} J)

ε_o Vacuum permittivity (8.854×10^{-12} C^2/Jm)

I mean excitation potential of the target

1.13 Ions Range in Solids

The ion range in a solid material is defined as the mean depth from the material surface at which the ion comes to a end. The range of ions in a solid can be expressed by the rate of energy loss $(dE/dx)_{total}$ along the track of the ion, which is given as under:

$$R = \int \frac{1}{|dE/dx|_{total}} dE$$

Where,

E_0 is the incident ion energy at the target surface

x is the distance measured along the ion path

dE/dx is the energy loss (which has both nuclear and electronic energy loss part) of the ions

R is the range of ion of energy E_0

1.14 Track Pattern by Swift Heavy Ions

Interaction of solids with heavy ions leads to damage zones in the material. When a solid is bombarded by swift heavy ions, the material in environs of the ion trajectory may be changed into a disordered state, giving rise to the so-called track (damage zone created along the paths of fast heavy ions).

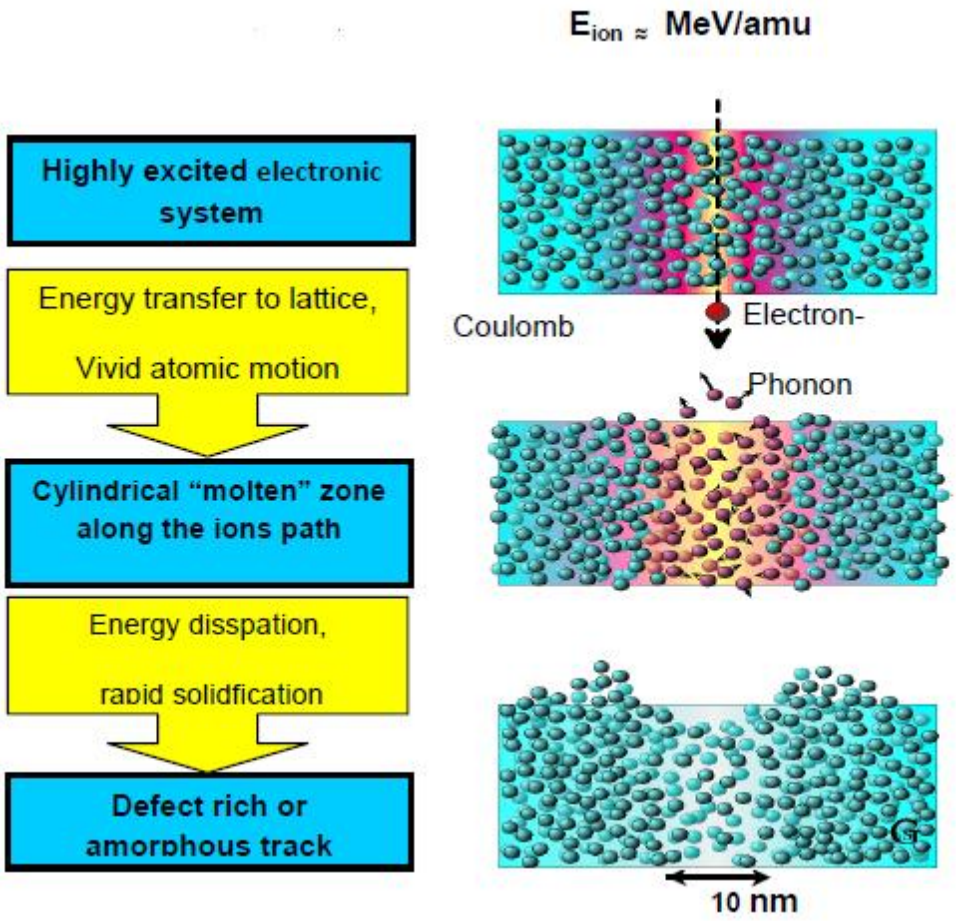

Figure 1.5: Evolution of Ion Track Formation

The formation of latent track by fast heavy swift ions in nanocomposites film and modification results in amorphous metals are related to material dependent thresholds in the electronic excitation density at the centre of the track (Schiwietz et al. 1999). Two different mechanisms can be considered for track formation as illustrated in Figure 1.5. The track formation in the material can be explained by the famous coulomb explosion and thermal spike models (Toulemonde et al. 1992).

1.15 Literature survey

Optical properties can be modified by doping of semiconducting particles in polymer matrix. The electron state at interface plays a very important role for modifying the optical properties (Jiaqi Yu' at al 1998). The design, synthesis and characterization of nanoparticles doped polymer become the subject of strong research. Because of their large surface to volume ration, there is an enhancement in optical, physical and chemical properties (Swapna S at al 2005). Irradiation of polymer has been recognized itself as the desired adequate method to modify polymer and nanocomposites properties extensively (Singh et al 2005).

In recent time, the interaction of radiation has been investigated in all type of polymer all types of polymers. Irradiation can alter the optical, physical and structure properties of the polymer. It is because of chain scission which cracks the macromolecules and cross linking that find the degree of degradation of those properties. There are various factors like type of interaction, energy, fluence, target material play a key role in predicting the behaviour of polymeric material under radiation.

The optical properties of polymers and its composites were studied by using UV-Visible spectroscopy (El-Badery, 2008; Singh and Prasher, 2004). They have reported that the irradiation direct to the shift of absorption edge from lower to higher wavelength region which specified that band gap energy decrease after irradiation. These results explained by chain scission of the polymers due to irradiation. The research in ion beam treatment of material like polymers and its composites has impressed in modern time. Wielunski et al. (1997) have reported that ion beam irradiation can enhanced the mechanical, optical, chemical and structural properties of various polymer films and its composites. The ion beam irradiation of polymer material makes

unalterable changes in their structure like ionizing radiations such as neutron, gamma, etc. In a controlled manner, it can be used to modify the various properties of the polymer films.

Swift heavy ions in materials like polymers destroy the original assembly of atoms by cross-linking, chain scission and emission of atoms and molecules (Marletta, 1990). This change in the structure of polymers shows the way to modification of their properties like optical absorption (Davenas et al. 1990), crystallinity and average crystallite size (Virk, 2002; Rajesh et al. 2006, Ramola et al. 2009). The results of irradiation on materials like polymer films depend upon the different parameters like molecular weight, temperature, etc. of target and energy, mass, fluence of ions.

In the last two decades, the research on the interaction of ion-beam irradiation with polymers at low and high dose has attracted much interest of the scientist worldwide at various institutes. The huge change induced in electrical conductivity studied by Forest et al. (1982) have characterized the temperature dependence and some doping effects induced in polymers by different ions. Marletta et al., (1989) have reported and found the correlation among the change in chemical, structural and electrical properties of polymers like Polystyrene. Liu et al. (2000) studied ion induced crystalline structure and chemical modifications by means of FTIR, XRD techniques and XRD results show significant loss of crystallinity after irradiation. Many researchers reported loss of crystallinity after heavy ion irradiation (Sun et al. 2003). Optical and electrical properties were also studied with 60 MeV protons by Mishra et al. (2000). Further, Singh et al. (2003) reported the chemical and electrical properties of 230 μm PET film by 50 MeV Li^{3+} ions. (Fink et al. 1994) have done IR studies on polycarbonate using the beam of low energy argon ions where Rajulu et al. (2000) have reported the modification in the chemical properties of polymers like polypropylene and polymethylmethacrylate/ polystyrene blend by 60

MeV silicon ion beam. The modification in optical, structural and chemical properties by swift heavy ions (SHI) was reported by Sun et al. 2003.They reported that material suffers a high degree of degradation through scissoring and cross linking. Alkynes formation after heavy irradtion was found.

Fink et al. 1995 reported that when energetic ions pass through the polymers, carbonaceous clusters produced along latent tracks in polymers. The value of optical band gap (*Eg*) can be calculated by famous Tauc's expression (Rajesh et al. 2006). Zhu et al. 2000, reported the energy loss on chemical modifications of polystyrene (PS) irradiated with 1.37 GeV Ar ion are studied through FTIR and optical absorption measurements. They found that PS underwent much degradation under ions irradiation. Incorporation of nanoparticles in polymer matrix can lead to an unexpected performance for many applications in different fields. Composites made of inorganic nanoparticles embedded in polymer matrix are used in automobile industry, medical applications (Thien-Phap Nguyen at 2011).

1.16 Objective and Scope of the study

The objective of this thesis work is to study the optical, structural and chemical properties of metal doped nanocomposites polymer films. The main attention and objectives of the research work are:

(1) The goal of research work presented in the Thesis to prepare polymeric nanocomposites. Metal nano particles of Ni and Cu are to be prepared with the help of micro emulsion method. Also semiconducting nanoparticles like CdS and ZnS are to be synthesized.

(2) These nanoparticles are to be introduced in polymer matrix. The thickness of the film is to be decided by the mass of the particles. In addition the uniform doping of nanoparticles in

polymer matrix has to be kept during the synthesis. The synthesis and doping part of the work studied as well. The first challenge is to make the metal nanoparticles of small size and uniform distribution in polymer matrix. Then to make the film of uniform thickness. The thickness has to be kept very low of the order of micron so it could not be brittle. The aim is the film should be transparent so that in future the optical properties of metal doped nanocomposites film can be modified.

(3) Next step is to irradiate the nanocomposites film with Swift Heavy Ions. Swift Heavy Ions is very powerful tool for the modification in materials.

(4) Final goal is to study the optical, structural and chemical properties of metal doped nanocomposites.

The focus of this research work is to investigate the radiation effect of swift heavy ions (SHI) on the optical, structural and chemical properties of nanocomposites polymer films. Goal is to produce smart nanomaterials which can be potentially used for various applications like sensors, optical devices, filters, magnetic data storage nano systems and more over. In this work, the optical band gaps of the materials under investigations have been engineered for the purpose of possible applications in industry.

REFERENCES

Jose-Yacam an M., Rendon L., Arenas J. Serra Puche, M. C. 1996. Maya Blue Paint: An Ancient Nanostructured Material". Science 273 (5272): 223–5.

Cook, I. 2006. Materials research for future energy. Nat. Mater. 5(2):77-80.

Xua X, Colemana M. R, Mylera U, Simpsona P. J., 1998. Ion beam irradiation-an efficient method to modify the sub nanometre scale microstructure of polymers in a controlled way. Mater. Res. Soc. Proceeding 540:255.

Mehta, G. K., 2003. Accelerator based material science based research in India. Nuclear Instruments and Methods. B 212:8-19.

El-Badry, B. A, Zaki, M. F, Hegazy, M. T, Morsy A. A., 2008. An optical method for fast neutron dosimetry using CR-39. Radiation Effects and Defects Solids 163:821-825.

Thien-Phap Nguyen, 2011. Surface & Coatings Technology, Surface & Coatings Technology 206, 742–752.

F. Iskandar, 2009. Adv. Powder Technol. 20, 283.

Tugba Orhan Lekesiza, Kadir Kalelia, Tamer Uyarb, Ceyhan Kayrana, Jale Hacaloglua, 2014. Preparation and characterization of polystyrene-b-poly (2-vinylpyridine) coordinated to metal or metal ion nanoparticles. Journal of Analytical and Applied Pyrolysis 106, 81–85.

Kesong Hu, Dhaval D. Kulkarni, Ikjun Choi, Vladimir V. Tsukruk, 2014. Graphene-polymer nanocomposites for structural and functional applications Progress in Polymer Science (in press).

Huang X, Yin Z, Wu S, Qi X, He Q, Zhang Q, Yan Q, Boey F, Zhang H, 2011. Graphene-based materials: synthesis, characterization, properties, and applications. Small 1876–902.

Young RJ, Kinloch IA, Gong L, Novoselov KS, 2012.The mechanics of graphene nanocomposites: a review. Compos Sci Technol. 72, 1459–76.

Sun X, Sun H, Li H, Peng H, 2013.Developing polymer composite materials: carbon nanotubes or graphene. Adv Mater 25, 5153–76

Krasheninnikov, A.V., Banhart, F., 2007. Engineering of nanostructured carbon materials with electron or ion beams. Nature Mater. 6, 723-733.

Davenas, J, Thevenard, P., 1993. The multi-aspects of ion beam modification of insulators. Nuclear Instrument and Methods B 80-81, 1021-1027.

Ziegler, J. F, Biersack, J. P, Littmark, U. 1985 (New Ed. in 1996). The Stopping and Range of Ions in Matter (Pergamon, New York).

Lee, E. H., 1999. Ion-beam modification of polymeric materials-fundamental principles and applications. Nucl. Instr. and Meth. B 1-4, 29-41.

Schiwietz, G, Xiao, G, Grande, P. L, Luderer, E, Pazirandeh, R, Stettner, U, 1999. Determination of the electron temperature in the thermal spike of amorphous carbon. Europhys. Lett. 47(3), 384- 390.

Toulemonde, M, Dufour, C., Paumier, E., 1992. Transient thermal process after a high energy heavy-ion irradiation of amorphous metals and semiconductors. Phys. Rev. B 46, 14362-1436.

Kim G., Kim Y., Ihm J., 2005. Encapsulation and Polymerization of acetylene molecule inside a carbon nano tube. Chem Phys. Lett. 415, 279-82.

Shvarcz M. Carbanions, 1968. Living polymer and electron transfer processes. Interscience Publishers, John Wiley and Sons, Inc., New York.

Ruckenstein E, Li Z.F., 2005.Surface modification and functionalization. Adv colloid Interface Sci. 113, 43-63.

Wang J-S, Matyjaszewski K., 1995. Controlled living radical polymerization. Atom transfer radical polymerization in the presence of transition metal complexes. J Am Chem Soc 117, 5614-5.

Matyjaszewski K, 2005. Macromolecular engineering from rational design through precise macromolecular synthesis and processing to targeted macroscopic material properties. Progress in Polymer Science 30, 858-875.

Zou, B.S., Little R.B., Wang, J.P., EI-Sayed, M.A.,1999. Effect of different capping environments on the optical properties of CdS nanoparticles in reverse micelle. Int. J. Quantum Chem. 72, 439

Margaret A. Hines, Philippe Guyot-Sionnest, 1996. Synthesis and Characterization of Strongly Luminescing ZnS-Capped CdSe Nanocrystals. Journal of Physical Chemistry 100, 468-471.

B.O. Dabbousi, J.Rodriguez-Viejo, F.V. Milkulec, J.R. Henie, H. Mattoussi, R. Ober, K.F. Jensoen, M.G. Bawendi, 1997. J. Phys. Chem. B 101, 9463.

S.Y. Lu, M.L. Wu, H.L. Chen, 2003. Polymer nanocomposite containing CdS–ZnS core–shell particles: Optical properties and morphology. Journal of Applied Physics 93, 5789.

J. Lee, V.C. Sunder, J.R. Heine, M.G. Bawendi, and K.F. Jensen, 2000. Full colour emission from II–VI semiconductor quantum dot–polymer composites. Advanced Materials, 12, 1102 (2000).

H. Mattoussi, L.H.Radzilowski, B.O. Dabbousi, E.L. Thomas, M.G. Bawendi and M.F.Fubner, 1998. Electroluminescence from heterostructures of poly (phenylene vinylene) and inorganic CdSe nanocrystals. Journal of applied Physics 83, 7965 (1998).

R.N. Bhargava and D.Gallagher, 1994. Optical properties of manganese-doped nanocrystals of ZnS. Physics Review Letter 72, 416.

Colvin, V.L., Schlamp, M.C., Alivisatos, A.P., 1994. Light-emitting diodes made from cadmium selenide nanocrystals and a semiconducting polymer. Nature 370, 354-357

Harrison, M.T., Kershaw, S.V., Burt, M.G., 2000. Colloidal nanocrystals for telecommunications. Complete coverage of the low-loss fiber windows by mercury telluride quantum dot. Pure and Applied Chemistry 72, 295-307.

Peng, X., Schlamp, M.C., Kadavanich, A., Alivisatos, 1997. A.P.J. Am. Chem. Soc. 119, 7019.

Reiss, P., Bleuse, J., Pron, A, 2002. Highly luminescent CdSe/ZnSe core/shell nanocrystals of low size dispersion. Nano Letter 2, 781-784.

Ebenstein, Y., Mokari, T., Banin, U., 2002. Fluorescence quantum yield of CdSe/ZnS nanocrystals investigated by correlated atomic force and single particle fluorescence microscopy. Applied Physics Letter 80, 4033-4035

Gerion D., Pinaud F., Williams S. C., Parak W. J., Zanchet D., Weiss S. & Alivisatos, A., 2001. Synthesis and properties of biocompatible water-soluble silica-coated CdSe/ZnS semiconductor quantum dots. Journal of Physics Chemistry B 105, 8861-8871.

Tugba Orhan Lekesiza, Kadir Kalelia, Tamer Uyarb, Ceyhan Kayrana, Jale Hacaloglua, 2014. Preparation and characterization of polystyrene-b-poly (2-vinylpyridine) coordinated to metal or metal ion nanoparticles, Journal of Analytical and Applied Pyrolysis 106, 81–85

L. Guo, S. Chen, L. Chen, 2007. Colloid Polymer Sci. 285, 1593.

Thien-Phap Nguyen, 2011.Polymer-based nanocomposites for organic optoelectronic devices: A review, Surface & Coatings Technology 206, 742–752.

Jiaqi Yu, Huimin Liu, Yanyun Wang, F.E. Fernandez, Weiyi Jia, 1998. Optical properties of ZnS: Mn2+ nanoparticles in polymer films, Journal of Luminescence 76&77, 252-255.

Swapna S. Nair, Mercy Mathews, M.R. Anantharaman, 2005. Evidence for blue shift by weak exciton confinement and tuning of band gap in super paramagnetic nanocomposites, Chemical Physics Letters 406, 398–403.

Singh, N. L, Shah, N, Singh, K. P, Desai C. F. 2005. Electrical and thermal behaviour of proton irradiated polymeric blends. Radiation Meas. 40, 741-745.

El-Badry, B. A, Zaki, M. F, Hegazy, T. M, Morsy, A. A. 2008. An optical method for fast neutron dosimetry using CR-39. Radiation Eff. Defects 163, 821-825.

Singh, S. and Prasher, S. 2004. The etching and structural studies of gamma irradiated induced effects in CR-39 plastic track recorder. Nuclear Instruments Methods B 222, 518-524.

Sun, Y, Xia, Y. 2002. Shape-Controlled Synthesis of Gold and Silver Nanoparticles. Science 298, 2176-2179.

Marletta, G. 1990. Chemical reactions and physical property modifications induced by KeV ion beams in polymers. Nuclear Instruments Methods B 4, 295-305.

Davenas, J, Thevenard, P, Boiteux, G, Fallaver, M, Xu, X. L., 1990. Hydrogenated carbon layers produced by ion beam irradiation of PMMA and polystyrene. Nuclear Instruments Methods B 46, 317–323.

Ramola R. C, Chandra, S, Negi, A, Rana, J. M. S, Annapoorni, S, Sonkawade, R. G, Kulriya P. K., Srivastava, A., 2009. Study of optical band gap, carbonaceous clusters and structuring

in CR-39 and PET polymers irradiated by 100 MeV O7+ ions. Physica B: Condensed Matter 404, 26-30.

Virk, H. S., 2002. Physical and chemical response of 70 MeV carbon ion irradiated Kapton-H polymer. Nuclear Instruments Methods B 191, 739-743.

Forrest, S. R, Kaplan, M. L, Schmidt, P. H, Venkatesan, T, Lovinger A. J., 1982. Large conductivity changes in ion beam irradiated organic thin films. Appl. Phys. Lett. 41:708-711.

Marletta, G, Pignataro, S, Oliveri C., 1989. Reflection electron energy loss spectroscopy (REELS) of conductive polymers obtained by KeV bombardment. Nuclear Instruments and Methods B 39, 773-777.

Liu C, Zhu Z, Jin Y, Sun Y, Hou M, Wang Z, Chen X, Zhang C, Liu J, Li B, Wang Y, 2000. Chemical modifications in polyethylene terephthalate films induced by 35 MeV/u Ar ions. Nuclear Instruments and Methods B 166-167, 641-645.

Sun Y, Zhu Z, Wang Z, Jin Y, Liu J, Hou M, Zhang Q, 2003. Swift heavy ion induced amorphization and chemical modification in polycarbonate. Nuclear Instruments and Methods B 209, 188-193.

Rajulu A. V, Reddy R. L, Avasthi D K, Asokan K, 2000. Infrared spectroscopic investigation of some polymers and polymer blend films irradiated by a 28 Si ion beam. Radiation Eff. Defects Solids 152, 57-66.

Fink D, Chung W. H, Klett R, Schmoldt A, Cardoso J, Montiel R, Vazquez M. H, Wang L, Hosoi F, Omichi H, Goppelt-Langer P. 1995. Carbonaceous clusters in irradiated polymers as revealed by UV-Vis spectrometry. Radiation Eff. Defects Solids 133, 193-208.

Fink D, Klett R, Chadderton L.T Cardosa, J, Montiel R, Vezquez H, Karanovich A, 1996. Carbonaceous clusters in irradiated polymers as revealed by small angle X-ray scattering and ESR. Nuclear Instruments Methods Phys. Res. B 111, 303–314.

Rajesh Kumar, Udayan De, Rajendra Prasad, 2006. Physical and chemical response of 70 MeV carbon ion irradiated polyether sulphone polymer. Nuclear Instruments and Methods in Physics Research B 248, 279–283.

CHAPTER 2

Materials and Experimental Methods

2.1 Introduction

This chapter gives the complete details about the nanocomposites polymer and experimental techniques used in the present work. The working principle of each experimental technique is also explained. Detailed descriptions of the following subject matters are given in this chapter:

- Target Materials
- Synthesis of Nanocomposites Polymer
- Pelletron Accelerator
- Irradiation (Material Science Beam Line)
- Calculation of Ion Range and its Energy Loss using SRIM-2008
- X-ray Diffraction (XRD) Technique
- UV-Visible Spectroscopy
- Fourier Transforms Infrared (FTIR) Spectroscopy
- Scanning Electron Microscopy (SEM)

2.2 Materials

Following materials have been used in the present work:

2.2.1 Polystyrene (PS)

Polystyrene (PS) is a polymer which is transparent, colour less and used widely for many applications. It is less expensive and available commercially in many shapes. There are few shortcomings in polystyrene (PS) like low impact strength, poor weather capacity and

poor chemical resistance. Many tailored results which try to find a solution to correct these deficiencies are commercially available.

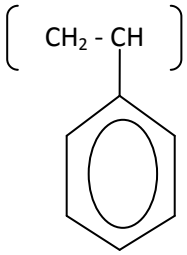

Figure 2.1: The Structure of PS

Polystyrene (density 1.06 g/mL) of average molecular weight 35,000. Polystyrene is a hard, transparent glass-like plastic made by polymerizing a benzyl derivative of ethylene called styrene. Ethylene itself can be polymerized into another plastic called polyethylene. If the starting material is styrene, polystyrene is the product. Ethylene is manufactured from petroleum and styrene is then manufactured from the ethylene. Polystyrene (PS) is the plastic most often used in "scotch" tape dispensers and transparent, hinged plastic boxes. Polystyrene (PS) can even be cast into cheap plastic lenses.

2.3 Synthesis of nanoparticles by Microemulsion Technique

Nowadays, nanoparticles of semiconductor are under strong investigation because of their modified photo reactivity and photo catalytic properties due to the quantum confinement and the dependence of the photo physical and photo chemical properties on their nano size as it comes close to the radius of exciton. This growing curiosity has direct to a wide range of preparative approaches to nanostructures like sol-gel, electron beam method and micro emulsion method.

2.3.1. Advantage of microemulsion over other techniques

This method of synthesis of nanoparticles offers many advantages: microemulsion is a very smooth procedure, not required intense temperature and pressure conditions, can be used to do various chemical reactions and not required any particular set of apparatus. Microemulsion method is a unique procedure as a sort of soft technique, which is appropriate way for synthesising the homogeneous and small size nanoparticles. The use of an inorganic phase in water-in-oil microemulsion has received significant attention for synthesis of nano particles. This is affecting unique method, which allows synthesis of ultrafine nano particles within the range 5 nm<particle diameter<50 nm.

2.3.2. Synthesis of CdS/ZnS nanoparticles by Micro-emulsion technique

Amongst the various studied methods, the use of micro-emulsions to obtain nanoparticles represents an efficient pathway. “Water-in-oil” micro-emulsions consist of nano meter sized water droplets that are distributed in a continuous oil medium and stabilised by surfactants molecules localized at water/oil interface (K et al 1997). This reverse micellar methods are diverse on a molecular scale, but very durable thermodynamically. Nanoparticles are obtained by reverse micelles. Reverse micelles are suitable reaction medium, since small water droplets signify nano reactors which support the configuration of tiny crystallites with a very fine size distribution (Cizeron, J et al 1995). There are many researchers who worked on this on the factors which have an effect on the size and shape of nanoparticles obtained in micro-emulsions, such as the droplet size, surfactant concentration and so on.

Though, the task performed by the several concerns prevailing the preparation of nano particles is yet to be explained and accurate procedure of their development has to be sort out (Herron, N et al 1990). The application of nanoparticles acquired in microemulsion method, as functional materials in chemical reaction, for optoelectronic devices, such as LED (Bowen Katari, J.E et al 1998) needs their effective revival and stabilisation. But there is some issue

in the revival method. The origin of the main issue in the revival method is large surface energy of very small nanoparticles, which creates them solidify permanently when reverse micelles are damaged without any safety treatment. This issue has been resolved by surface modification of the nanoparticles with several organic molecules (Kanjilal, D at al 1993).

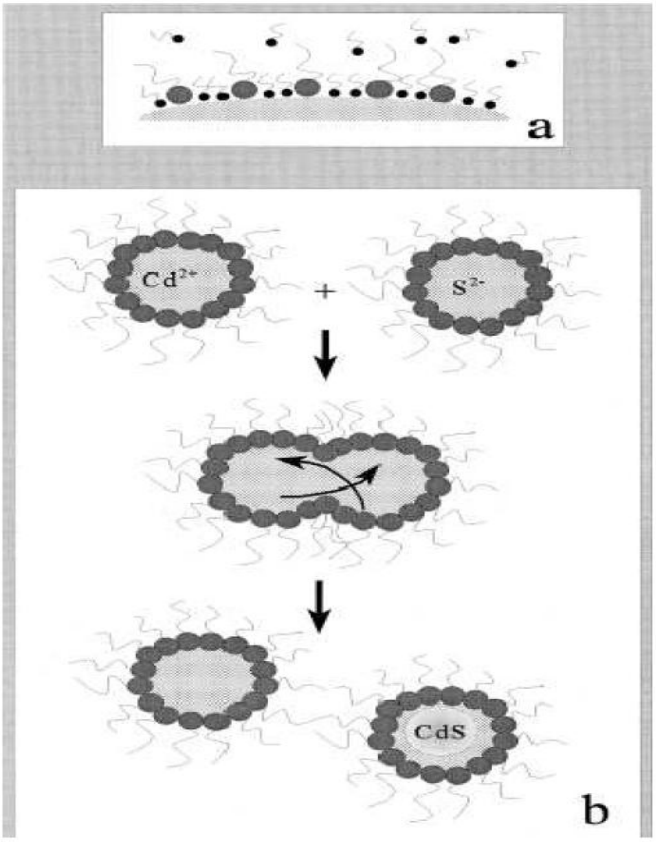

Figure 2.2: (a) Synthesis of quantum-sized CdS in reverse micelles; and (b) Water-in-oil" reverse micelle formed by CTAB as surfactant and n-pentanol, as co surfactant

The present work deals with the use of a quaternary water-in-oil microemulsion, the cetyltrimethylammonium bromide (CTAB)/ *n*-pentanol/*n*-hexane/water system, which offers many advantages over the various micro-emulsions already tested. It has been verified that at a certain composition (CTAB concentration of around 0.1 M, with molar ratio pentanol/CTAB in the range 8–20 and water content of up to 80 mol of water per mole of CTAB) or ATP the system consists of almost spherical reverse micelles stabilized by

pentanol, which acts as a co surfactant (Giustini, M et al 1996). The presence of a co surfactant in this micro-emulsive system allows modulation of the water droplets dimension and surface dynamics by varying either the water content.

The nanoparticles of cadmium sulfide (CdS) have been prepared in this procedure to use this extra parameter, and inspections have meant to look at the main features controlling the size, the distribution and the stability of CdS nano clusters. It seems that the transforming to a quaternary micro emulsion rises the growth of variables regulating the system, and make difficult to the clarification of the procedures engaged in the preparation of the nanoparticles, demanding, as a outcome, some extra tidy on the features, which can affect progress, particles preparation and stabilization. In the visible range by the absorption spectroscopy the characterization can be done of CdS suspension.

When the nanoparticles of semiconducting material are adequately small (20 nm diameter) such that the diameter of the nanoparticles becomes very close to the diameter of the first excited-state orbital of the conduction band electrons, the quantum size effect is come into the existence (Brus, L.E., et al 1984). With the reduced size of particle, the optical band-gap of the semiconductor turns out to be larger and the absorption spectrum appears to be shifted towards the lower wavelength. The upper limit of wavelength of the UV–vis absorption size has been shown in the theoretical work. SEM permits one to look into the arrangement of nanoparticles and find out the average size and size-distribution of nanoparticles.

2.3.3 Preparation of CdS/PS nanocomposites films

The nanoparticles of cadmium sulfide (CdS) were synthesized by micro emulsion method. In this method the nanoparticles of CdS were prepared by the reactions of sodium sulfide and cadmium nitrate in water-in-oil micro emulsion system. In this synthesis method surfactant plays a crucial role so for that purpose cyclohexane was used. The nanoparticles of

cadmium sulfide (CdS) of the size of 50-60 nm were synthesized. The purpose is to disperse semiconducting nanoparticles evenly in polymer and to make nanocomposites film. In this work the cadmium sulfide (CdS) nanoparticles were dispersed in polystyrene (PS) matrix. In the procedure the first step was that polymer was dissolved in chloroform and in the second step, 3 ml of synthesized CdS nanoparticles were added to the polymer solution and dispersed by ultrasonic agitation to make sure a uniform arrangement. Now after this process uniform mixture is obtained, the mixture was poured on to a clean Petri dish. The solvent was evaporated at room temperature (25^0C) to get thin films (thickness ~ 20 μm) of polymer composites which were then dried in vacuum oven at 30° C (Rong et al, 2003; Singh et al., 2011).

2.3.4 Synthesis of ZnS nanoparticles and nanocomposites films

Nanoparticles of ZnS were synthesis by the reaction of Zinc chloride ($ZnCl_2$) and sodium sulfide (Na_2S) in water-in-oil micro emulsion system (Kulkarni et al 2001). Micro-emulsion of $ZnCl_2$ and Na_2S have 0.46 g of n-pentanol, 3.37 g of Triton X-100, 7.64 g of cyclohexane and 1 g of water. Molar ratio of water and surfactant was maintained at 11 while for sulfide and zinc ions was constant (=1). Concentration of sulfide and zinc were estimated per aqueous phase (Jovanović et al 2007).

The confirmation of the nanoparticles was confirmed by in the SEM image (Fig. 1). The nanocomposites of ZnS doped polystyrene were synthesized by solution cast method. The polystyrene (PS) polymer can be dissolved in chloroform. ZnS nanoparticles were added to this solution of polystyrene followed by ultrasonic agitation for uniform arrangement. The obtained solution of ZnS and polystyrene was poured on to a clean glass petri disc floating on Hg to maintain uniform thickness of prepared sample. The solvent was allowed to evaporate at room temperature (25^0C) to get thin films of polymer composites and finally films were then dried in vacuum oven at 30° C to remove the solvent content (Singh et al 2011). The

thickness of prepared thin films have been found 20µm and calculated as per weight, area and density relation.

Figure 2.3: Nanocomposites Film Preparation Method

2.4 Sources of Irradiation

The irradiation by the swift heavy ions (SHI) has been done at Material Science chamber in IUAC, New Delhi, India. In order to irradiate the nanocomposites polymer film, 60 MeV Ni^{5+} ions have been used to conduct the experiments. The beam current was 0.5 pnA. Two fluences, 10^{10} and 10^{11} ions/cm^2 have been selected for irradiation. The samples of nanocomposite of size 1.5 cm × 1.5 cm were prepared and these samples were mounted on the four side of vertical ladder. The ladder was mounted in general purpose scattering chamber. A high vacuum of the order of ~ 6×10^{-6} Torr was done in chamber.

2.4.1 The Pelletron Accelerator

A Pelletron Accelerator which can produce high energy ions (Figure 2.3) is running at Inter University Accelerator Centre (IUAC), New Delhi. This accelerator is being used for basic sciences and applied physics in nuclear physics, atomic physics, materials science,

biosciences and other allied fields (Kanjilal et al., 1993).

A high voltage up to 15 million volts can be produced in the portion of Pelletron known as terminal. A 15UD Pelletron accelerator is competent of accelerating any ion from proton to uranium (except inert gases) up to energies of a few hundred MeV depending upon the nature and type of the ion. It has been installed by the Electrostatic International Inc., USA. This is a Tandem Van de Graff accelerator, in which the charge carrier belt is replaced by a chain of pellets. The digit 15 stands for 15 MV terminal voltages and UD stands for Unit Double. It is mounted in a vertical arrangement in an insulating steel tank of height 26.57 and width 5.5 m. This tank has sulfur hexafluoride (SF6) gas at a pressure of 4.0 Torr to stop sparking and discharging for insulation purpose. The SNICS (Source of Negative Ion by Cesium Sputtering) ion source acts as a source of negative ions which are analyzed by the injector magnets. A high voltage terminal with 1.52 mm diameter and 3.81 mm length in the middle of the tank can be charged by a high potential varied from 4 to 16 MV using an electrostatic charge transfer device. This terminal is connected to the tank vertically through ceramic titanium tubes known as the accelerating tube.

These tubes help in keeping a potential gradient. Negative ions from the ion source are infuse on the way to terminal and stripped off a few electrons through stripper foils. The yield is transformed into positive ions. These ions are further accelerated as they proceed towards the bottom of the tank at ground potential. As a result, the ions from the accelerator gain energy, as given in Equation 2.1.

$$E = V_{\pi}\ (q + 1)\text{MeV} \qquad 2.1$$

In the above equation Vπ is the terminal potential and ‘q’ is the number of positive charges (charge states) on the ions after stripping. A heavy ion of charge state ‘q’ will get a final

kinetic energy equal to (q + 1) × 16 MeV.

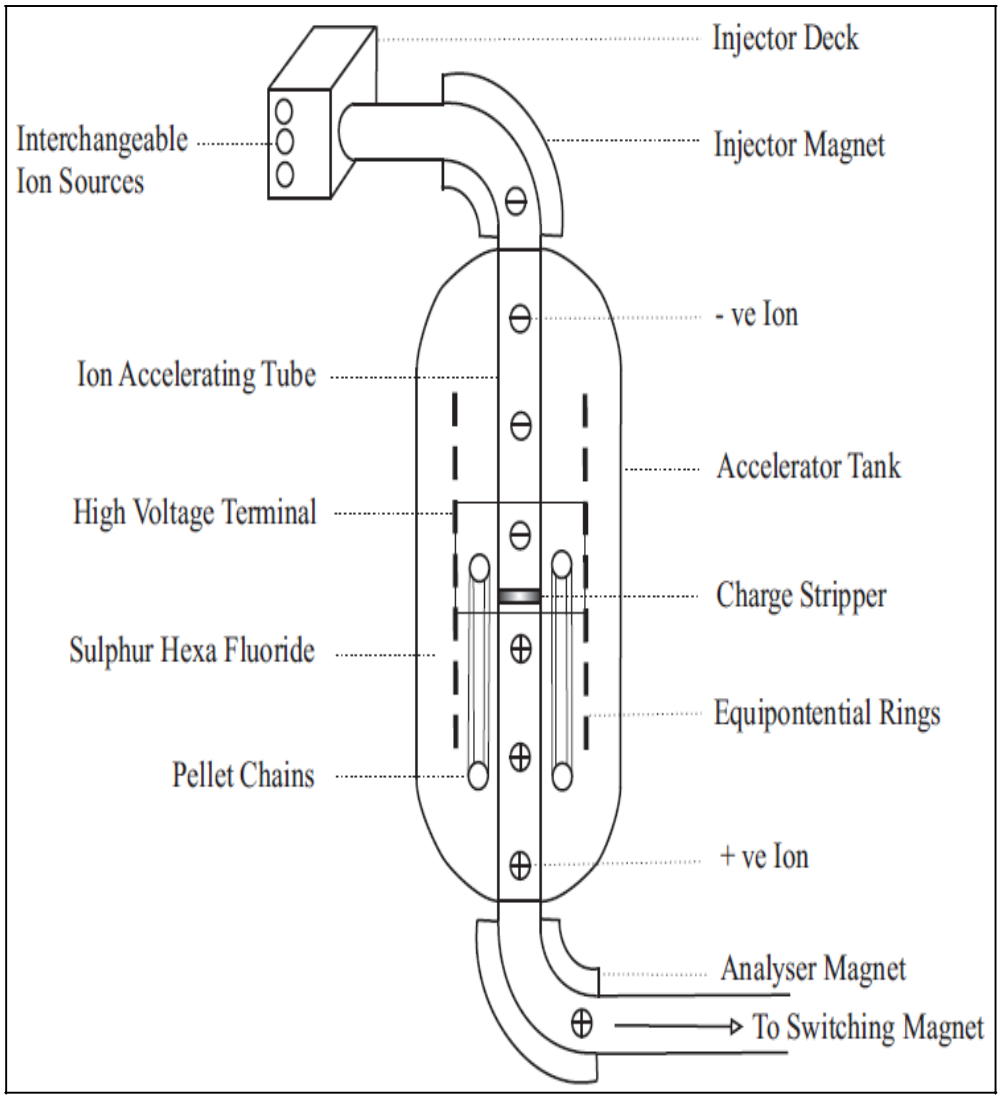

Figure 2.4: Diagram of 15UD Pelletron Accelerator

Thus protons accelerated to a full terminal voltage would have energy equal to 32 MeV. By using proper magnets with respect to the charge states and energies, the high energetic ions are analyzed and are bent at 90° to the vertical position by using analyzer magnet. These redirected ions are focussed to the desired experimental area in the beam hall with the help of multi-port switching magnet. These switching magnets have the ability to

redirect the beam to any one of the seven beam lines (NSC school on accelerator physics, 1989).

2.4.2 Material Science Beam Line

The samples are irradiated in the material science beam line of IUAC, New Delhi. The beam line setup is shown in Figure 2.4.

Figure 2.5: Material Science Beam Line for Irradiating Materials

This beam line is at 150° angle with respect to the direction of the unswitched direct beam. The beam line is sustained at ultra-high vacuum of the order of 10^{-9} Torr and the irradiation process is carried out in the high vacuum chamber (HVC). It is fixed in Material Science beam line of Pelletron. It has a system of temperature control from low temperature to high temperature, dose control which includes positive bias to the target for secondary electron suppression (Faraday cup) and proper mechanical support and alignment. The vacuum in the

target chamber is generally kept below 10^{-6} Torr.

Several samples of different size can be mounted on all the four sides of a specially designed ladder, which is 10cm long copper block of rectangular cross-section. Each sample was fixed on the ladder with the help of silver paste. Conducting path was provided by using a line of silver paste from the top surface of the sample to the copper block. The target ladder is mounted through a Wilson seal from the top flange of the chamber. This top flange is connected to the chamber through a flexible bellow that can be expanded up to 11 cm from its least position. A stepper motor in conjunction with a suitable mechanical assembly is used to control the up and down motion of the ladder. The beam on the ladder can be observed by observing the luminescence of the beam on the quartz crystal mounted on all sides of the ladder. After the observation of the beam on the quartz, the sample to be irradiated is brought to the same position as that on the quartz by moving the ladder in the desirable position. A CCD camera is attached to one of the ports of the chamber for viewing the sample and the quartz position.

The positions of ladder can be monitored regularly using close circuit television (CCTV) in the data acquisition room. The magnetic scanner that can be swept the beam 25 mm in y- direction and 10 mm in x-direction to ensure the uniform irradiation of samples. A cylindrical enclosure of stainless steel surrounds the sample ladder, which is kept at a negative potential of 120V. This enclosure suppresses the secondary electrons coming out of the sample during the irradiation. An opening in the suppresser allows the ion beam to fall on the sample. The total number of particles/charges falling on the sample can be estimated by a combination of the current integrator and the pulse counter (Faraday Cup) from which the irradiation fluence can be measured.

2.5 Fluence Calculation

The calculation of fluence was done by knowing duration of irradiation and the value of ions beams current as follows,

$$I = \frac{Q}{T} = \frac{Dqe}{T} = \frac{\emptyset Aqe}{T} \qquad 2.2$$

$$\therefore T = \frac{\emptyset Aqe}{I} \qquad 2.3$$

Where I = ion current (nA)

Q = total charge

D = dose = ion fluence (φ) in ions/cm^2 × area (A) of irradiation in cm^2

q = charge state

e = electronic charge = 1.6×10^{-19} C

T = time of irradiation

Since, the number of particles per nano ampere of beam current $= \frac{\mathrm{I}}{\mathrm{qe}}(pnA)$

$$T = \frac{\emptyset A}{I(pnA)} \qquad 2.4$$

Using the Equation 2.4, the required time was calculated for all ions fluence. During the experiment, keeping current of the ion beam constant, the samples were irradiated for pre-determined time.

2.6 Calculation of Range and Energy Loss

Stopping and Range of Ions in Matter (SRIM) is software for computing the range and energy loss in the materials like polymers when ions interact with matter; the core of SRIM is a program Transport of ions in matter (TRIM) (Ziegler et al. 2008). In 1983, Ziegler and Biersack developed this software programs and are being continuously upgraded. SRIM is based on a Monte Carlo simulation method, namely the binary collision approximation with a random selection of the impact parameter of the next colliding ion. As the input parameters, it needs the ion type and energy (in the range 10 eV-2GeV) and the material of one or several target layers for doing the calculations. Standard applications include:

Ion Stopping and Range in Targets: SRIM can calculate the attribute of the energy loss of ions in materials (Ziegler et al. 2008). SRIM is able to do fast calculations which generate tables of stopping powers, range and straggling distributions for any type of ion at any energy range in any elemental target. Using targets with complex multi-layer configuration requires more detailed computations. In the present research work, the projected range, nuclear and electronic losses are calculated using SRIM code by Ziegler et al. (2008) for all target materials. Details of the samples for heavy ions and ionizing radiations are given in Table 2.1.

Ion Implantation: The electronic and chemical properties of materials can be modify by a beam of ions. When ion beam passes through the material it causes harm to solid targets by doing the displacement of atoms. Generally the kinetic effect is connected with the physics of the type of interactions is found in the stopping and range of ions in materials package.

Sputtering: In the phenomenon of sputtering, the beam of SHI knocks out target atoms. All the computations of sputtering by any ion in any energy range have been done by SRIM package.

Table 2.1 Irradiation Details of the Samples

S. No.	Target	Fluence (ions/cm^2)	Current (pnA)	Range	*Se* (eV/A^0)	*Sn* (eV/A^0)	Energy and Ions
1.	PS	1×10^8	0.5	19.71	5.2×10^2	1.21	60 MeV Ni^{5+}
		1×10^{11}					
2.	PS/CdS:Cu	1×10^8	0.5	17.56	5.94×10^2	1.67	60 MeV Ni^{5+}
		1×10^{11}					
3.	PS/CdS:Ni	1×10^8	0.5	17.24	6.03×10^2	1.69	60 MeV Ni^{5+}
		1×10^{11}					
4.	PS/ZnS	1×10^{10}	0.5	18.16	5.68×10^2	1.49	60 MeV Ni^{5+}
		1×10^{11}					
5.	PS/ZnS:Cu	1×10^{10}	0.5	16.48	6.36×10^2	1.74	60 MeV Ni^{5+}
		1×10^{11}					
6.	PS/ZnS:Ni	1×10^{10}	0.5	16.14	6.47×10^2	1.78	60 MeV Ni^{5+}
		1×10^{11}					

2.7 Characterization Techniques

2.7.1 X-ray Diffraction (XRD)

The X-ray diffraction (XRD) is the most broadly used technique for qualitative and quantitative analysis as well as for characterizing a broad range of materials including polymers, fluids, metals, nanocomposites, plastics, ceramics, semiconductor etc. XRD studies the structure of unknown crystals and materials, identify the crystalline phase, and determine the spacing between layers. The orientation of a single crystal or grain can be find out by XRD technique. This technique is able to measure the size and stress of crystalline regions

and determine the crystallinity of the thin films.

In an X-ray diffractometer, the production of X-rays is done within a sealed tube (anode) consisting of the metal target (copper metal) and a tungsten metal filament (cathode). Other metals such as chromium, iron, nickel, silver and tungsten can also be used as target for specific purposes. A current (10-15 mA) is passed through the filament within the tube that current warms the filament, the number of electrons emitted from the filament depend on the amount of current passing in the filament, the higher the current the larger the number of electrons. X-rays are produced when high potential voltage (typically 15-60 kilovolts is applied within the tube so that the generated electrons are accelerated and interact with it to produced X-rays. The wavelength of X-rays depends upon the target metal's properties. The characteristics X-rays are produced, when electrons with adequate energy remove inner shell electrons of the target material. When the vacancy of this inner cell i.e. K is filled by an electron originating from any of the outer shell e.g. L and M, the emitted radiation is called Kα (8.06 KeV) and K_β. (8.93 KeV) Usually K lines are used in XRD since the longer wavelength lines are too easily to be absorbed. Kα consists of Kα1 and Kα2 X-rays. The Kα1 transition will occurs almost exactly twice the frequency of Kα2 transition and the resulting X-rays will have twice the intensity as that of Kα2. There is a need for producing monochromatic X-rays for diffraction. This need of producing monochromatic X-rays is done by filtering, by foils or crystal. The wavelength of Kα1 and Kα2 X-rays are very close so an average of the two can be used for calculation purpose.

When a collimated beam of X-rays, with definite wavelength is incident on a crystal, it is coherently scattered from all atoms and undergoes constructive interference (shown in Figure 2.5) in certain directions and destructive interference in other directions giving rise to diffracted beam. It is important to note that only those crystallites or atoms whose reflecting planes are parallel to the sample surface will add to reflected intensities. The Bragg condition

for the angle of the diffraction is thus:

$$n\lambda = 2dSin\theta \qquad 2.5$$

where n is an integer called the order of diffraction, λ is the wavelength of the X-ray, θ is the diffraction angle and d is the interplanar spacing in crystalline material.

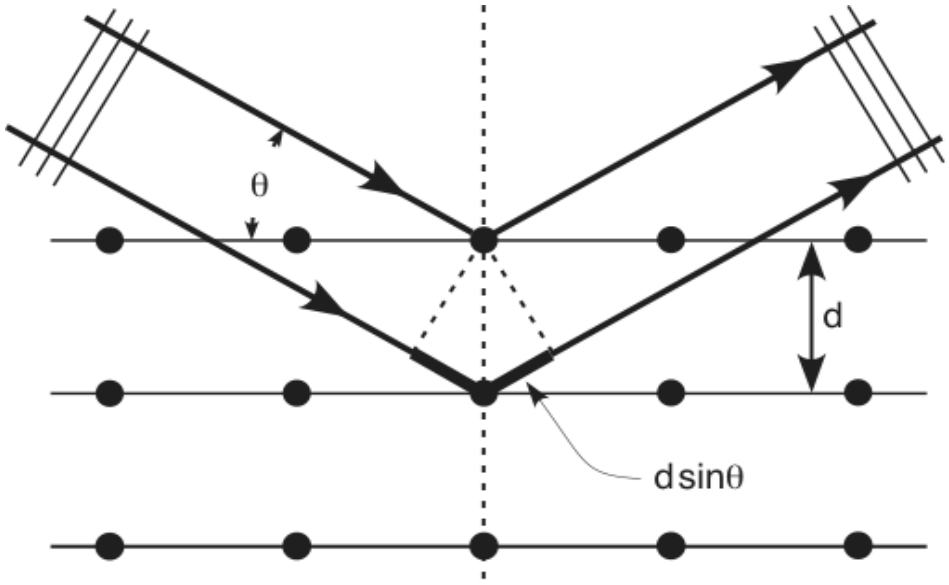

Figure 2.6: Reflection of X-rays from Parallel Planes in a Solid

For homogeneous phase λ is fixed and for a set of lattice planes d is fixed, hence the degree of diffraction will depend on the glancing angle θ. With the help of Bragg's equation it is possible to determine the spacing d between successive lattice planes if λ is known and θ is measured.

Determination of Crystallite Size

The main contribution to the XRD peak intensity is due to grain size, lattice vibrations or strain, instrumental broadening and defects. We can estimate the average crystallite size using

Scherer equation (Scherer, 1918; Patterson, 1939):

$$L = \frac{k\lambda}{b\cos\theta} \qquad 2.6$$

Where λ=1.54 nm is the wavelength of the Cu-Kα X-ray radiation used, b is the FWHM of the diffraction peak and θ is the Bragg angle (in radians), k is the Scherer constant (usually taken as unity), L is crystallite size (A^0).

Determination of Percentage Crystallinity

The crystallinity can be calculated by separating intensities due to amorphous and crystalline phase on diffraction pattern. Percentage of crystallinity (Xc %) is measured as the ratio of crystalline area to total area (Ramola et al. 2009).

$$X_{c\%} = \left(\frac{A_c}{A_a + A_c}\right) \times 100 \qquad 2.7$$

where A_C = area of crystalline phase, A_a = area of amorphous phase and X_C = percentage of crystallinity.

XRD experiment was performed on thin films by using a Bruker D8 advanced, AXS, X- ray diffractometer with Cu-Kα radiation in a wide range of Bragg's angle at 40kV/30mA and having Cu-Kα radiation selected by a graphite monochromator.

2.7.2 UV-Visible Spectroscopy

Ultraviolet-visible spectroscopy is a tool for doing the measurement of the attenuation of the light after it passes through a specimen or after reflection from a specimen surface. UV-visible studies include transmittance, absorption and reflection measurements in the UV, visible and near infra red wavelength region. The UV-visible spectroscopy is generally used

to find out functional group of molecules and inorganic ions in solution. The UV-visible is extremely valuable for quantitative measurements. The strength of the sample in a solution can be determined by computing the absorbance at some wavelength and using the Beer-Lambert Law i.e. $I = I_0 e^{-\sigma l N}$, where I_0 and I are the intensity of the incident light and transmitted light, respectively; σ is the cross section of light absorption by a single particle and N is the density of absorbing particles. In the visible and ultraviolet region, organic compounds absorb UV radiation which leads promotion of electrons in σ, π and n-orbitals from the lower state to upper energy state. These upper energy states are express by molecular orbitals that are vacant in the lower state and are mostly known as anti bonding orbitals. These anti bonding orbitals connected with σ bond is called the σ* orbital and that connected with π bond is called the π* orbital.

[a] Principle of UV Visible Spectroscopy

When thin films of materials are exposed to UV-Visible light having an energy which is according with a possible electronic transition within the molecule, some of the light energy will be absorbed as the electron is raised from lower to a higher energy orbital. An optical spectrometer in UV-visible spectroscopy traces the wavelengths at which absorption takes place and degree of absorption at each wavelength simultaneously. The absorbance of any material or sample will depend on the number of molecules absorbed by the light beam in the spectrometer (e.g. their molar concentration in the sample tube), it is a requirement to take the exact value of the absorbance for this and other operational factors for doing the comparison of the spectra of different compounds in a significant way.

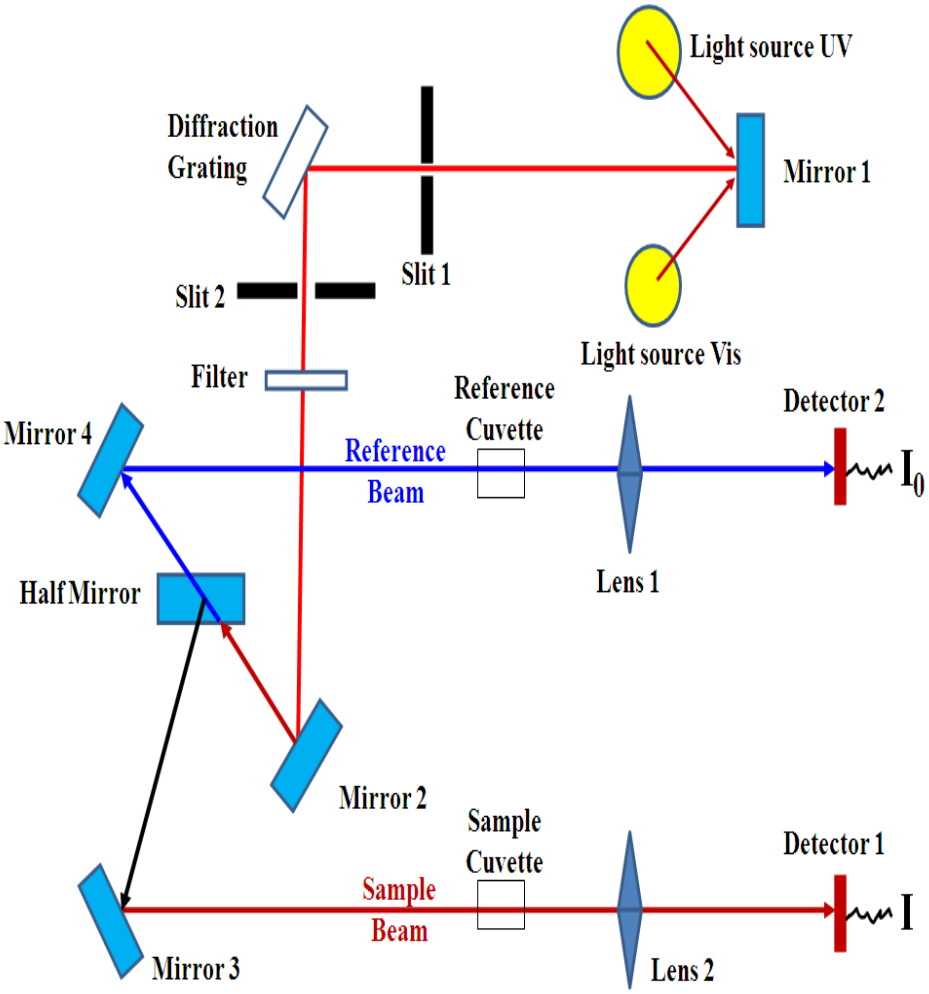

Figure 2.7: Schematic Diagram of UV-Visible Spectroscopy

The exact value of absorption is known as "molar absorptivity" and is mainly useful in the comparison of the spectra of dissimilar compounds and find out the comparative strength of light absorbing functions. A schematic diagram of UV-visible spectrometer with all necessary components is shown in Figure 2.6. In the present studies absorption spectra of UV Visible were recorded using a Hitachi U-3300 UV Vis Spectrophotometer.

[b] Determination of Optical Band Gap Energy

The UV-visible spectral data is used for the determination of the energy band gap (i.e. the gap between the conduction band and the valence band) in case of various polymers by using the relation given by Zaki, (2008).

$$\alpha(v) = B\left(hv - E_g\right)^n / hv \qquad 2.8$$

where hν is the energy of photon of the incident light, Eg is the value of the optical band gap energy between the valence band and the conduction band and the value of n describes the direct or indirect electronic transition during the absorption process in the K space. In particular, n is 1/2, 3/2, 2 and 3 for direct allowed, direct forbidden, indirect allowed and indirect forbidden transitions, respectively.

The dependency of factor B is on the transition probability and does not change within the optical frequency range. So factor B can be understood to be constant within that frequency range. The calculation of the value of optical band gap is done by plotting $(\alpha h\nu)^{1/n}$ against (hν). The materials which are amorphous, n = 2 is a fit case for indirect transition; n= ½ is a reasonable fit for a direct transition.

In the present research work, the values of optical band gap were calculated by plotting $(\alpha h\nu)^{1/2}$ and $(\alpha h\nu)^{2}$ as a function of the photon energy (hν) respectively, taking into account the linear portion of the fundamental absorption edge of the UV-visible spectra

[c] Determination of Number of Carbon Atoms

The number of carbon atoms (N) per conjugation length for a linear structure (Ramola et al., 2008) is given by

$$N = {2\pi\beta}/{E_g} \qquad 2.9$$

Where 2β gives the band structure energy of a pair of adjacent Π sites. The value of β is taken to be -2.9 eV as it is associated with π-π* optical transition in the –C=C- structure.

From the Robertson relation cluster size can be calculated by Nouh et al. (2003) and the number of carbon atoms per cluster can be calculated by using the following relation (Gupta et al., 2000):

$$E_g = \frac{34.3}{\sqrt{N}}\ eV \qquad 2.10$$

2.7.3 Fourier Transforms Infrared Spectroscopy (FTIR)

This spectroscopy is a main tool for finding the presence of functional group in organic materials. FTIR is an easy method to identify the presence of certain functional groups in organic molecule. This technique can also be used for the collection of absorption bands and for the detection of pure composites or the presence of specific impurities. The spectrometer of FTIR simultaneously records data in a broad range of spectra. So this spectrometer gives a significant advantage over a dispersive spectrometer which records intensity over a narrow range of wavelengths at a time. In FTIR spectroscopy, the term Fourier transform spectroscopy reflects the fact that in all these techniques, raw data is converted into the actual spectrum by Fourier transform and in many of the cases in optics involving interferometers is based on the Wiener-Khinchin theorem. This theorem states that the power spectral density of a wide-sense-stationary random process is the Fourier transform of the corresponding autocorrelation function.

In FTIR-spectroscopy, the interference signal of a two-beam interferometer is measured. The beam splitter divides the collimated IR beam into two beams. One of the beams is transmitted to the moving mirror and other reflected in the fixed mirror. These two IR beams are then reflected back to the beam splitter by the mirrors. The reflected IR beams superimpose and interfere constructively or destructively depending on the wavelength of the light and the optical path difference between the mirrors. These IR beams recombined and then go through the sample (or the reference) and arrives at the detector. Helium-Neon laser controls the position and movement of the movable mirror. The optical schematic of an FTIR Spectrometer is shown in Figure 2.7. The Resolution of FTIR spectrometer plays an important role and depends generally by the highest value of path difference between the interferometer wings.

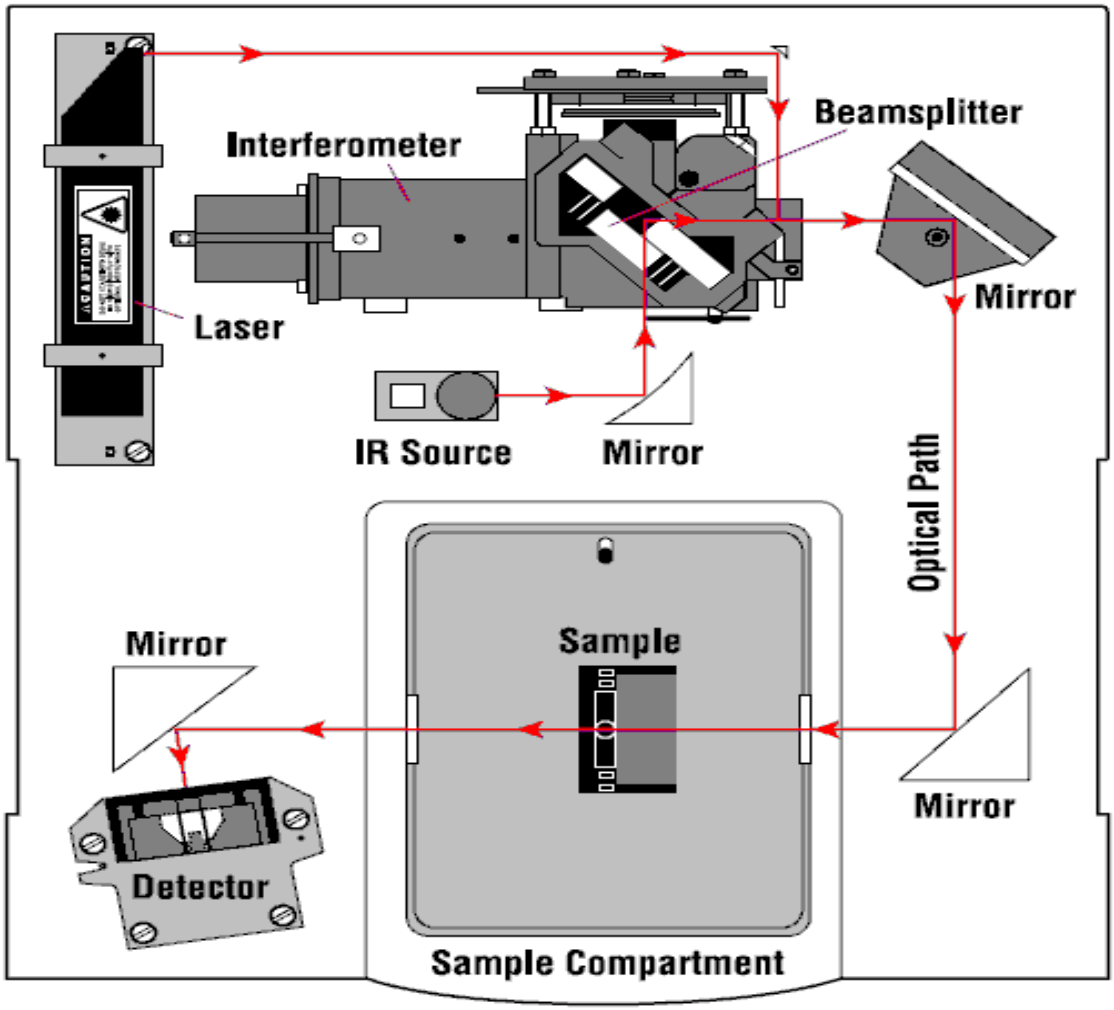

Figure 2.8: Optical Schematic of a FTIR Spectrometer

The optical arrangement of the interferometer during shifting of mirrors is very important. Hence shifting the mirror (so called scanner) have an effect on the efficiency of the device which is very crucial. In FTIR spectroscopy, the study is done on the effect of interaction of radiation with chemical materials. In the interaction of electromagnetic radiation with a sample (solid or liquid), it has been found that some particular frequencies of the radiation are absorbed by the molecules of the substance guiding to the molecular vibrations. The modern IR spectrometers are producing good results and these days considered to be superior to the dispersive IR spectrometers. The infrared spectrum is

obtained by FTIR (Fourier Transform Infrared). In this procedure an interferogram of a sample signal is collected by using an interferometer, then doing a Fourier Transform on the interferogram to get the spectrum.

An FTIR Spectrometer is a type of equipment that produces the infrared spectrum. This infrared spectrum is obtained by collecting and digitizing the interferogram and then performing the FT function. An interferometer is the most important part of Fourier Transform Infrared (FTIR) spectroscopy. This interferometer divides a beam of light into two beams and then recombines them such that these recombined beams produce an interference pattern which depends on wavelength. The interferometer which commonly used is the Michelson interferometer. The Michelson interferometer is the heart of all modern FT-IR spectrometers. In the present work, the FTIR measurements on the films were carried out by using Thermo Nicolet NEXUS 670 FTIR system.

2.7.4 Scanning Electron Microscopy

This is one of the most useful and versatile tool for the investigation of surface topography, micro structural feature etc. It provides a pictorial display of the surface layer with a high depth of a focus greater than that possible in electron microscope thus providing details than that by the replica technique.

In scanning electron microscope (SEM), a fine and focused beam of electrons takes the picture of a sample by scanning it in a raster scan pattern. When electrons interact with the atoms of the sample, after the interaction electrons give an idea about the properties of the sample like surface topography, composition and electrical conductivity etc. In most of the applications, image is produced by the data which has been taken over a selected area of the surface of the sample. This is a two-dimensional image that displays spatial variations in these properties. The range of selected areas remains approximately 1 cm to 5 μ in width can be imaged in a scanning mode using conventional SEM techniques (magnification ranging

from 20X to approximately 30,000X, spatial resolution of 50 to 100 nm). Some of the selected point locations on the materials or sample can also be studies by SEM technique. The crystalline structure, crystal orientations and chemical compositions (using EDS) can be found out by this approach which is able to do qualitatively and semi-quantitatively analysis.

When electrons are incident on the solid sample, in the interaction of electron-sample, accelerated electrons have significant amounts of kinetic energy. This energy is dissipated as a variety of signal produced by the interaction of electrons and sample. These signals produced by electron-sample interaction include secondary electrons (that produce SEM images), backscattered electrons, diffracted backscattered electrons, photons, visible light and heat. Images of the sample are commonly taken by the secondary electrons and backscattered electrons. These secondary electrons are mostly used to see the morphology and topography of sample's surface and backscattered electrons are for demonstrating contrasts in composition in multiphase samples.

X-ray is produced, when high speeding electrons collide with electrons in discrete orbitals (shells) of atoms in the materials or sample. This is inelastic collision. The excited electrons make a transition to the lower energy states and produced X-rays. These X-rays are of a fixed wavelength and called characteristic X-rays. Thus, excited electrons in elements produced characteristic X-rays. Scanning Electron Microscope (SEM) is a non-destructive technique; i.e. X-rays produced by electron-sample interactions do not harm the sample. So there is no volume loss of the materials and it is possible to use the same materials repeatedly. Schematic diagram of SEM is shown in Figure 2.8. For doing the analysis in SEM, there are some special preparations which need to be done to the sample because SEM utilizes vacuum conditions and uses electrons to form an image. Water would vaporize in vacuum so all water must be removed from the sample. All metals samples can be used without any preparation because metals are conductive.

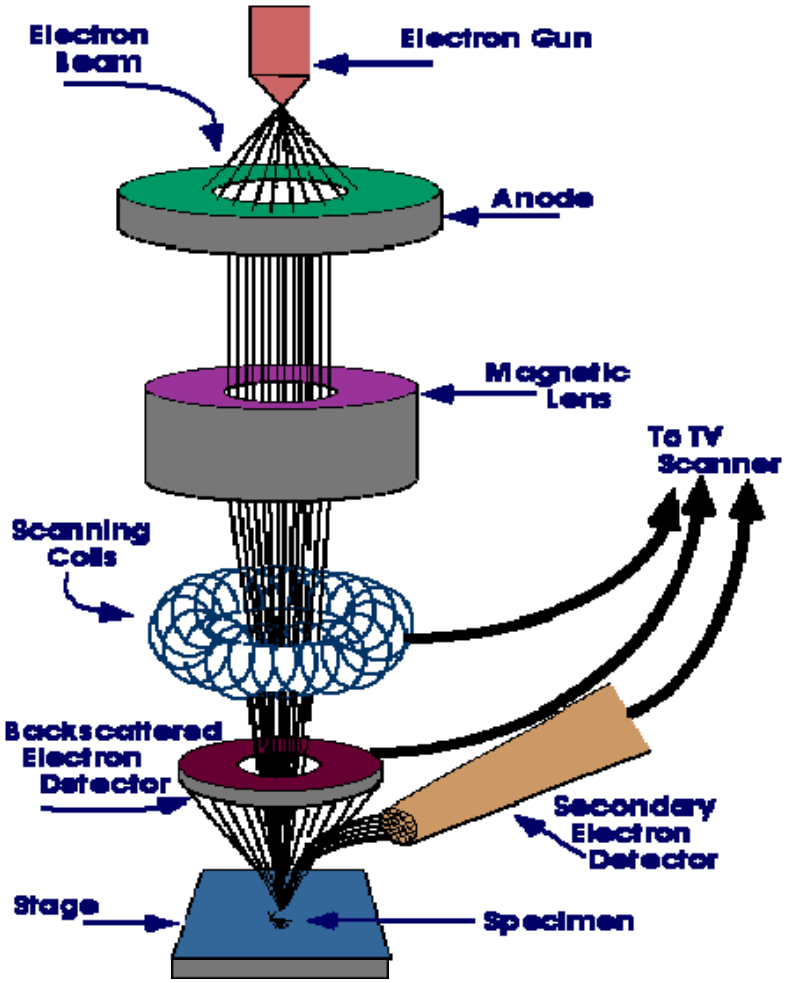

Figure 2.9: Schematic of Working Principle of SEM

The samples of all non-metals need some preparations before being used. These samples of non-metals need to be made conductive by covering the sample with a thin layer of conductive material. This is done by using a device called a "sputter coater." In the present studies SEM images were obtained by using JEOL (JSM-6490 LV) scanning electron microscope.

[REFRENCES]

Ko-no, K., 1997. Synthesis and characterization of microparticles reversed micelles. In: Esumi, K., Veno, M. (Eds.). Structure-Performance Relationship in Surfactant, S. S. Series, 70. Marcel Dekker,

Cizeron, J., Pileni, M.P., 1995. Solid solution of CdyZn12yS nano sized particles made in reverse micelles. J. Phys. Chem. 99, 17410–17416.

Herron, N., Wang, Y., Eckert, H., 1990. Synthesis and characterization of surface-capped size-quantised CdS clusters. Chemical control of cluster size. J. Am. Chem. Soc. 112, 1322–1326.

Bowen Katari, J.E., Colvin, V.L., Alivisatos, A.P., 1994. X-ray photoelectron spectroscopy of the CdSe nanocrystals with applications to studies of the nanocrystals surface. J.Phys. Chem. 98, 4109–4117.

Giustini, M., Palazzo, G., Colafemmina, G., Della Monica, M., Giomini, M., Ceglie, A., 1996. Microstructure and dynamics of the water-in-oil CTAB/n-pentanol/n-hexane/water micro émulsion: a spectroscopic and conductivity study. J. Phys. Chem. 100, 3190.

Brus, L.E., 1984. J. Chem. Phys. 80, 4403–4409.

Rong,M.Z.,Zhang,M.Q., Liang, H.C., Zeng, H.M.,2003.Surface modification and particles size distribution control in nano-CdS/polystyrene composite film. Chem. Phys.286, 267–276.

Singh N.L, Shah S., Qureshi A., Tripathi A., Singh F., Awasthi D. K., Raole P.M., 2011. Effect of ion beam irradiation on metal particles doped polymer composites. Bull. Mater. Sci. 34(1), 81-88

Kanjilal, D, Chopra, S, Narayanan, M. M, Iyer, I. S, Jha, V, Joshi, R, Datta, S. K. 1993. Testing and operation of the 15UD Pelletron at NSC. Nucl Instr. Methods A 328:97-100

NSC school on accelerator physics, 1989.

Ziegler, J. F, Biersack, J. P, Ziegler, M. D. 2008. The Stopping and Range of Ions in Matter. Lulu Press Co.

Scherrer, P. 1918. Gottinger Nachrichten Gesell.2: 98.

Patterson, A. L. 1939. The Scherrer Formula for X-ray Particle Size Détermination. Phys. Rev. 56:978-982.

Ramola R. C, Chandra, S, Negi, A, Rana, J. M. S, Annapoorni, S, Sonkawade, R. G, Kulriya, P. K. Srivastava, A. 2009. Study of optical band gap, carbonaceous clusters and structuring in CR-39 and PET polymers irradiated by 100 MeV O^{7+} ions. Physica B: Condensed Matter 404:26-30.

Zaki, M. F. 2008. Gamma-induced modification on optical band gap of CR-39 SSNTD. J. Phys. D: Appl. Phys. 41:175404.

Nouh, S. A, Abdel-Salamb, M. H, Morsy, A. A. 2003. Electrical, optical and structural behaviour of fast neutron-irradiation-induced CR-39 SSNTD. Radiat. Meas. 37:25-29.

Gupta S, Choudhary D, Sarma A, 2000. Study of carbonaceous clusters in irradiated polycarbonate with UV-vis spectroscopy. J. Polym. Sci., Part B: Polym. Phys. 38:1589-1594.

S.K. Kulkarni, U. Winkler, N. Deshmukh, P.H. Borse, R. Fink, E. Umbach, 2001. Appl. Surf. Sci. 169-170, 438-446.

D.J. Jovanović, Ivana Lj.Validžić, I.A. Janković, N. Bibić, J.M. Nedeljković, 2007. Materials Letters 61, 4396–4399.

CHAPTER 3

SHI Induced Modifications in Nano-CdS/ polystyrene Composite Films

3.1 Introduction

The nanoparticles of cadmium sulphide (CdS) of size of 50-60 nm were prepared by one of the best chemical method i.e. micro-emulsion method. Ni and Cu metals are doped in the polystyrene/CdS (PS/CdS) nanocomposites. The pristine and metal doped nanocomposite films were irradiated with 60 MeV Ni^{5+} ions. The result of doping of Cu and Ni metals and swift heavy ion irradiation at different fluence was discussed for observing the change in the structural, optical and chemical properties of PS/CdS nanocomposite films. In XRD spectra of irradiated polystyrene (PS), the fall in the amorphous nature has been observed at higher fluence of radiation. In the UV-visible studies, shifting of the absorption peaks towards the visible region in irradiated and doped nanocomposites sample was found. The absorption peak shifting in case of Cu and Ni doped nanocomposites was more prominent than those of pure polystyrene (PS) and PS/CdS nanocomposite films. The increase in absorption was attributed to the creation of a conjugated system of bonds. The fall in optical band gap energy in case of Ni metal doped PS/CdS sample was found much while in case of Cu doped PS/CdS sample it was less and the ion irradiation further decreased the optical band gap energy value. In FTIR pattern of Cu and Ni metal doped PS/CdS composites film the absorption peak of Cd-S bond was noticed at 405 cm^{-1}. There is a dip in the intensity of polystyrene (PS) absorption lines in all SHI irradiated samples.

Nanocomposites polymer signify a growing field in nanoscience and nanotechnology. The small size of metal or semiconductors nano- particles as compare to the wavelength of visible

light gives the nanocomposites polymer an innovative perception for optical materials. Doping of the suitable nanoparticles in the polymer matrix can modified the optical properties of nanocomposites and properties also can be modified by swift heavy ions. The optical, structural, chemical, magnetic, electrical and other properties of the polymers and polymer nanocomposites can be change by the controlled beam of SHI (Tombrello et al., 1994; Steckenreiter et al., 1997; Kulshrestha et al., 2006; Kumar et al., 2006; Vijay et al, 2006). The interaction of the incoming swift heavy ions with the target material can be occurred by two methods i.e. elastic and inelastic. In elastic collision, the energetic ions interact with nuclei of the atoms and in inelastic collision the energetic ions interact with electrons of the target atoms depending upon the energy of the arriving ion. At higher energy of the order of 10 MeV the inelastic collision dominates and responsible for modifications in optical, structural and chemical properties (Kanjilal, 2001). A large amount of energy of SHI is lost in process of ionizing atoms and exciting electrons. Ionization of atom causes bond cleavages, degradation, free radical formation and cross- linking of polymeric chains and formation of unsaturated bonds (Fink et al., 1996; Picq et al., 1998). There are various parameters of SHI like mass, charge state, energy and dose of the impinging ions which can modify the materials. Linear energy transfer (LET) value of incoming ion can defined these parameter (Lee et al., 1999). The alteration in properties also depends upon the type (molecular arrangement and stuffing of polymeric chains etc) of target polymers (Singh et al., 2013, Balanzat et al., 1994).

Metal doped PS/CdS followed by irradiation with SHI may give extreme alteration in its properties like structural, optical and chemical etc. The small size and strong confinement properties make these metal doped polymer nanocomposites valuable for wide applications such as light-emitting diodes (Tesster et al., 2002), lasers (Artemyev et al., 2001) and devices (Zhu et al., 2005). Zhu et al, 2005 reported that CdS doped polymers are one of the highly studied

polymers due to their size dependent properties. The emission conduct of nanocomposites changes with the change in the size, which can be restricted during the synthesis by surface capping molecules and by controlling the temperature (Alivisatos et al., 1996). In the literature, it has been reported that CdS nanoparticles can be synthesis by various methods (Peng et al., 2001; Gorelikov et al., 2004; Peng et al., 1997). There are various methods available for the synthesis of nanocomposites such as microemulsion, sol-gel template, chemical aerosol flow synthesis, ion beam synthesis, ultrasonic's irradiation in an aqueous solution, two phase approach and in situ micelle-template-interface reaction route. In all these methods, microemulsion is very efficient technique for controlling the size of nanoparticles. The synthesis of nanocomposites has been done by Micro- emulsion method. The inclusion of CdS nanoparticles in the polymer matrix has been reported in literature (Farmer et al., 2001; Wu et al., 2004; Han et al., 2005). The doping of nanoparticles in the polymer with varying concentration has been found in the literature (Chen et al., 2007; Rong et al., 2003). But, few data is available in the literature for the modification in the properties like optical, structural and chemical by swift heavy ions beam irradiation.

To control the energy band gap and crystallite size of nanocomposites polymer, SHI irradiation is very effective tool. In SHI irradiation the desired beam of ions can be produced by controlling the beam parameters like current, energy, fluence etc. Further, the energy band gap and crystallite size can also be restricted by doping of nanoparticles with varying concentration. The main aim of the present research work in this chapter is to discuss the optical properties for the change in optical band gap energy by the two methods: doping with metals (Ni and Cu) and ion beam treatment (irradiation). In addition to it the impact of ion beam irradiation on chemical and structural properties are also discussed.

3.2 Synthesis of CdS/PS Nanocomposites Film

3.2.1 Materials

Polystyrene (PS) is a polymer which is transparent, colour less and used widely for many applications. It is less expensive and available commercially in many shapes. Polystyrene (PS) (density 1.06 g/mL) of average molecular weight 35,000 and all other chemicals/solvents were purchased from Sigma Aldrich. All the chemicals were used as- recieved without any further treatment.

3.2.2 Preparation of CdS/PS Nanocomposites Film

The nanoparticles of cadmium sulfide (CdS) were synthesized by the reaction of sodium sulfide and cadmium nitrate in water-in-oil micro emulsion system. In this synthesis method surfactant plays a crucial role so for that purpose cyclohexane was used. The nanoparticles of cadmium sulfide (CdS) of the size of 50-60 nm were synthesized. The purpose is to disperse semiconducting nanoparticles evenly in polymer and to make nanocomposites film. In this work the cadmium sulfide (CdS) nanoparticles were dispersed in polystyrene (PS) matrix. In the procedure the first step was that polymer was dissolved in chloroform and in the second step, 3 ml of synthesized CdS nanoparticles were added to the polymer solution and dispersed by ultrasonic agitation to make sure a uniform arrangement. Now after this process uniform mixture is obtained, the mixture was poured on to a clean Petri dish. The solvent was evaporated at room temperature (25^0C) to get thin films (thickness ~ 20 μm) of polymer composites which were then dried in vacuum oven at 30° C (Rong et al, 2003; Singh et al., 2011).

3.3 Scanning Electron Microscope (SEM)

In scanning electron microscope (SEM), a fine and focused beam of electrons takes the picture of a sample by scanning it in a raster scan pattern. The interaction of electrons with the atoms gives valuable information about the surface topography. The SEM image of synthesized CdS nano particles is shown in Fig. 3.1.The white dots appearing in the image suggesting the formation of CdS nanoparticles. The CdS nanoparticles of 50-60 nm size can be seen in this SEM image.

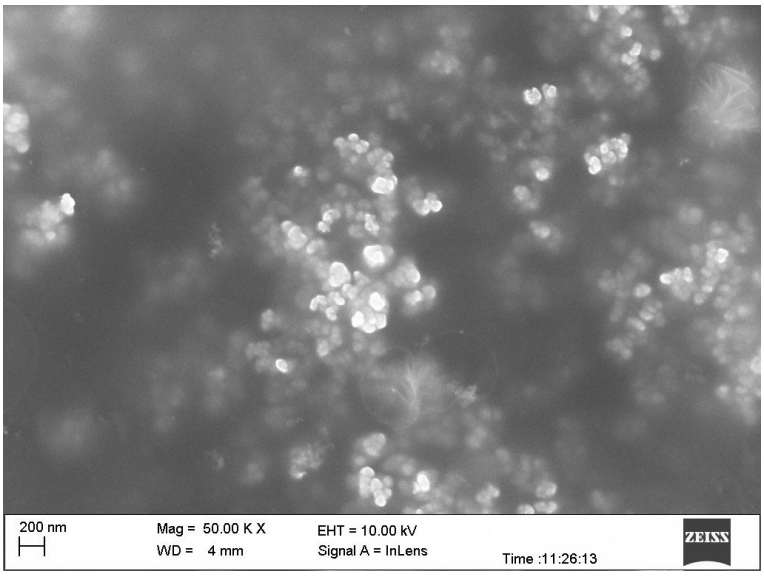

Figure 3.1: SEM image of Synthesized CdS nano particles

3.4 Irradiation

The nanocomposite films of the size (1.5 cm × 1.5 cm) were prepared for swift ions irradiation. These small specimens of nanocomposites were mounted on a vertical vacuum shield ladder and irradiated in general purpose scattering chamber (GPSC) with 60 MeV Ni^{5+} ions beam from 15 UD Pelletron accelerator at Inter University Accelerator Centre (IUAC), New Delhi,

India to the fluences of 10^8 and 10^{11} ions/ cm^2. For minimizing thermal decomposition, the beam current was kept ~ 0.5 pnA. UV–visible, FTIR and X-ray diffraction were used for the study of optical, chemical and structural properties of pristine and irradiated samples. UV–visible spectroscopy for find out the band gap energy was carried out in the wavelength range 250–800 nm using U- 3300 Hitachi system. Preliminary structural studies were carried out by using Bruker AXS system with Cu-K_α radiation (1.54 Å) for a wide range of Bragg angles 2θ ($5 \leq 2\theta \leq 50$). Infrared measurements were performed in transmission mode using Nicolet Nexus 670 FTIR spectrometer.

3.5 SRIM (Stopping and Range of ions in Materials) calculations

Energy losses can be calculated by SRIM calculations. As we know that two type of losses (electronic and nuclear) are found in the interaction of SHI with the materials. The electronic energy loss (S_e), nuclear energy loss (S_n) and projected range of Ni ions in target polymer and polymer nano-composites were calculated by using SRIM- 2008 code (Ziegler, 2010). All these calculated values are mentioned in Table 3.1. The S_e values for our target samples are 100 times larger than those of their S_n values ensuring nuclear energy loss to be nearly negligible. In all the samples the nuclear energy losses are very less as compare to electronic losses. The values of projected range are almost equal to our sample thickness (20 μm), hence very little probability is there for ion implantation.

Table 3.1. SRIM calculated Se, Sn values and projected range of 60 MeV Ni ion beams for Target samples

Target Material	S_e (eV/ Å)	S_n (eV/ Å)	Projected range (μm)
Polystyrene (PS)	5.20×10^2	12.1	19.71
PS\CdS:Cu	5.94×10^2	16.7	17.24
PS\CdS:Ni	6.03×10^2	16.9	17.56

3.6 Results and discussion

3.6.1 X-ray diffraction

XRD characterization had been carried out with the narrow objectives of investigation to variation of intensity of the XRD peaks with different ion fluence to see loss of crystallinity with irradiation and in this work no effort has been made in a direction to find the whole structure of the polymer nanocomposite films. The structural properties were studied by X-ray power diffraction (XRD). The analysis of all XRD spectra was carried out with a Philip analytical X-ray B.V. Diffractometer, using graphite-monochromatized Cu Kα radiation (λ = 1.54178 A°) at IUAC New Delhi. These nanocomposite samples are irradiated by 60 MeV Ni^{5+} ions beam under the high vacuum of $4^{\times}10^{-6}$ Torr to the fluence of 10^8 to 10^{11}ions/cm^2. The properties of the nanocomposites materials can be modified in an organize way by controlling the parameter like energy and ion fluence of ion beam radiation. When ionizing radiation interact with the material it causes degradation and cross linking in polymers. A scanning rate of 2° per minute was applied to record the pattern in the 2θ range between 5° and 80°. Cu and Ni metal doped polystyrene nanocomposite films of 20 microns thick are irradiated by 60 MeV Ni^{5+} ions beam.

In Figure 3.2, the XRD spectra of virgin and irradiated samples of polystyrene (PS) are shown. The polystyrene (PS) film was irradiated by SHI at fluence of 10^8 and 10^{11} ions/cm^2. The amorphous nature of polystyrene (PS) can be verified in X-ray diffraction spectra of virgin PS sample. The X-ray diffraction pattern of virgin polystyrene (PS) sample conforms to the XRD spectra reported by Singh and Samra, 2008. The major diffraction peaks with maximum intensity of virgin polystyrene (PS) was found at $2\theta = 19.76^{\circ}$. For all irradiated samples no phase change has been found (Guzman et al., 1985) as their XRD peak positions do not change. The peak width of the X-ray diffraction pattern of polystyrene (PS) increases at a fluence of 10^8 ions/ cm^2 where as successive irradiation at still higher fluence (10^{11} ions/ cm^2) causes decrease in peak width. This indicates the alignment of the polymeric chains in a regular pattern and hence amorphous nature is decreased at higher fluences. Figure 3.3 shows the X-ray diffraction patterns of as-prepared Ni doped PS/ CdS and Cu doped PS/ CdS composite films. All the intensity X-ray diffraction peaks indicates the cubic structure of CdS crystals by comparing with the literature (Wu et al, 2004).

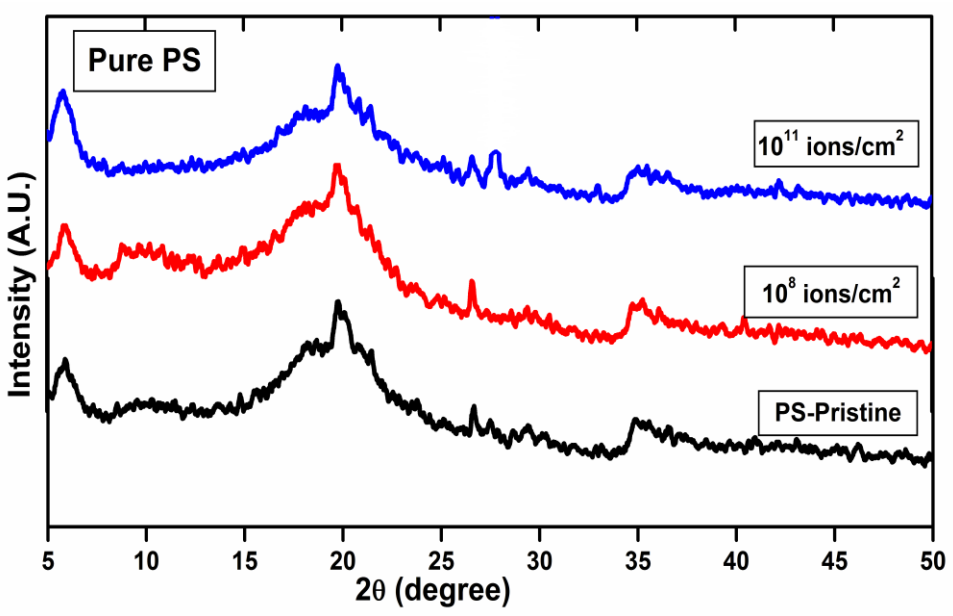

Figure 3.2: X- ray diffraction patterns of pristine and Ni^{5+} irradiated polystyrene polymer films

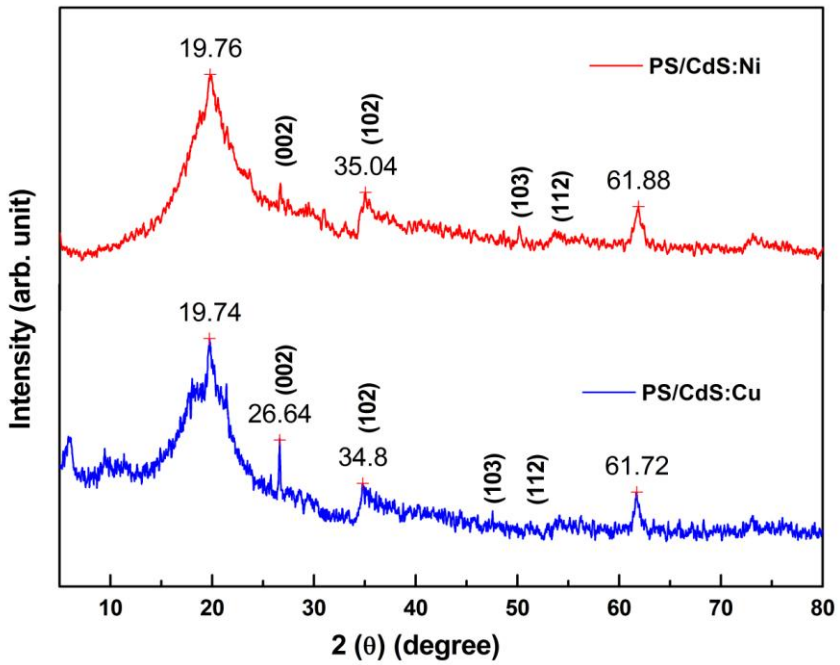

Figure 3.3: X- ray diffraction patterns of PS/ CdS: Cu and PS/ CdS: Ni nanocomposites

X-ray diffrcation spectra of virgin and irrdaiated Ni doped PS/CdS and Cu doped PS/CdS nanocomposite films are shown in Figure 3.4 and 3.5 respectively. The diffraction pattern of pristine PS/CdS: Ni and PS/CdS: Cu nanocomposite films peak at 2θ~19.74 and 2θ~19.76 show the peak with maximum intensity and shows the amorphus nature. When these nanocomposite films are irradiated with 60 MeV Ni^{5+} ions dose of fluence of 10^{8} to 10^{11} ions/cm^{2} , the intensity of the diffracton peak of Cu doped PS/CdS composites increases at a dose of 10^{10} ions/cm^{2} and further decraese at the ions dose of 10^{11} ions/cm^{2} led to disordering characters. Broadening of XRD peak at higher dose of ions noticed in all nanocomposites polymer films.

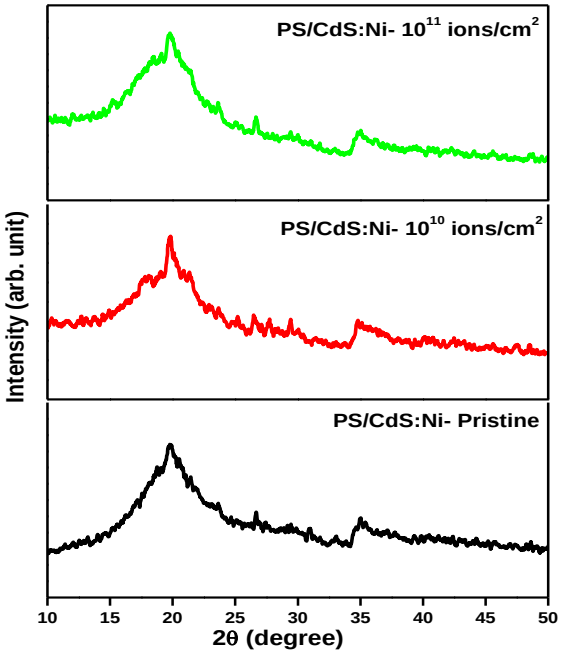

Figure 3.4: X- ray diffraction patterns of Ni^{5+} irradiated PS/ CdS: Ni nanocomposites

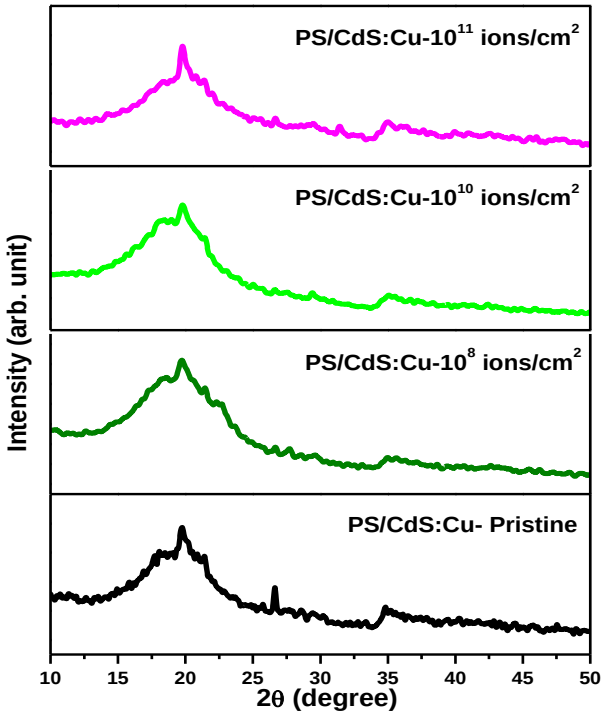

Figure 3.5: X- ray diffraction patterns of Ni^{5+} irradiated PS/ CdS: Cu nanocomposite

A noticeable shift in the X-ray diffraction peak by SHI irradiation was found. This changes in X-ray diffraction peak are due to disorderning of original strcture of Polystyrene. The crystallite size of irradited nanocomposite films was found to be increased which may due to cross-linking in polymers.

Table 3.2: Bragg Angle and Crystal Size of Pristine and Irradiated Nanocomposite Polymer Films

Sample	Fluence (ions/cm^2)	Bragg angle (2θ)	C.S. L (A^0)
PS	Pristine	19.76	20
	10^8	19.72	20
	10^{11}	19.72	24
PS/CdS: Cu	Pristine	19.74	19
	10^8	19.72	20
	10^{11}	19.85	20
PS/CdS: Ni	Pristine	19.76	19
	10^{10}	19.72	20
	10^{11}	19.72	20

3.6.2 UV-visible spectroscopy

In the prsesnt work, the attention is given on the optical properties of Ni and Cu doped PS/CdS nanocomposite films with the idea of possible applications as bio sensors, light emiiting diode,s optical data storage. For the biosensors application viewpoint the investigation of the optical properties of the synthesized particles is most important feature. Nanocomposites with the doping of metals are focus of latest concern because of their extraordinary magnetic, optical, electronic properties, which often different from their bulk properties. The reasons for modification in these properties are higher surface to volume ratio, confinement of electronic and vibrational excitation and quantum size effect [S. J. Ahmadi et al 2004].

The optical properties become very important when the particle size is small. At the nnaoscale level the energy levels are discrete and band gap changes. Due to that band gap energy the colours, wavelength etc change and cause the optical properties. In today's time, the optical properties of these small size dimensions systems have attracted growing interest in both the applied science and technology. Similar to various other properties of nanoparticles, interaction with electromagnetic radiation depends on the size of the particles and thus allows one, for example, to engineer tailor-made materials for new optical applications.

UV- visible spectra of virgin and irradiated films of pure polystyrene (PS), Cu doped PS/ CdS and Ni doped PS/ CdS are shown in Figs. 3.1, 3.2 and 3.3 respectively. In Fig 3.1-3.3, the spectra of pure PS, Cu doped PS/ CdS and Ni doped PS/ CdS composite films reveals the shift of absorption peak from ultraviolet to visible wavelength region. This shifting of absorption peak towards the visible region is because of the development of extended system of conjugated bonds (Singh et al, 2007; El-Badry et al., 2009). The absorption bands are associated with π- π^* electronic transitions (Singh et al, 2007). The values of optical energy band gap of the virgin and irradiated nanocomposite films were calculated by using Tauc's expression (Tauc et al., 1996) as per following equation

$$(\alpha h\nu) = B\,(h\nu - E_g)^{1/2} \qquad (1)$$

Here α is the absorption coefficient, $h\nu$ is the photon energy, B is band tailing parameter (Metwally et al., 1901) and E_g is the value of energy band gap. The E_g values of the films were calculated by the extrapolation of the plot of $(\alpha h\nu)^2$ versus $(h\nu)$ to the energy axis. The band gap plots of pure PS, Cu doped PS/ CdS and Ni doped PS/ CdS are shown in fig 3.4, 3.5 and 3.6 respectively. The calculated values of E_g are tabulated in Table 2.

Table 3.3: Calculated values of band gap energy (Eg) and number of carbon hexagon rings per conjugation length (N) for PS, PS/ CdS:Cu and PS/ CdS:Ni nanocomposite films

Sample	Fluence (ions/cm^2)	E_g (eV)	Value of N
PS	Pristine	4.35	62
	10^8	2.80	150
	10^{11}	2.34	215
PS\CdS:Cu	Pristine	3.95	75
	10^8	3.60	91
	10^{11}	2.73	158
PS\CdS:Ni	Pristine	3.42	100
	10^8	2.99	131
	10^{11}	2.66	166

The value of energy band gap of pristine polystyrene (PS) is very close to the value reported by Singh and Samra, 2008; Singh et al, 2007. There is fall in the band gap (E_g) value of composites with doping of metal ion as well as with ion irradiation. The band gap (E_g) of pure polystyrene (PS) is found to be 4.35 eV and further on the doping of Cu and Ni to PS/CdS composites, band gap decreases 3.95 and 3.42 eV respectively. Swift heavy irradiation (SHI) decreases the band gap value further to quite a drastic level. There is 35%, decrease in band gap value from their pristine value for irradiated samples of PS at a fluence of 10^8 ions/cm^2, whereas this decrease is 46%, at a fluence of 10^{11} ions/cm^2. There is 9% and 12% decrease in band gap from their pristine values for irradiated samples of Cu doped PS/CdS and Ni doped PS/CdS films respectively at a fluence of 10^8 ions/cm^2, whereas this decrease is 31% and 22% at a fluence of

10^{11} ions/ cm^2. It has been reported in the literature that this fall in band gap energy may be due to carbon enriched regions formed in polymers during SHI irradiation (Fink et al., 1996; Phukan et al., 2003).

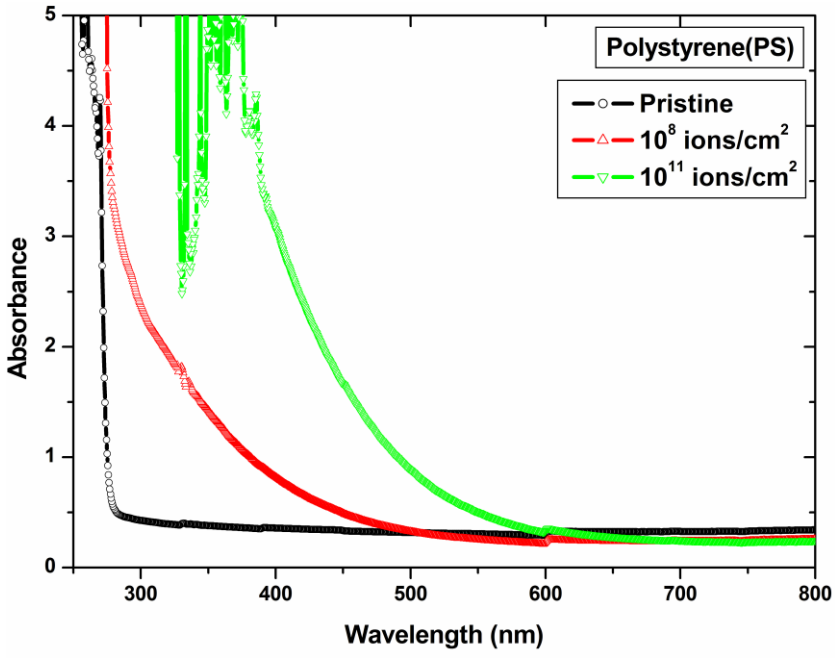

Figure 3.6: UV-visible spectra of pristine and Ni^{5+} irradiated polystyrene (PS) polymer films

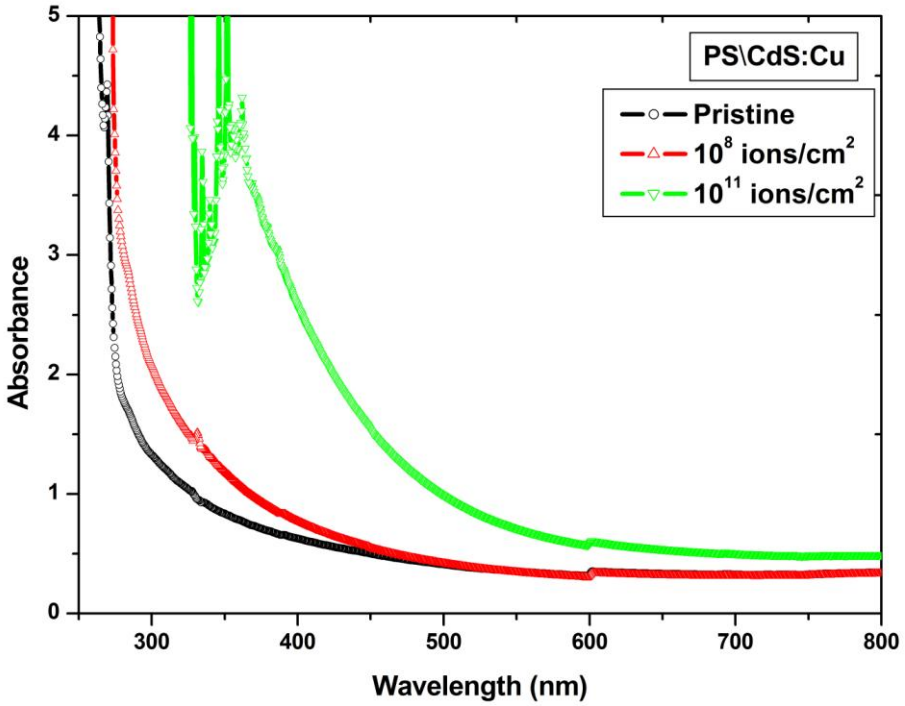

Figure 3.7: UV-visible spectra of pristine and Ni^{5+} irradiated PS/ CdS: Cu films

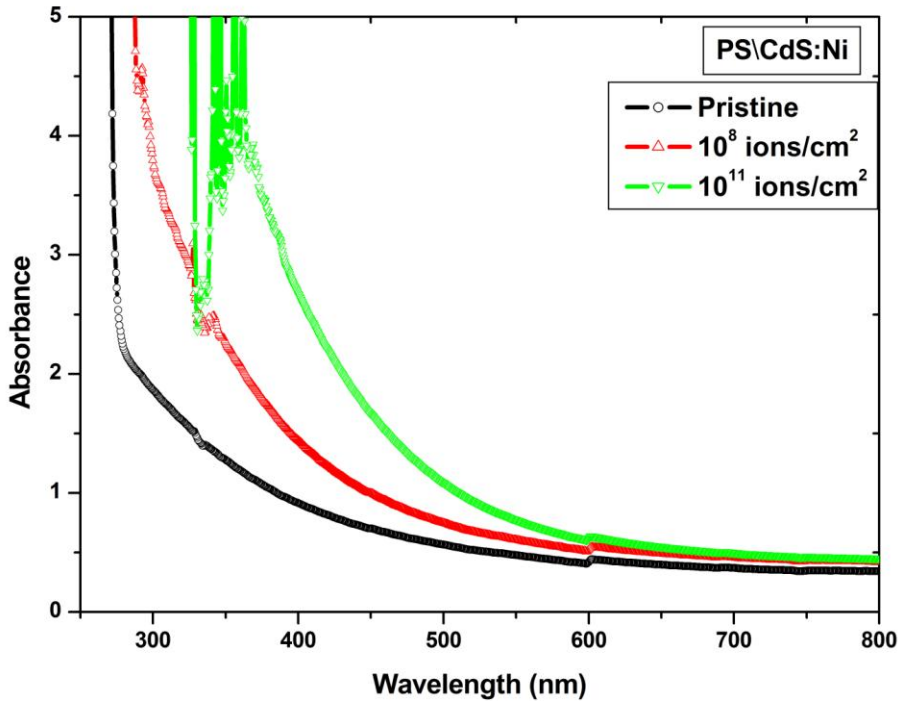

Figure 3.8: UV-visible spectra of pristine and Ni^{5+} irradiated PS/ CdS: Ni films

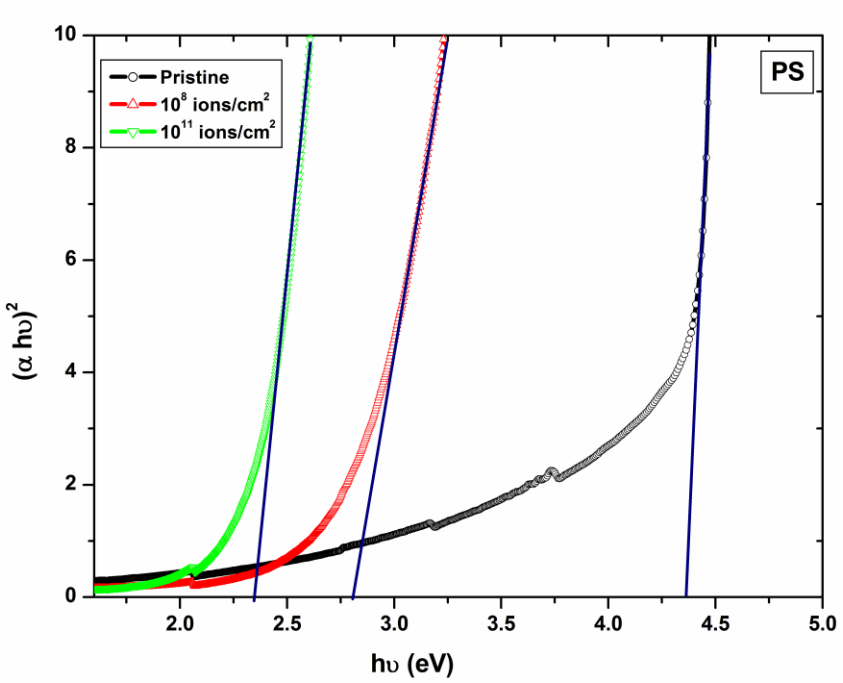

Figure 3.9: Band gap spectra of pristine and Ni^{5+} irradiated polystyrene (PS) polymer films

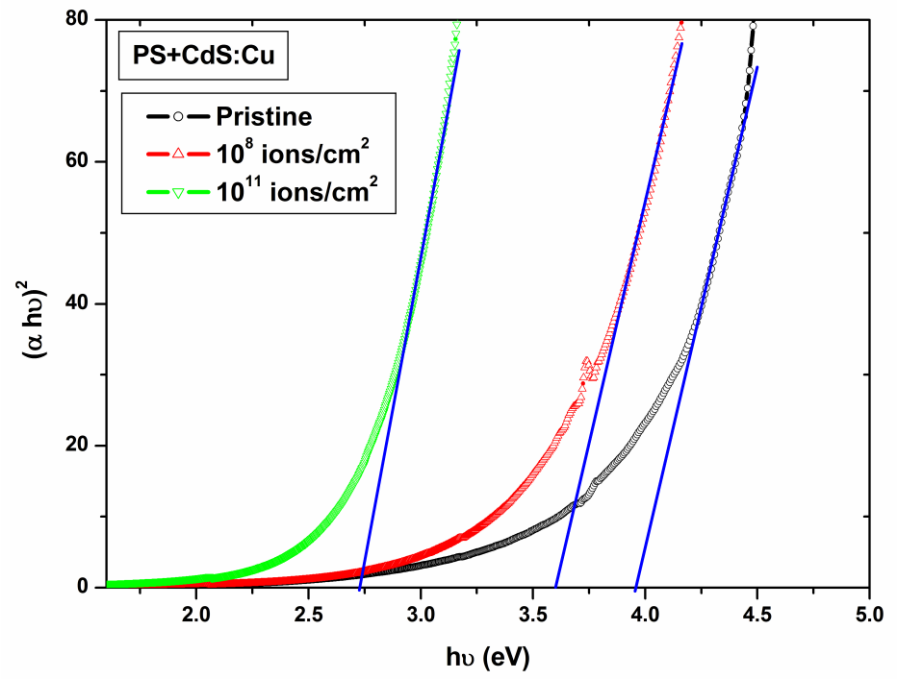

Figure 3.10: Band gap spectra of pristine and Ni^{5+} irradiated PS/ CdS: Cu films

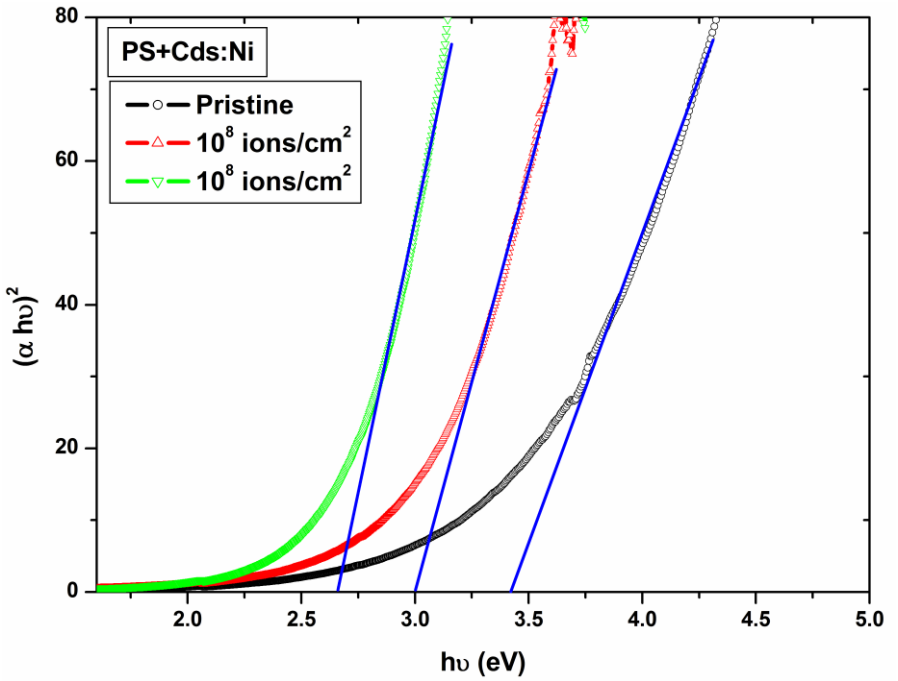

Figure 3.11: Band gap spectra of pristine and Ni^{5+} irradiated PS/ CdS: Ni films

No. of carbon hexagon rings per conjugation length (N) were calculated from the modified Robertson relation (Kumar et al., 2011) using following equation

$$E_g \approx (34.3/N^{1/2}) \quad (2)$$

The calculated values of N are tabulated in Table 3.3. The values of N are increasing with doping and ion irradiation as well as with higher ion fluence.

3.6.2 FTIR spectroscopy

The FTIR spectra of pristine polystyrene (PS) in Fig. 3.12 conforms to the spectra reported by Evelyn et al, 1999. The FTIR spectrum shows the lines due to aromatic ring C-H stretching vibrations at 3081, 3060 and 3026 cm^{-1}, C-H stretch vibrations in CH_2 group at 2922 and 2851 cm^{-1}, the aromatic ring vibrations at 1602 and 1493 cm^{-1} and the lines due to the CH_2

deformation vibrations at 1452 cm^{-1} (Kondyurin et al, 2008; 2006). The fall in the intensity has been found in all lines after SHI irradiation. Additionally it has been found that C-H bending vibrations (675-950 cm^{-1} region) reduced in deeper layers at the fluence of 10^{11} ions/cm^2. Some of the frequency bands in the range 1755-2000 cm^{-1} vanished entirely at the higher fluence of 10^{11} ions/cm^2. In all swift heavy ions irradiated PS samples, no new absorption lines were noticed in spectrum.

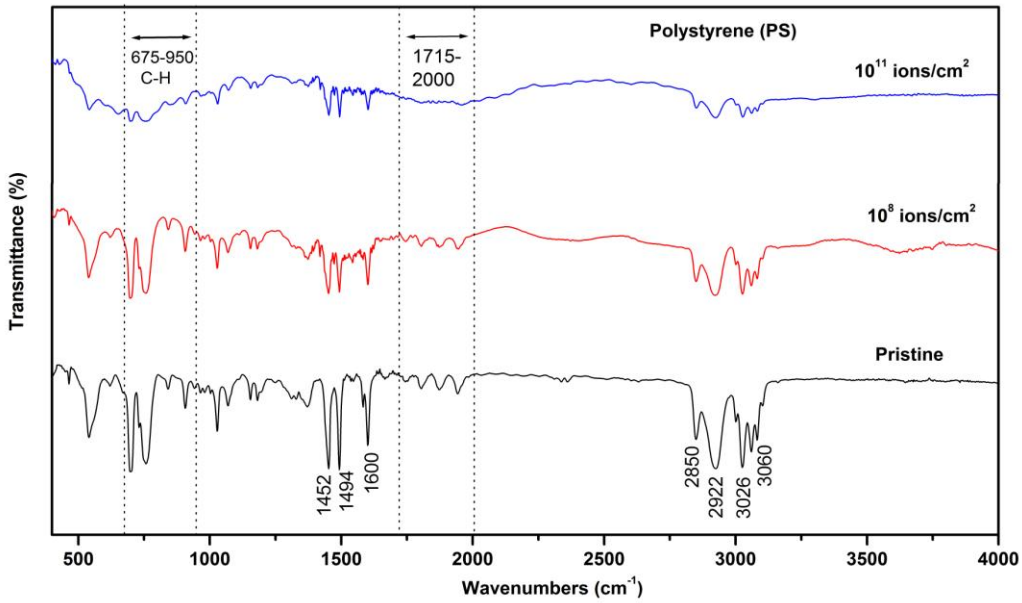

Figure 3.12: FTIR spectra of pristine and Ni^{5+} irradiated polystyrene (PS) films

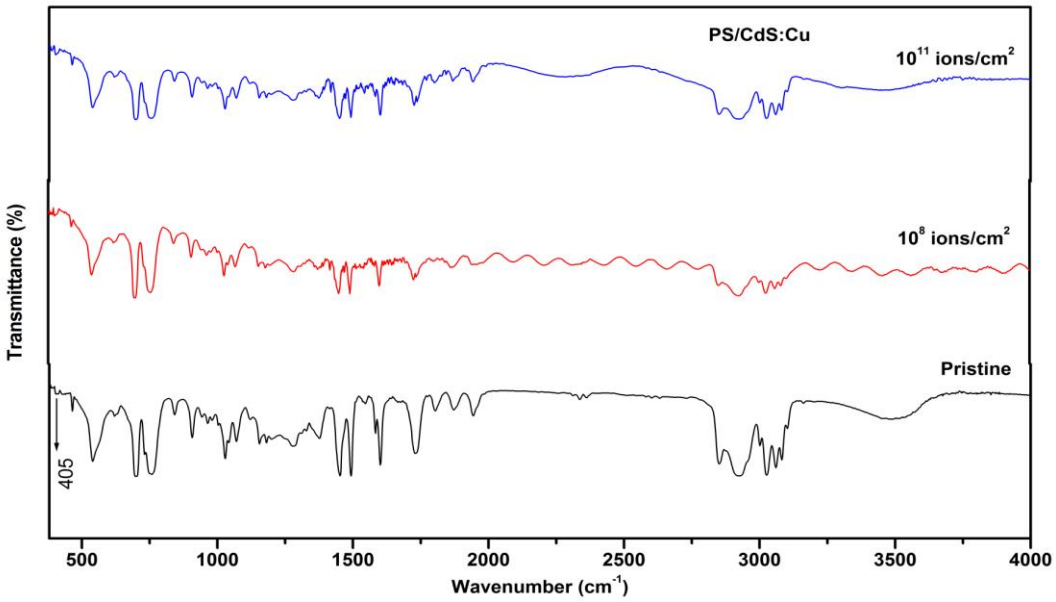

Figure 3.13: FTIR spectra of of pristine and Ni^{5+} irradiated PS/ CdS: Cu films

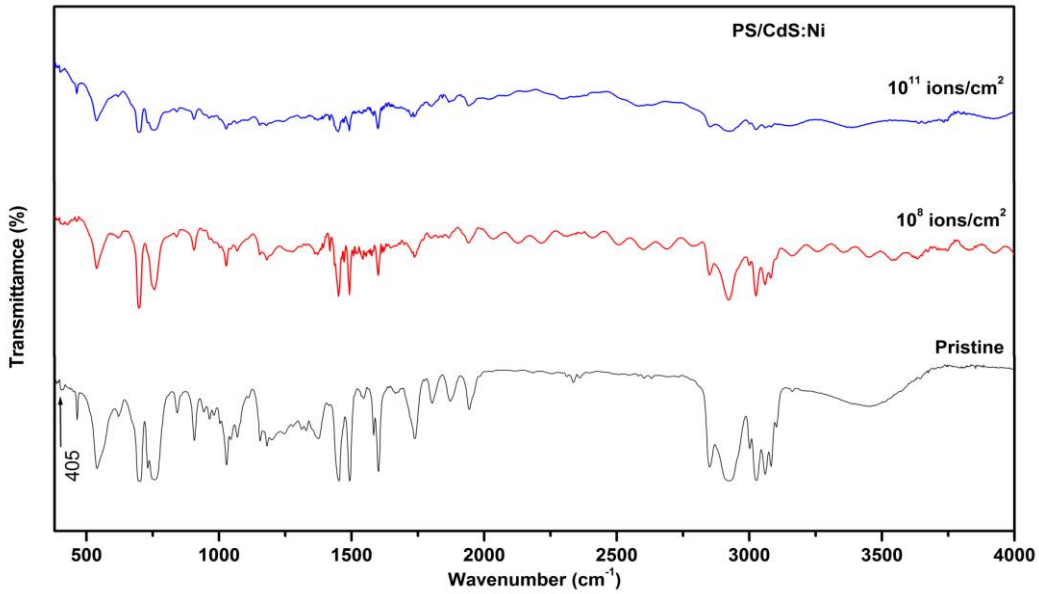

Figure 3.14: FTIR spectra of pristine and Ni^{5+} irradiated PS/ CdS: Ni films

The FTIR spectra of pristine and irradiated samples of Cu doped PS/CdS and Ni doped PS/CdS nanocomposites are shown in Figs. 3.13 and 3.14 respectively. The vibrational absorption peak of the Cd-S bond has been observed at 405 cm^{-1} in both figures (Wu et al, 2004).

There is a dip in the intensity of styrene absorption lines (3081, 3060, 3026, 2922, 2851, 1602, 1493 and 1452 cm^{-1}) in all SHI irradiated nanocomposite films of both the figures. In all swift heavy ions irradiated films no new peak could be observed in the FTIR spectra in above figures.

3.6.3 Conclusion

Swift heavy ion (SHI) beam irradiation is an efficient tool to modify the optical, structural and chemical properties of materials. The nanoparticles of cadmium sulfide (CdS) of average size 50-60 nm were prepared by micro-emulsion method. Ni and Cu metals were doped with PS/CdS nanocomposites and irradiated by 60 MeV Ni^{5+} radiations. The result of doping of Ni and Cu metals in polymer matrix (PS) and SHI irradiation were carried out for modification of optical, structural, and chemical properties. The inclusion of Ni and Cu metals in polymer matrix reduced the band gap energy. When the doped films of PS/CdS were irradiated by Ni^{5+} ions, the band gap energy was decreased. This fall in optical band gap energy by 60 MeV Ni^{5+}irradiation was further approved by the formation of conjugated bonds. The amorphous nature of polystyrene (PS) was also found to be decreased after SHI irradiation at fluence of 10^{11} ions/cm^2. In all irradiated sample, it has been found that the intensity of styrene absorption lines diminished in FTIR spectra. No new band formation was noticed after Ni^{5+} ion beam irradiation in FTIR spectra of PS, Ni metal doped PS/CdS and Cu metal doped PS/CdS samples. So it can be concluded that SHI irradiation is an effective tool for controlling the optical band gap energy of polymer nanocomposites. The optical band gap energy of nanocomposites can be engineered for various applications by monitoring the SHI irradiation beam line and its parameters such as beam current, ion mass, charge and energy.

REFERENCES

S. J. Ahmadi, Y. D. Huang, W. LI Journal of Material Science 39 (2004) 1919 –1925

Alivisatos, A.P., 1996. Semiconductor clusters, nanocrystals, and quantum dots. Science 271 (5251) 933-937.

Artemyev, M.V., Woggon, U., Wannemacher, R., Jaschinski, H., Langbein, W., 2001. Light trapped in a photonic dot: microspheres act as a cavity for quantum dot emission. Nano Lett. 1, 309-314.

Awasthi, K., Kulshrestha V., Avasthi D.K., Vijay Y.K., 2010. Optical, chemical and structural modification of oxygen irradiated PET. Radiat. Meas. 45, 850-855.

Balanzat, E., Bouffard, S., Cassani, A., Dooryhee, E., Protin, L., Grandin, J. P., Doualan, J. L., Margerie, J., 1994. Defect creation in alkali-halides under dense electronic excitations: experimental results on NaCl and KBr. Nucl. Instrum. Methods Phys. Res., Sect. B 91, 134-139.

Chen, L., Zhu, J., Li, Q., Chen, S., Wang, Y., 2007. Controllable synthesis of functionalized CdS nanocrystals and CdS/PMMA nanocomposite hybrids. Eur. Polym. J. 43, 4593-4601.

El-Badry B. A., 2009. Ion bombardment of poly-allyl-diglycol-carbonate (CR-39). Vacuum 83, 1138-1142.

Evelyn, A.L., Ila, D., Zimmerman, R.L., Bhat, K., Poker, D.B., Hensley, D.K., Klatt, C., Kalbitzer, S., Just, N., Drevet, C., 1999. Ion beam modification of PES, PS and PVC polymers. Nucl. Instrum. Methods Phys. Res., Sect. B 148, 1141-1145.

Farmer, S. C., Pattern, T. E., 2001. Photoluminescent polymer/quantum dot composite nanoparticles. Chem. Mater. 13, 3920-3926.

Fink, D., Klett, R., Chadderton, L.T., Cardosa, J. M., Montiel, R., Vezquez, H., Karanovich, A., 1996. Carbonaceous clusters in irradiated polymers as revealed by small angle X-ray scattering and ESR. Nucl. Instrum. Methods Phys. Res., Sect. B 111, 303-314.

Gorelikov, I., Kumacheva, E., 2004. Electrodeposition of polymer-semiconductor nanocomposite films. Chem. Mater. 16, 4122- 4127.

Guzman, A. M., Carlson, J.D., Baras, J.E., Pronko, P.P., 1985. Chemical and physical changes induced in polyvinylidene fluoride by irradiation with high energy ions. Nucl. Instrum. Methods Phys. Res., Sect. B 7–8, 468-472.

Han, Z., Zhu, H., Bulcock, S. R., Ringer, S. P., 2005. One-step synthesis and structural features of CdS/montmorillonite nanocomposites. J. Phys. Chem. B 109, 2673-2678.

Kanjilal, D., (2001). Swift heavy ion-induced modification and track formation in materials. Current Science 80, 1560- 1566.

Kondyurin, A., Gan, B.K., Bilek, M.M.M., McKenzie, D.R., Mizuno, K., Wuhrer, R., 2008. Argon plasma immersion ion implantation of polystyrene films. Nucl. Instrum. Methods Phys. Res., Sect. B 266, 1074-1084.

Kondyurin, A., Gan, B.K., Bilek, M.M.M., Mizuno, K., McKenzie, D.R., 2006. Etching and structural changes of polystyrene films during plasma immersion ion implantation from argon plasma. Nucl. Instrum. Methods Phys. Res., Sect. B 251, 413-418.

Kulshrestha, V., Awasthi, K., Acharya, N. K., Singh, M., Bhagwat, P. V., Vijay, Y. K., 2006. Structural, optical, thermo mechanical and transport property of ion irradiated polymer membranes. Polymer Bull. 56, 427–435.

Kumar, R., Ali, S. A., Singh, P., Prasad, R., 2011. Physical and chemical response of 145 MeV Ne^{6+} ion irradiated polymethylmethacrylate (PMMA) polymer. Nucl. Instrum. Methods Phys. Res., Sect. B 269, 1755–1759.

Kumar, R., De, U., Prasad, R., 2006. Physical and chemical response of 70 MeV carbon ion irradiated polyether sulphone polymer. Nucl. Instrum. Methods Phys. Res., Sect. B 248, 279- 283.

Lee, E. H., Rao, G. R., Mansur, L. K., 1999. LET effect on cross- linking and scission mechanisms of PMMA during irradiation. Radiat. Phys. Chem. 55, 293- 305.

Metwally, H. S., 1901. Electrical and optical studies in $Ge_{100-x}S_x$ chalcogenide thin films. Acta Phys. Pol., A 99, 683- 690.

Peng, X., Schlamp, M. C., Kadavanich, A. V., Alivisatos, A. P., 1997. Epitaxial growth of highly luminescent CdSe/ CdS core/ shell nanocrystals with photostability and electronic accessibility. J. Am. Chem. Soc. 119, 7019- 7029.

Peng, Z. A., Peng, X., 2001. Formation of high quality CdTe, CdSe and CdS nanocrystals using CdO as precursor. J. Am. Chem. Soc. 123, 183- 184.

Phukan, T., Kanjilal, D., Goswami, T. D., Das, H. L., 2003. Study of optical properties of swift heavy ion irradiated PADC polymer. Radiat. Meas. 36, 611-614.

Picq, V., Ramillon, J. M., Balanzat, E., 1998. Swift heavy ions on polymers: Hydrocarbon gas release. Nucl. Instrum. Methods Phys. Res., Sect. B 146, 496-503.

Rong, M. Z., Zhang, M. Q., Liang, H. C., Zeng, H. M., 2003. Surface modification and particle size distribution control in nano-CdS/Polystyrene composite film. Chem. Phys. 286, 267-276.

Singh, L., Samra, K.S., 2008. Opto-structural characterization of proton (3 MeV) irradiated polycarbonate and polystyrene. Radiat. Phys. Chem. 77, 252-258.

Singh, L., Samra, K.S., Singh, R., 2007. Opto-chemical response of CR-39 and polystyrene to swift heavy ion irradiation. Nucl. Instrum. Methods Phys. Res., Sect. B 255, 350-356.

Singh, N. L., 2011. Effect of ion beam irradiation on metal particle doped polymer composites Bull. Material. Sci. 34 (1), 81–88

Singh, P., Kumar, R., Prasad, R., 2013. Free volume evolution in 50 MeV Li $^{3+}$ ion-irradiated polymers studied by positron annihilation lifetime spectroscopy. Radiat. Eff. Defects Solids 168, 97-105.

Steckenreiter, T., Balanzat, E., Fuess, H. Trautmann, C., 1997. Chemical modifications of PET induced by swift heavy ions. Nucl. Instrum. Methods Phys. Res., Sect. B 131, 159–166.

Tauc, J., Grigorovici, R., Vancu, A., 1996.Optical Properties and Electronic Structure of Amorphous Germanium Phys. Status Solids 15, 627-637.

Tesster, N., Medvededev, V., Kazes, M., Kan, S., Banin, U., 2002. Efficient Near-Infrared Polymer Nanocrystal Light-Emitting Diodes. Science 295, 1506-1508.

Tombrello, T. A., 1994. Predicting latent track dimensions. Nucl. Instrum. Methods Phys. Res., Sect. B 94, 424–428.

Vijay Y.K. Kulshrestha Vaibhav, Awasthi Kamlendra, Acharya N.K., Jain A., Singh M. Dolia S.N.. Khan S.A., Avasthi D.K., 2006. Characterization of nanocompsoite polymeric membrane. J. Polym. Res. 13,357-360.

Wu, D., Ge, X., Zhang. Z., Wang, M., Zhang, S., 2004. Novel One-Step Route for Synthesizing CdS/Polystyrene Nano- composite Hollow Spheres. Langmuir 20, 5192-5195.

Ziegler, J. F., 2010. SRIM – The stopping and range of ions in matter (2010). Nucl. Instrum. Methods Phys. Res., Sect. B 268 1818–1823.

Zhu, L., Zhu, M. Q., Hurst, J. K., Li, A. D. Q., 2005. Spiropyran-based Photochromic Polymer Nanoparticles with Optically Switchable Luminescence. J. Am. Chem. Soc. 127, 8968-8970.

CHAPTER 4

SHI Irradiation of Metal Doped Zinc Sulphide Polymer Nanocomposites Synthesized Using Micro Emulsion Method

4.1 Introduction

The nanoparticles of zinc sulfide (ZnS) of the size in the range of 50-60 nm were synthesized by micro emulsion method. A ZnS/PS nanocomposite film in which ZnS nanoparticles were embedded in to polystyrene, doped by metal (Ni, Cu) using solution cast method. Conformation of ZnS nanoparticles is done by SEM image. Ion beam irradiation is effective tool which have huge potential for modifying the optical, structural and chemical properties. The films of Ni doped PS/ ZnS and Cu doped PS/ ZnS were irradiated with Ni^{5+} ions of energy 60 MeV to different fluences of 10^{10} and 10^{11} ions/cm^2.Modification due to heavy ions in optical, chemical and structural modifications were studied by UV- Visible Spectroscopy (UV- Vis), Fourier Transform Infrared spectroscopy (FTIR) and X- Ray Diffraction Spectroscopy (XRD). The peak width of XRD spectra at higher fluence (10^{11} ions/cm^2) of the nanocomposites film decrease after SHI irradtion as evidenced the decrease in the amorphous nature. The UV-Vis spectra of SHI irradiated sample shift from ultraviolet to visible region. The value of band gap in Ni doped PS/ZnS decrease more to the Cu doped PS/ZnS nanocomposites after irradiation by SHI. In the FTIR spectra of Ni and Cu metal doped PS/ZnS the absorption peak of Zn-S was observed at 465 cm^{-1}.The intensity of all vibrational absorption peak of all irradiated metal doped composites decrease with higher fluence of ions.

The polymer and nanoparticles intermixing to form nanocomposites has been widely practiced because of their large number of applications; such as those in optoelectronics, sensors, medical devices, drug delivery and membrane industry etc (Kumari et al 2010). The control over the shape, size and functional properties of nanoparticles may be used for the improvement in mechanical, thermal, tribological, optical, electrical, magnetic and chemical properties of the polymer nanocomposites (Carrion et al 2007). There is wide range of literature available upon the different type of polymer nanocomposites, their synthesis and applications; but our focus is upon the ZnS nanoparticles intermixed with polystyrene polymer. ZnS is an important II-VI group semiconductor material. Zinc blende and wurtzite are the two different crystal strcture of ZnS and both the strcture have the same band gap energy (3.68 eV). It is widely used as phosphor in photoluminescence, electroluminescence and optical sensor (Bodo et al 2012, Borah et al 2008). The large amount of work has been carried out upon the Zn based polystyrene nanocomposites synthesized by different methods in the last decade (Chae et al 2005,Chen et al 2006,Manzi et al 2009,Tu et al 2010, Cheng et al 2010,Awad et al 2011). In addition to it, some recent reports are published upon the Zn based polymer nanocomposites, other than polystyrene (Awad et al 2011, Kole et al 2014). The above cited reports have been focused upon the studies of polymer nanocomposites by changing the doping concentration of the nanoparticles in polymer matrix. The other idea to modify the material properties is by the way of controlled swift heavy ions (SHI) beam irradiation and ions implantation. There are some recent reports available on the ion beam modification of metal doped polymer nanocomposites (Fernandez et al 2005, Mishra et al 2008, Ray et al 2010). There is no data available upon the ion beam treatment of ZnS doped polystyrene nanocomposites to the best of information available to us. In this chapter, study is based upon the synthesis of ZnS nanoparticles by micro emulsion method; the

synthesized ZnS nanoparticles were intermixed with polystyrene by solution cast method to form nano composite thin films. The synthesized films were irradiated with 60 MeV nickel ions for studying the modification in optical, structural and chemical properties.

4.2Experimental

4.2.1 Materials and methods

Polystyrene (density 1.06 g/mL) of average molecular weight 35,000 and all other chemicals/solvents were purchased from Sigma Aldrich. All the chemicals were used as-received without any further treatment.

The structural, optical and chemical studies of pristine and irradiated samples were carried out at Inter University Accelerator Centre (IUAC), New Delhi, India. X- ray diffraction studies were carried out by using Bruker AXS system with Cu-K_α radiation (1.54 Å) for a wide range of Bragg angles 2θ ($5 \leq 2\theta \leq 80$). UV–visible studies were carried out in the wavelength range 250–800 nm using U-3300 Hitachi system. Infrared measurements were performed in transmission mode using Nicolet Nexus 670 FTIR spectrometer.

The synthesis of ZnS nanoparticles was carried out by the reaction of Zinc chloride ($ZnCl_2$) and sodium sulfide (Na_2S) in water-in-oil micro emulsion system (Kulkarni et al 2001). Micro- emlusion of $ZnCl_2$ and Na_2S have 0.46 g of n-pentanol, 3.37 g of Triton X-100, 7.64 g of cyclohexane and 1 g of water. Molar ratio of water and surfactant was maintained at 11 while for sulfide and zinc ions was constant (=1). Concentration of sulfide and zinc were estimated per aqueous phase (Jovanovic et al 2007).

ZnS nanopaticles were sucessfully doped through chemical method reported in lietrature (Ramasamy et al 2012, Murgadoss et al 2012). The 20- 60 nm sized nanoparticles were obtained

and confirmed in the SEM image (Fig. 4.1). The nanocomposites of ZnS and polystyrene were synthesized by solution cast method. Polystyrene (PS) polymer was dissolved in chloroform and ZnS nanoparticles were added to this solution followed by ultrasonic agitation for uniform arrangement. The obtained combination of solution was poured on to a fresh glass petri disc floating on Hg to maintain unvarying thickness of prepared sample. The solvent is then evaporated under normal room temperature (25ºC) condition and finally thin films of polymer composites were obtained. In the final step these films were then dried in vacuum oven at 30° C to remove the solvent content (Singh et al 2011). Average thickness of prepared thin films have been found 18μm (±2) and calculated as per weight, area and density relation.

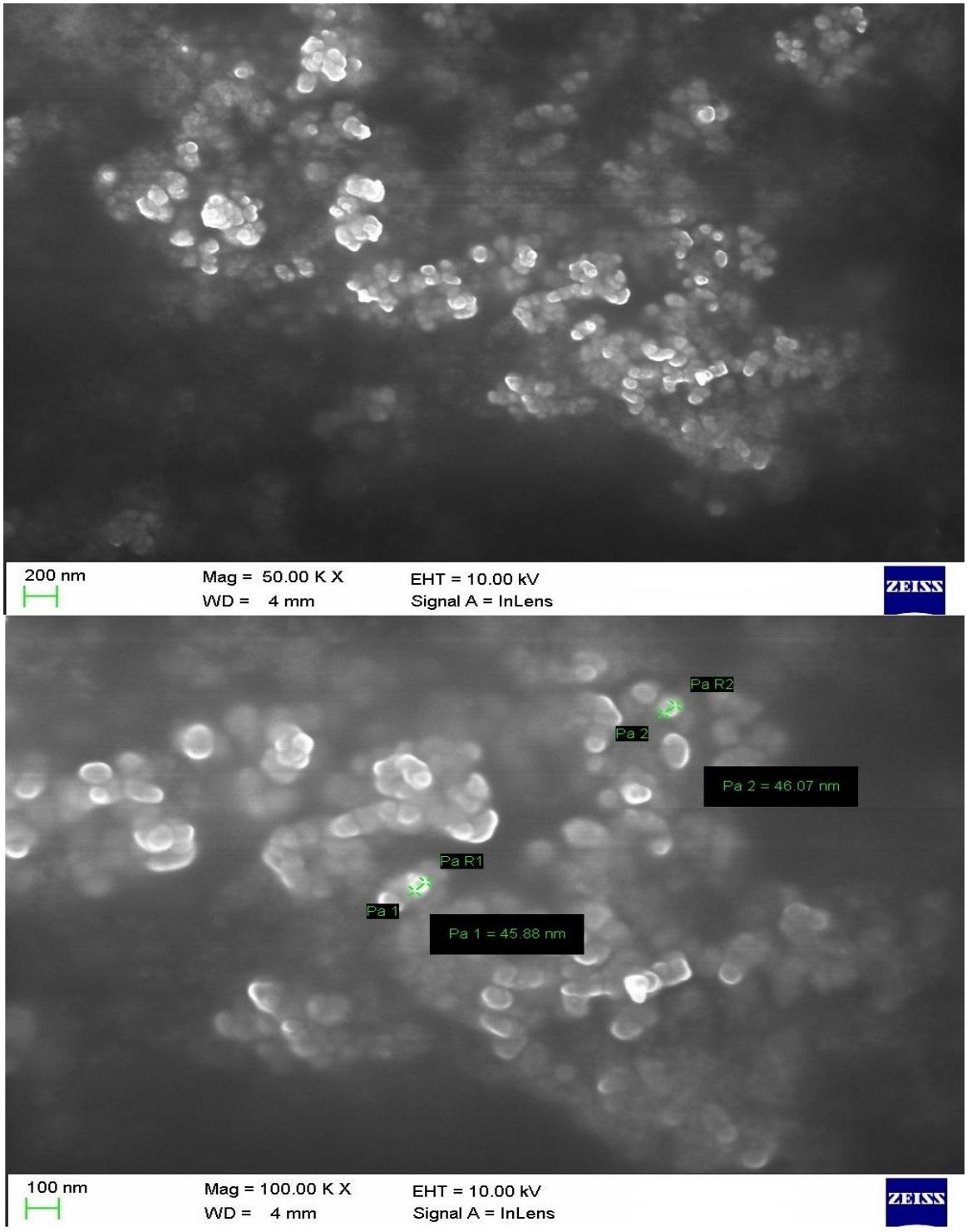

Figure 4.1: SEM image of ZnS nanoparticles synthesized by micro emulsion method

4.2.2 Irradiation

Polymer composites films were cut into small pieces of the size (1.5 × 1.5 cm^2) and these samples were mounted on a vertical vacuum shield ladder and irradiated in General Purpose Scattering Chamber (GPSC) by 60 MeV Ni ion beam from 15 UD Pelletron accelerators at Inter University Accelerator Centre (IUAC), New Delhi, India to the fluences of 10^{10} and10^{11} ions/ cm^2. The beam current was kept ~ 0.5 pnA to suppress thermal decomposition.

4.2.3 Preliminary calculations and ions irradiation

The preliminary calculations were carried out using SRIM-2010 code for ions range and energy loss inside the material (Ziegler et al 2010). The calculated values of electronic energy loss (S_e), nuclear energy loss (S_n) and projected range values are tabulated in Table 4.1. Our sample thickness of 18 μm is compatible with the SRIM calculated projected range for ions to pass through the sample; ensuring negligibly small ions implantation. The S_n values are also quite small, so the nuclear energy loss was least probable.

The irradiation experiment was carried out at Material Science chamber in IUAC, New Delhi, India. The composite samples of size 1.5 cm × 1.5 cm were mounted on the vertical ladder. The ladder was mounted in general purpose scattering chamber and the vacuum of the order of 6×10^{-6} Torr was done in the chamber. The 60 MeV Ni^{5+} beam was selected for irradiation; the beam current was 0.5 pnA. Two fluences, 10^{10} and 10^{11} ions/cm^2 were selected for irradiation.

Table 4.1: SRIM calculated Se, Sn values and projected range of 60 MeV Ni ion beams for target samples

Target material	Se (eV/Å)	Sn (eV/Å)	Projected range (μm)
PS	$5.20*10^2$	1.213	**19.71**
PS/ZnS	$5.68*10^2$	1.490	**18.16**
PS/ZnS: Cu	$6.36*10^2$	1.746	**16.48**
PS/ZnS: Ni	$6.47*10^2$	1.781	**16.14**

4.3 Characterization techniques

Optical, structural and chemical properties have been studied by UV–Visible, X-ray diffraction analyses and FTIR respectively. UV–Visible spectroscopy results were studied in the wavelength range 200–800 nm using U- 3300 Hitachi system. Preliminary structural studies were carried out by using Bruker AXS system with Cu- K_α radiation (1.54 Å) for a wide range of Bragg angles 2θ ($5 \leq 2\theta \leq 50$). Infrared measurements on unirradiated and irradiated samples were carried out in transmission mode using Nicolet Nexus 670 FT- IR spectrometer.

4.4. Optical studies by UV-visible spectroscopy

UV-visible spectroscopy results were discussed in the wavelength range of 200-800 nm at normal room temperature for pristine and SHI irradiated nanocomposite polymer films. Figs. 4.2 (a), 4.2 (b) and 4.2 (c) reveal the UV- visible absorption spectra of PS/ZnS, Cu doped PS/ ZnS and Ni doped PS/ZnS nanocomposites respectively. The shifting of the absorption peak towards the visible region (i.e longer wavelength) was observed. This shifting are due to the formation of

conjugated system of bonds after ion irradiation (Singh et al 2014, Dhillon et al 2014, Singh et al 2010). The shifting of absorption edge towards the longer wavelength is due to ion irradiation bond rupturing which leads to cross linking, free radical formation and resulting formation of the new bonds.The shift became more pronounced as the ion fluence was increased.

Some broadening of the absorption peak has been noticed in PS, PS/ZnS, Cu doped PS/ZnS and Ni doped PS/ZnS after irradiation. The reason of this broadening is beacuse of formation of conjugated system of bonds i.e formation of defects after SHI irrdation. The cause of maximum absorption is π–π^* electronic transition. These electronic transitions need an unsaturated group in the molecule to provide the π electrons.

The main aim of optical UV-vis spectra is to find out energy band gap (E_g) for nanocomposite polymer films.The band gap energy was observed to be decreased due to the formation of conjugated system of bonds. The energy band gap (E_g) was calculated using Tauc's relation as following (Reddeppa et al 2014, Singh et al 2014, Kumar et al 2015).

$$(\alpha h\nu) = B\,(h\nu - E_g)^2 \qquad (1)$$

Here α is the absorption coefficient, $h\nu$ is the photon energy, B is band tailing parameter and E_g is the value of energy band gap for indirect transition (Singh et al 2015). The band gap of the nanocomposites films were calculated by the extrapolation of the plot of $(\alpha h\nu)^{1/2}$ versus $(h\nu)$ (Singh et al 2015). The calculated values are tabulated in Table 4.2. There is quite observable decrease in the value of E_g after ion exposure, also the band gap energy was decreased with the doping of Cu and Ni as compared to the pure polystyrene (4.35 eV) as per our previous data reported in last chapter. On the similar grounds, the number of carbon hexagon rings (N) was observed to be increased in number with the increase of ion fluence as per the values given in

Table 2. The value of N was calculated using following equation (Singh et al 2014,Kumar et al 2013).

$$E_g \approx 34.3/N^{1/2}$$

It can be seen in Table 4.2 that band gap energy of PS, PS/ZnS, PS/ZnS:Cu and PS/ZnS:Ni nanocomposite polymer films suffers a decrease with increase in the fluence. Carbon enriched at domains formed in nanocopmositess during swift heavy ions irrdation. The variation in the optical bad gap energy is due to the strctural deformation phenomenon in nanocomposite polymer films.

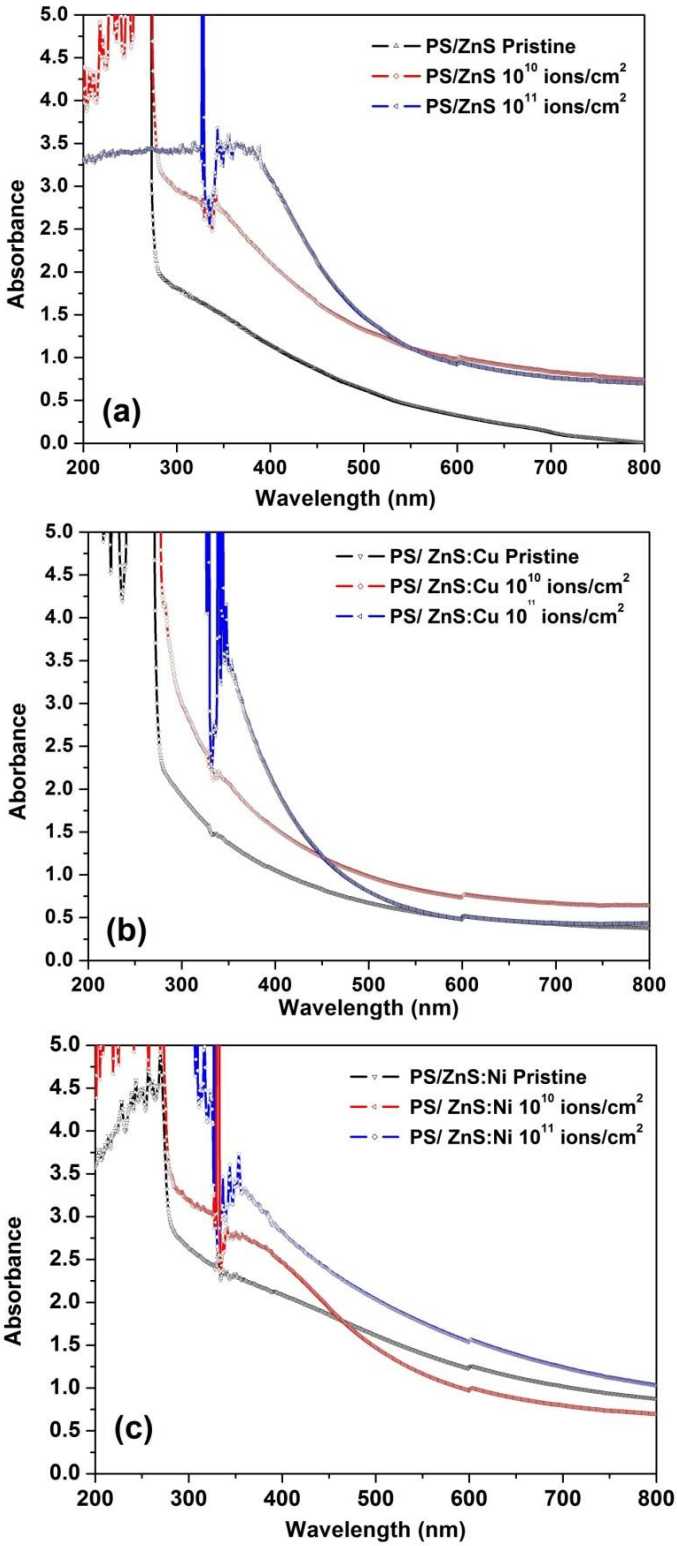

Figure 4.2: UV- visible absorption spectra of (a) PS/ZnS, (b) Cu doped PS/ ZnS and (c) Ni doped PS/ZnS nanocomposite

Fig 4.3 show the UV-vis spectra of Polystyrene, after irradiation of 60 Mev Ni^{5+} ions, the absorption edge is shifting towards the higher wavelength. This shifting of absorption edge may be due to the formation system of conjugate system of bonds. The band gap energy of pure PS was found to be reduced after irrdaiation due to formation of cojugate system of bonds.

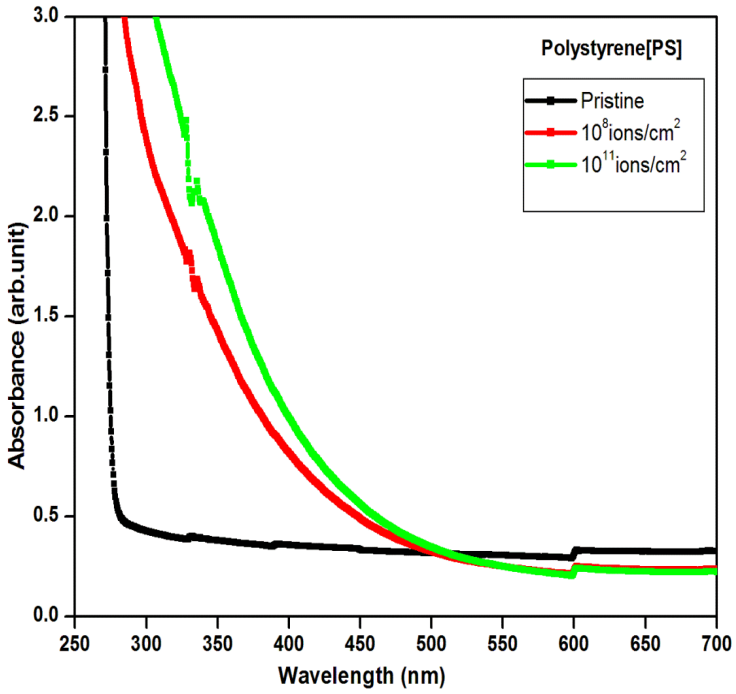

Figure 4.3. UV-Visible spectra of Polystyrene (PS) irradiated with 60 MeV Ni ion beam

No. of carbon hexagon rings per cluster (N) were calculated from the modified Robertson relation (Kumar et al., 2014) using eq. (2)

$$E_g \approx (34.3/N^{1/2}) \ldots\ldots\ldots\ldots\ldots\ldots\ldots\ldots (2)$$

The calculated values of N are tabulated in Table 4.2. The values are increasing with increase of ion fluence.

Table 4.2: Variation of absorption edge, band gap energy and number of carbon atoms for PS, PS/ZnS:Cu and PS/ZnS:Ni nanocomposite films.

Sample	Fluence (ions/cm^2)	Band gap E_g (eV)	Value of N
PS	Pristine	4.35	62
	10^{10}	2.73	158
	10^{11}	2.34	215 (Kumar et al 2014)
PS/ZnS:Cu	Pristine	4.20	67
	10^{10}	3.50	96
	10^{11}	3.06	126
PS/ZnS:Ni	Pristine	3.92	77
	10^{10}	2.81	149
	10^{11}	2.65	168

4.5 Structural studies by X- ray diffraction

The X- ray diffraction (XRD) was performed to determine the crystallographic orientation of ZnS nanoparticles. The Fig. 4.4 shows the diffraction patterns of Cu doped and Ni doped polystyrene ZnS (PS/ZnS) nanocomposites in 2θ mode. In general it has been found that polymers have both crystalline and amorphous region. When these polymers are doped with nanoparticles, change in the crystalline and amorphous region has been observed. The polystyrene broad peak was observed at 19.38° in both cases. The intensity of this peak increased

slightly after ion irradiation, which was insignificant for structural modifications. The prominent peaks observed at 35.35°, 39.44° and 53.73° are attributed to (002), (100) and (103) respectively, these peaks attribute the formation of ZnS nanoparticles and Zn blende structure (Bodo et al 2012, Ali et al 2006)

Increase in crystalline nature suggests cross- linking where as decrease in crystalline nature suggests scissoring of polymeric chains at higher fluences. Cross- linking and chain scissoring in nanocomposite films occurred, when high energy beam of swift heavy ions (SHI) interact with the films. The cross- linking and scissoring further depends upon LET values (Singh et al., 2012) and mechanism of ion- solid.

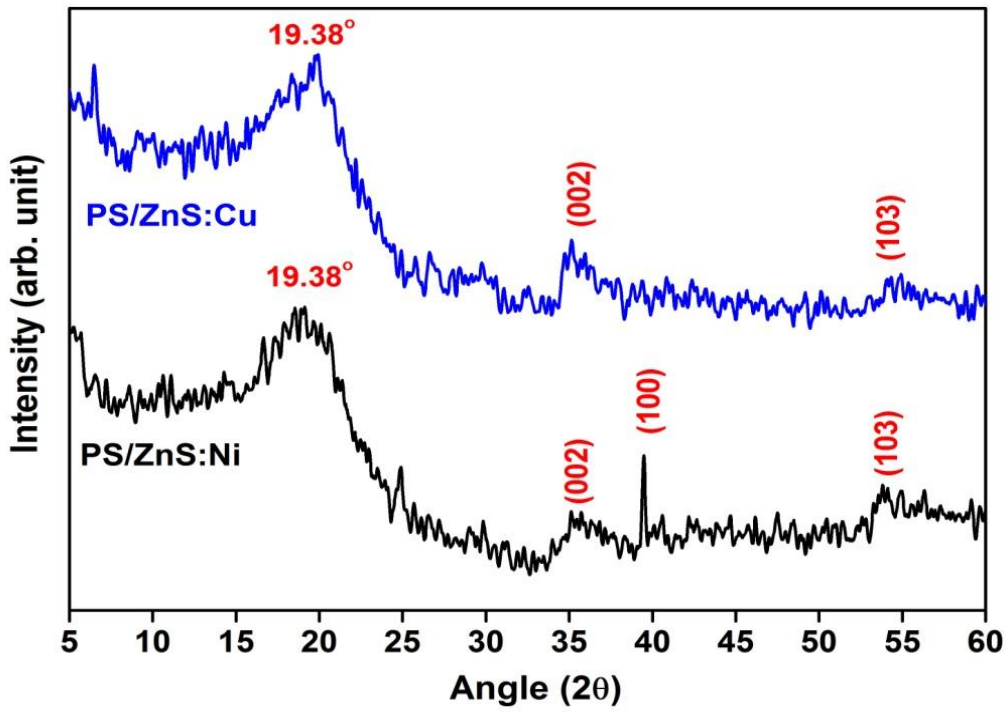

Figure 4.4: X-ray diffraction patterns of PS/ZnS: Cu and PS/ZnS: Ni nanocomposites

The broadening of XRD peaks are observed because of the small crystallite size. In the XRD pattern of Cu and Ni doped PS/ZnS composites the existence of cubic ZnS structure with some similarity of hexagonal ZnS structure observed. The diffraction peak in the figure can be indexed cubic zinc blend ZnS crystal by comparing with the literature but hexagonal type ZnS crystal cannot be excluded. So some of the diffraction peak indexed in XRD pattern which evidenced the hexagonal ZnS structure (Yu Bacherikov et al 2014, Lei Wang et al 2013, Yuwen Zhao et al 2004).

X-ray diffrcation patterns of pristine and irrdaiated PS/ZnS: Ni and PS/ZnS: Cu nanocomposites are shown in Figure 4.5 and 4.6 respectively. The diffraction spectra of pristine PS/ZnS: Ni and PS/ZnS: Cu nanocomposite films peak at 2θ~19.38 show the peak with maximum intensity and indicates the amorphus nature. After the irrdaition of 60 MeV Ni^{5+} with the fluence of 10^{10} and 10^{11} ions/cm^2 , the intensity of the diffracton peak of PS/ZnS: Cu increases at a flunce of 10^{10} ions/cm^2 and further decraese at the fluence of 10^{11} ions/cm^2 led to disordering characters. Broadening of XRD peak at higher fluence observed in all nanocomposites polymer films. A noticeable shift in the XRD peak towards the higher Bragg angle after irradiation by SHI was found. This changes in X-ray diffraction peak are due to disorderning of original strcture of material. The crystallite size of irradited nanocomposite films was found to be increased which may due to cross-linking in polymers.

Table 4.3: Bragg Angle and Crystal Size of Pristine and Irradiated Nanocomposite (PS/ZnS: Cu & PS/ZnS: Ni) Polymer Films

Sample	Fluence (ions/cm^2)	Bragg angle (2θ)	C.S. L (nm)
PS/ZnS: Cu	Pristine	19.38	3.6
	10^{10}	19.72	1.8
	10^{11}	19.72	1.4
PS/ZnS: Ni	Pristine	19.38	3.7
	10^{10}	19.72	0.8
	10^{11}	19.72	1.8

Crystallite size for the diffrent nanocomposite films has been shown in Table 4.3. In case of Cu doped PS/ZnS composites, it decreases with increase in fluence. This decrease in crystallite size may be becausue of disorderness in composite films at higher fluence. In Ni doped PS/ZnS coposites, the crystallite size decrease after irrdation at intial dose and then it increase at higher fluence. This increase in crystallite size may be due to the formation of some crystallite in the amorphus region of nanocomposite films.

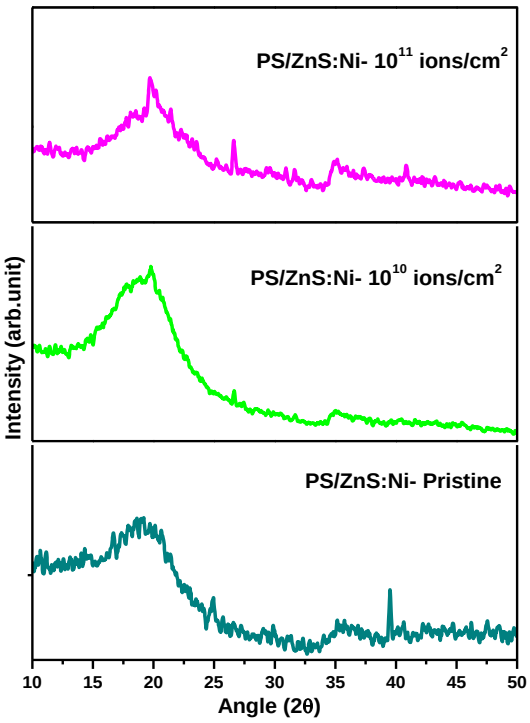

Figure 4.5: X-ray diffraction patterns of Ni^{5+} irradiated PS/ZnS: Ni nanocomposites

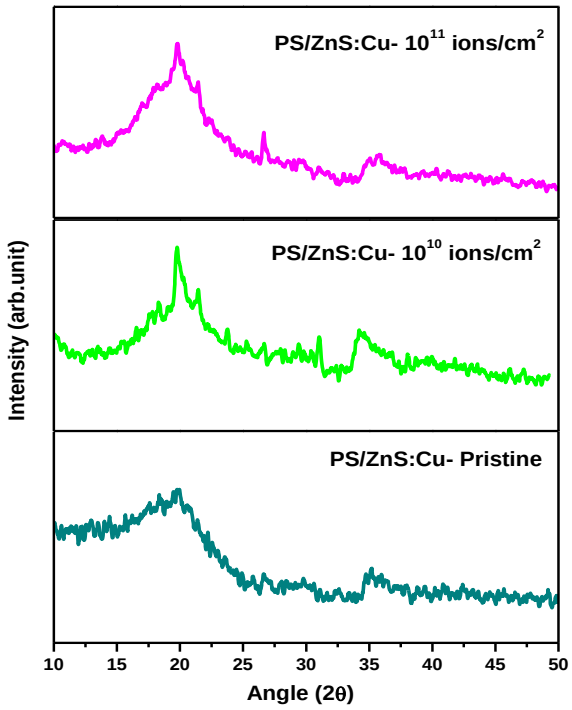

Figure 4.6: X-ray diffraction patterns of Ni^{5+} irradiated PS/ZnS: Cu nanocomposite

4.6 FTIR Spectroscopy

The FTIR spectra (in the wave number range of 400-4000 cm^{-1}) of pristine and irradiated samples of Cu doped PS/ ZnS and Ni doped PS/ ZnS are shown in Fig. 4.5 and Fig. 4.6 respectively. There is some decrease in intensity of typical bands associated with the funcional group present in the polymers. These nanocpmosite polymers have C and H group can be expected to infra red active.In FTIR spectra of Cu and Ni doped PS/ ZnS sample, the peak at 465 cm^{-1} is due to Zn-S bonding and the band at 1734 cm^{-1} correspond to the C=O stretching (Kole et al 2014). The peak at 1495 cm^{-1} are responsible for aromatic stretches and the bands in the range 1700 to 1950 cm^{-1} are responsible for aromatic overtone (Cheng et al 2010). The broad absorption band at 2915 cm^{-1} is assigned to C-H bond of PS (Arabi et al 2011). The peaks of frequency range 2850-3000 cm^{-1} are observed which indicate the presence of CH stretch bonds

which would confirm the functional group of alkanes. A small decrease in intesity may be due to degrdation of a chain.

The intensity of the bands changed after SHI irradiation. The intensity of some of the bands decreased very fast with increase of the ion fluence. The strong absorption band in the frequency range of 900-675 cm^{-1} showed the presence of aromatic group. FTIR spectra in of Cu doped PS/ZnS in Fig. 4.6 show sharp fall in intensity of the bands at 1450 cm^{-1} and 1500 cm^{-1} representing C-H stretch attributed to chain scission which may be taking place at the carbonate site with the formation of new hydroxyl group. FTIR spectra of Ni doped PS/ZnS in fig. 4.7 also show sharp fall in intensity of bands at 1450 cm^{-1} and 1500 cm^{-1} The intensity of the absorption band of C-C stretch at the frequency range of 1585 - 1600 cm^{-1} decreased after irradiation. It explains that chain scissoring took place in metal doped nanocomposites after ion irradiation.

However, the intensity of all the bands decreased after SHI irradiation. It is noticable decrease in the intensity of all peak as compare to pristine at all fluence. The decraese in intensity is due to the clevage of carbonate linkage.

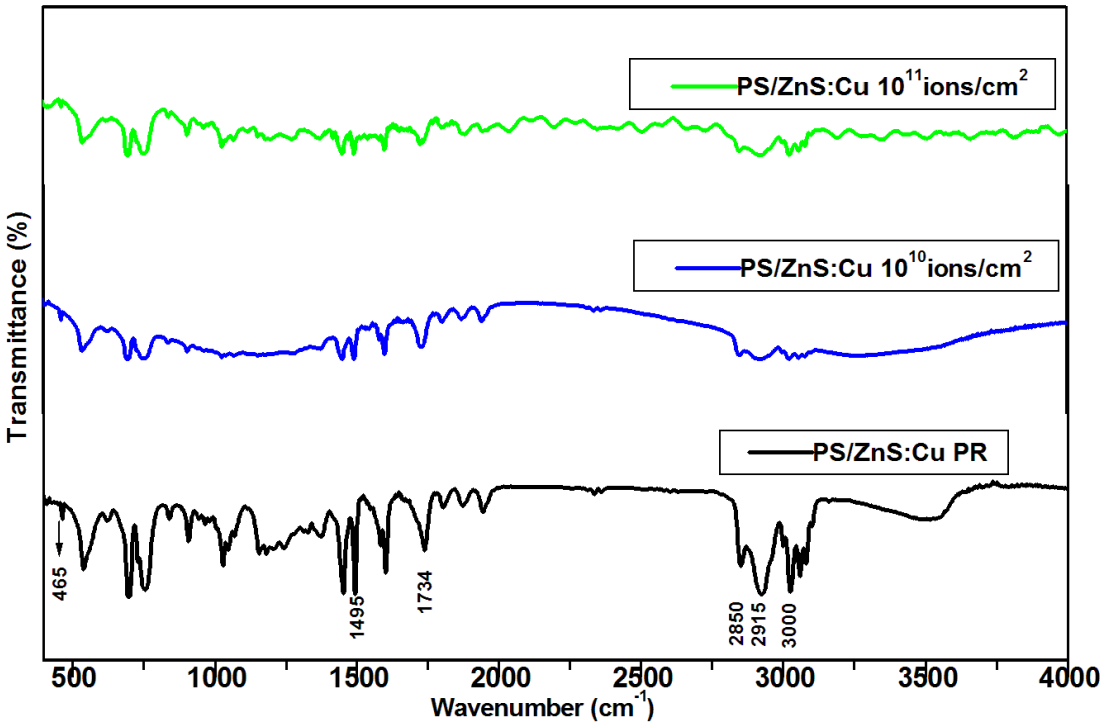

Figure 4.7: FTIR spectra of PS/ ZnS: Cu film irradiated with 60 MeV Ni ion beam

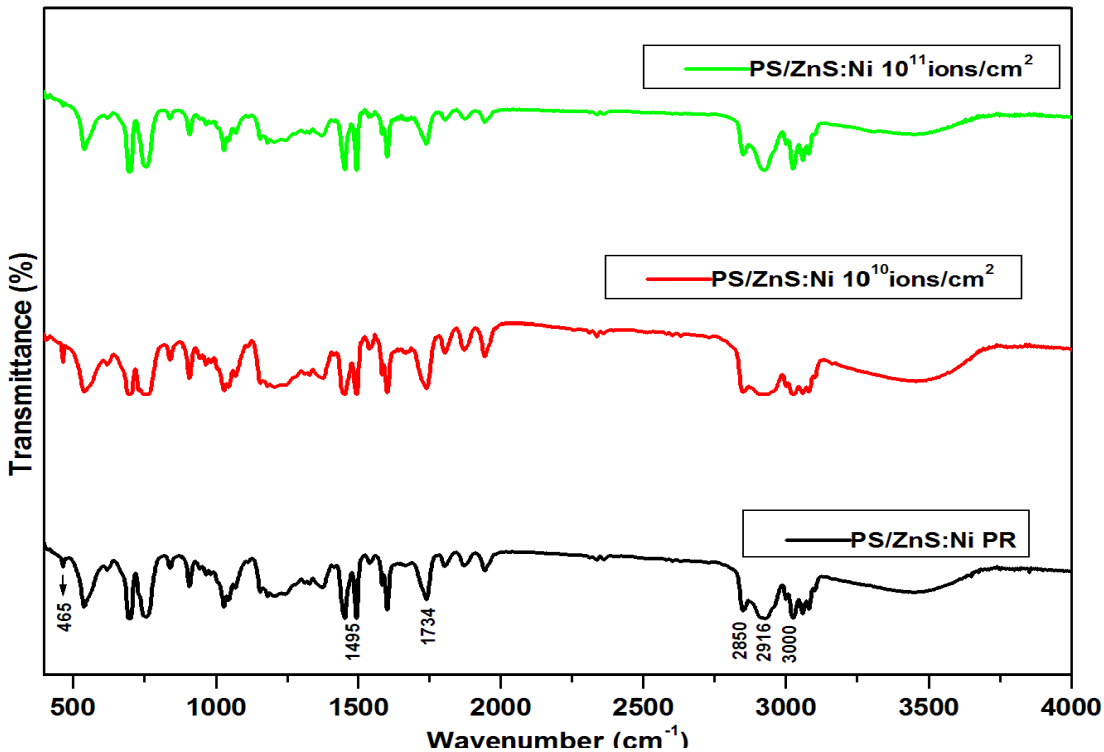

Figure 4.8: FTIR spectra of PS/ ZnS: Ni film irradiated with 60 MeV Ni ion beam

4.7 Conclusion

ZnS nanoparticles of average size 20-60 nm were synthesized, which was confirming by SEM image. The PS/ZnS nanocomposites were doped with Cu and Ni metal nanoparticles. These nanoparticles were confirmed by SEM image. The optical, structural, chemical and SHI irradiation study of doped PS/ZnS nanocomposites was done. The obtained Zn blende structure was confirmed by the (002), (100) and (103) peaks in the XRD results. The band gap energy was decreased in metal doped nanocomposites. This band gap energy of Cu and Ni doped nanocomposites was further decreased after SHI irradtion of 60 MeV Ni^{5+} ions. There was minor increase in the polymer broad X- ray peak at 19.38° after ion irradiation.This may be because of defects and creation of new energy states after irradiation. The amorphous nature of Cu and Ni doped PS/ZnS decrease at higher fluence. The shift of the absorption peak of UV-vis spectra towards the higher wavelength was observed due to the formation of conjugated system of bonds after ion irradiation. The shift became more pronounced at higher ion fluence. The optical band gap energy was observed to be decreased due to the formation of conjugated system of bonds. There was 27% and 32% decrease in the otical band gap energy of the PS/ZnS:Cu and PS/ZnS:Ni composites after swift heavy ion (SHI) irradiation at fluence of 10^{11} ions/cm^2. The intensity of absorption band in FTIR spectra decrease after irradtion. In FTIR spectra of Cu and Ni doped PS/ZnS no new band formation was observed. The Zn-S bonding was confirmed in the FTIR band at 465 cm^{-1}.Ion beam irradiation is a technique which can control the band gap energy of polymer nanocomposites.

REFERENCES

Kumari A, S. K. Yadav, S.C. Yadav, 2010. Biodegradable polymeric nanoparticles based drug delivery systems. Colloids Surf. B 75, 1–18.

F.J. Carrion, J. Sanes, M.D. Bermúdez,2007.Effect of ionic liquid on the structure and tribological properties of polycarbonate–zinc oxide nanodispersion. Mater. Lett. 61, 4531-4535.

B. Bodo, R. Singha, S.C. Das, 2012. Int. J. Appl. Phys. Maths. 02, 287-289.

J.P. Borah, J. Barman, K.C. Sarma, 2008. Structural and optical properties of ZnS nanoparticles. Chalcogenide Lett. 05, 201-208.

W. Chae, B.C. Kim, 2005. Characterization on Polystyrene/ Zinc Oxide nanocomposites prepared from solution mixing. Polym. Adv. Technol. 16, 846-850

Chen-Chi M. Ma, Yi-Jie Chen, Hsu-Chiang Kuan, 2006. Polystyrene nanocomposite materials-Preparation, mechanical, electrical and thermal properties, and morphology. J. Appl. Polym. Sci. 100, 508-515Manzi-Nshuti, D. Chen, S. Su, C.A. Wilkie, Polym. Degrad. Stab. 94 (2009) 1290-1297.

Y. Tu, L. Zhou, Y.Z. Jin, C. Gao, Z.Z. Ye, Y.F. Yang, Q.L. Wang, 2010. Transparent and flexible thin films of ZnO-polystyrene nanocomposite for UV-shielding applications. J. Mater. Chem. 20, 1594-1599.

X. Cheng, Q. Zhao, Y. Yang, S.C. Tjong, R.K.Y. Li, A facile method for the synthesis of ZnS/polystyrene composite particles and ZnS hollow micro-spheres, J. Mater. Sci. 45 (2010) 777–782.

S. Awad, H. Chen, G. Chen, X. Gu, J.L. Lee, E.E. Abdel-Hady, Y.C. Jean, 2011. Free volumes, glass transitions, and cross-links in zinc oxide/waterborne polyurethane nanocomposites, Macromolecules 44, 29-38.

K. Kole, S. Gupta, P. Kumbhakar, P.C. Ramamurthy, Nonlinear optical second harmonic generation in ZnS quantum dots and observation on optical properties of ZnS/PMMA nanocomposites, Opt. Commun. 313 (2014) 231–237.

de Julián Fernández, M.G. Manera, J. Spadavecchi, G. Maggioni, A. Quaranta, G. Mattei, M. Bazzan, E. Cattaruzza, M. Bonafini, E. Negro, A. Vomiero, S. Carturan, C. Scian, G. Della Mea, R. Rella, L. Vasanelli, P. Mazzoldi, 2005. Study of the gas optical sensing properties of Au-polyimide nanocomposite films prepared by ion implantation. Sens. Actuators, B 111-112, 225-229.

Y.K. Mishra, V.S.K. Chakravadhanula, U. Schürmann, H. Kumar, D. Kabiraj, S. Ghosh, V. Zaporojtchenko, D.K. Avasthi, F. Faupel, 2008. Controlled reduction of size of Ag nanoparticles embedded in Teflon matrix by MeV ion irradiation. Nucl. Instrum. Methods Phys. Res., Sect. B 266, 1804-1809.

S.S. Ray, 2010.A new possibility for microstructural investigation of clay-based polymer nanocomposite by focused ion beam tomography. Polymer 51, 3966-3970.

S.K. Kulkarni, U. Winkler, N. Deshmukh, P.H. Borse, R. Fink, E. Umbach,2001. Investigations on chemically capped CdS, ZnS and ZnCdS nanoparticles. Appl. Surf. Sci. 169-170, 438-446

J. Jovanović, Ivana Lj.Validžić, I.A. Janković, N. Bibić, J.M. Nedeljković, 2007. Synthesis and characterization of shaped ZnS nanocrystals in water in oil microemulsions. Materials Letters 61, 4396–4399.

V. Ramasamy, K. Praba, G. Murugadoss, 2012. Synthesis and study of optical properties of transition metals doped ZnS nanoparticles. Spectrochim. Acta A 96, 963‑971.

G. Murugadoss, 2012. Luminescence properties of co-doped ZnS:Ni, Mn and ZnS:Cu, Cd nanoparticles. J. Lumin. 132, 2043‑2048

N.L. Singh, S. Shah, A. Qureshi, A. Tripath, F. Singh, D.K. Avasthi, P.M. Raole; Effect of ion beam irradiation on metal particle doped polymer composites Bull. Mater. Sci. 34 (1) (2011) 81–88.

J.F. Ziegler, M.D. Ziegler, J.P. Biersack, SRIM—the stopping and range of ions in matter (2010), Nucl. Instrum. Methods Phys. Res., Sect. B 268 (2010) 1818-1823.

H.A. Ali, A.A. Iliadis, L.J. Martinez-Miranda, U. Lee, 2006. Structural and Rectifying Junction Properties of Self-assembled ZnO Nanoparticles in Polystyrene Diblock Copolymers on (100) Si Substrates. Solid-State Electron. 50, 1105–1112P. Singh, R. Kumar, Adv. Polym. Technol. 33 (3) (2014), pp. 09.

R.K. Dhillon, P. Singh, S.K. Gupta, S. Singh, R. Kumar, 2013. Study of high energy (MeV) N6+ ion and gamma radiation induced modifications in low density polyethylene (LDPE) polymer. Nucl. Instrum. Methods Phys. Res., Sect. B 301, 12-16.

P. Singh, R. Kumar, H.S. Virk, R. Prasad, 2010. Modification of optical, chemical and structural response of polymethylmethacrylate polymer by 70 MeV carbon ion irradiation. Indian J. Pure Appl. Phys. 48, 321-325.

N. Reddeppa, A.K. Sharma, V.V.R. Narasimha Rao, W. Chen, Measurement 47 (2014) 33–41.

P. Singh, R. Kumar, J. Cyriac, M.T. Rahul, P.M.G. Nambissan, R. Prasad, 2014. High energy (MeV) ion fluence dependent nano scale free volume defects studies of PMMA films. Nucl. Instrum. Methods Phys. Res. Sect. B 320, 64-69.

R. Kumar,P.Singh 2015. Influence of SHI upon nanohole free volume and micro scale level surface modifications of polyethyleneterephthalate polymer films. Appl. Surf. Sci. 337, 19-26.

P. Singh, R. Kumar, P.M.G. Nambissan, 2015. Investigation of in-depth and surface properties of polyethyleneterephthalate thin films after SHI and gamma radiation treatment by means of PALS and AFM studies.Vacuum 115, 31-38.

P. Singh, R. Kumar, R. Singh, A. Roychowdhury, 2015. The influence of cross-linking and clustering upon the nanohole free volume of the SHI and γ-radiation induced polymeric material. Appl. Surf. Sci. 328, 482-490.

P. Singh, S.A. Ali, R. Kumar, 2014. Modifications of structural, optical and chemical properties of Li3+ irradiated polyurethane and polyetheretherketone. Radiat. Phys. Chem. 96, 181-185.

R. Kumar, P. Singh, 2013. UV–visible and infrared spectroscopic studies of Li3+ and C5+ irradiated PADC polymer. Results Phys. 3, 122-128.

A.M. Arabi, T. Ebadzadeh, A.A. Yousefi, M. Pishvaei, E.M. Rad, C. Zamani, 2011. Hydrothermal synthesis of highly stabilised ZnS–polystyrene hybrid nanoparticles. Micro & Nano Letters 6, 844–847.

Yu Bacherikov, A. Kuchuk, A. Zhuk, Yu Polischuk, V.Kladko, T.Kryshtab, N.Korsunska, 2014. Correlation between luminescent characteristics and phase composition of ZnS: Cu powder prepared by self-propagating high temperature synthesis. Journal of Luminscene; 145, 970-975.

Lei Wan, Lixin Cao, Ge Su, Wei Liu, 2013. Chenghui, Huajian Zhou. Prepration and characterization of water-soluble ZnSe:Cu/ZnS core/ shell quantum dots. Applied Surface Science 280, 673-678.

CHAPTER 5

Conclusion and Future Scope of Research

5.1 Conclusion

This chapter sum up and concludes the thesis work. The directions and possible scope for further research in this area are also suggested.

In the process of interaction of ionizing radiation with the material, it liberated an electron from atom or molecule, generating ions which are atoms or molecules with net electric charge. The degree of ionization depends on energy and nature of particle. In the interaction of ionizing radiation to the nanocomposite polymer films, incident energy is transported to the medium as an effect of ionization and excitation of the target molecules.

Swift heavy ions are valuable resources for nanocomposite polymers by improving their properties over non-irradiated nanocomposites and offering significant advantages over other methods of modification. The swift heavy ions (SHI) irradiation in a controlled way has been used to modify the optical, structural, chemical, magnetic, electrical and other properties of the polymers and polymer nanocomposites. Drastic modifications in structural, optical and chemical properties of Ni and Cu metal doped PS/CdS and PS/ZnS composites film followed by irradiation with SHI have been found. In this work, we have synthesis the nanocomposites and made systematic characterization of nanocomposites polymer films before and after irradiation. The outcomes and findings of thesis can be divided into the following parts:

First part **(Chapter-2)** covers the synthesis of CdS and ZnS nanoparticles by micro emulsion procedure and Cu and Ni doped PS/CdS, PS/ZnS composite films by the solution cast methods. For the synthesis of nanoparticles, micro- emulsion method is very valuable and impressive for controlling the size of nano- particles among the other methods available such as chemical aerosol flow synthesis, sol-gel template, ion beam synthesis, ultrasonic's

irradiation in an aqueous solution, two phase approach and in situ micelle-template-interface reaction route.

In the second part **(Chapter-3)** the nanoparticles of cadmium sulphide (CdS) of size of 50-60 nm were prepared by one of the best chemical method i.e. micro- emulsion method. Ni and Cu metals are doped in the polystyrene/CdS (PS/CdS) nanocomposites. The pristine and metal doped nanocomposite films were irradiated with 60 MeV Ni^{5+} ions. The result of doping of Cu and Ni metals and swift heavy ion irradiation at different fluence was discussed for observing the change in the optical, structural and chemical properties of PS/CdS nanocomposite films. In XRD spectra, the decrease in the amorphous nature of SHI irradiated polystyrene (PS) has been observed. In the UV-visible studies, shifting of the absorption peaks of all irradiated and doped samples from ultraviolet to the visible region was found. The absorption peak shift in UV-visible spectra of Cu and Ni metal doped composites was more prominent than those of pure polystyrene (PS) and PS/CdS nanocomposite films. The cause for increase in absorption was due to the production of a conjugated system of bonds. The fall in optical band gap energy value in case of Ni metal doped PS/CdS composite was larger that of Cu doped PS/CdS composites and the SHI irradiation further reduced the optical band gap energy. In FTIR pattern of Cu and Ni metal doped PS/CdS composites film the absorption peak of Cd-S bond was noticed at 405 cm^{-1}. In all SHI irradiated samples of polystyrene (PS), a dip in the intensity of absorption lines has been found. The band gap energy (E_g) of metal doped nanocomposite polymer films can be controlled by swift heavy ions (SHI) with highly focused and controlled ion beam. Thus band gap energy (E_g) of nanocomposite polymer films can be engineered as per requirements by taking care of the beam parameters such as ion mass, current, charge and energy.

In the third part **(Chapter-4)** ZnS nanoparticles of average size 50-60 nm were synthesized, which was confirm by SEM image. The PS/ZnS nanocomposites were doped

with Cu and Ni metal nanoparticles. The optical, structural, chemical and SHI irradiation study of doped PS/ZnS nanocomposites was done. The band gap energy was decreased in metal doped nanocomposites. This band gap energy of Cu and Ni doped nanocomposites was further decreased after SHI irradtion of 60 MeV beams of Ni^{5+} ions. This may be because of defects and formation of new energy states after irradiation. The amorphous nature of Cu and Ni metal doped PS/ZnS composites decrease at higher fluence. In FTIR pattern, the intensity of all absorption bands decreased in all SHI irradiated nanocomposite films. In FTIR spectra of Cu and Ni doped PS/ZnS no new band formation was noticed. Swift Heavy Ion (SHI) beam irradiation is a technique which can control the band gap energy, can also do the modification in the structural and chemical properties of nanocomposites polymer.

The research work presented in this thesis is the unique approach to study the effect of swift heavy ions on the properties of Ni and Cu doped nanocomposites (PS/CdS:Cu, PS/CdS:Ni, PS/ZnS, PS/ ZnS: Cu and PS/ ZnS: Ni) at various fluence. Significant changes have been found with the increase of fluence. The irradiation parameters like energy, ion, mass, fluence, charge etc and type of the target material itself appears to be responsible for the differences that have been observed in the studied properties of the nanocomposite polymer films. It can be concluded that changes in band gap are dominant at higher fluence. These studies show a straightforward demonstration of the prospective applications of nanocomposite polymers in optoelectronics and sensors.

5.2 Future Scope

The research work presented in this thesis opens up a wide area for the future work in the field of nanocomposite polymers. In the continuation of this experimental work, the research can be elongated in several new directions. The future scope for this research work that falls in the range of same field can be considered in the following area:

- Synthesis of polymer nanocomposites with doping of metals by varying the concentration.
- It can modify the properties of nanocomposites and further the properties can be modified with Swift Heavy Ions (SHI).
- The effect of Swift Heavy Ions (SHI) with different energy range and with different ions on the optical, structural, chemical properties of these nanocomposites can be explored.
- Also the synthesized nanocomposites can be employed as part of sensors, devices etc.

Appendix-A: Samples Details for Heavy Ions Irradiation

S. No.	Target	Fluence (ions/cm^2)	Current (pnA)	Range	*Se* (eV/A^0)	*Sn* (eV/A^0)	Energy and Ions
1.	PS	1×10^8 1×10^{11}	0.5	19.71	5.2×10^2	1.21	60 MeV Ni^{5+}
2.	PS/CdS: Cu	1×10^8 1×10^{11}	0.5	17.56	5.94×10^2	1.67	60 MeV Ni^5
3.	PS/CdS: Ni	1×10^8 1×10^{11}	0.5	17.24	6.03×10^2	1.69	60 MeV Ni^{5+}
4.	PS/ZnS	1×10^{10} 1×10^{11}	0.5	18.16	5.68×10^2	1.49	60 MeV Ni^{5+}
5.	PS/ZnS: Cu	1×10^{10} 1×10^{11}	0.5	16.48	6.36×10^2	1.74	60 MeV Ni^{5+}
6.	PS/ZnS: Ni	1×10^{10} 1×10^{11}	0.5	16.14	6.47×10^2	1.78	60 MeV Ni^{5+}

Appendix B: FTIR Bands of PS, Cu and Ni doped PS/CdS composite films

Band Position (cm^{-1})	Assignments
3081,3060 and 3026	C-H stretching vibrations
2851 and 2922	C-H stretch vibrations in CH_2 group
1602 and 1493	Aromatic ring vibrations
405	Vibrational absorption peak of the Cd-S bond

Appendix C: FTIR Bands of Cu and Ni doped PS/ZnS composite films

Band Position (cm^{-1})	**Assignments**
2915	C-H bond of PS
2850 - 3000	Presence of CH stretch bonds
1700 - 1950	Aromatic overtone
1734	C=O stretching
465	Zn-S bonding

List of Publications

Paper Published in International Journals

1. **Satyendra Kumar,** Paramjit Singh, R. G. Sonkawade, Kamlendra Awasthi, Rajesh Kumar, 60 MeV Ni ion induced modification in nano-CdS/polystyrene composite film, ***Radiation Physics and Chemistry*** 94(2014) 49-53.

2. **Satyendra Kumar,** Paramjit Singh, R. G. Sonkawade, Kamlendra Awasthi, Rajesh Kumar, SHI irradiation of metal doped zinc sulfide polymer nanocomposites synthesized by microemulsion method, ***Nuclear Instruments and Methods in Physics Research B*** 358 (2015) 258-262.

3. Paramjit Singh, **Satyendra Kumar,** Rajesh Kumar, Study of physical and chemical modification induced by 50 MeV Li^{3+} ion beam in polymers, ***Radiation Physics and Chemistry*** 94(2014) 54-57.

4. Sanjeev Kumar Gupta, Paramjit Singh, **Satyendra Kumar,** Rajesh Kumar, Gamma Radiation induced modification in Physicochemical Properties of Makrofol (KG and N) Polycarbonate, ***Advances in Polymer Technology,*** Vol. 0, No. 0 (2015), DOI 10.1002/adv.21510.

Conference Contribution (National/International)

1. **Satyendra Kumar,** R. G. Sonkawade, Rajesh Kumar, Kamlendra Awasthi, Anil Sharma, F. Singh, Effect of irradiation on Band Gap of Doped Polystyrene/CdS composite, Book of abstract pp.84, International Conference on Radiation Environment Assessment, Measurement and its Impact (RADENVIRON-2012), BBA University Lucknow, April 12-14, 2012.

2. Sanjeev Kumar Gupta, Paramjit Singh, **Satyendra Kumar,** Rajesh Kumar, Modification induced by gamma exposure on structural, optical and chemical properties of Polyamide Nylone-6, 6 polymer, Proceeding of SSNTDs-18, 2013.

3. Lalit Mohan Singh, **Satyendra Kumar,** Rajesh Kumar, Study of natural radioactivity, radon exhalation rate and radiation doses in coal and fly ash samples from Thermal Power Station, Delhi India, Book of Abstract pp.146, 26th International Conference on Nuclear Tracks in Solids (ICNTS-26), Kobe, Japan, Sept 15-19, 2014.

4. Anil Sharma, R G Sonkawade, **Satyendra Kumar,** Assessment of Radon exhalation rate in soil sample collected from NTPC Badarpur, Delhi, India, International Conference in Material Science and Ionizing Radiation Safety & Awareness, (ICMSIRSA-2016), University of Kolhapur, Kolhapur, January 28-30, 2015.

5. Anil Sharma, R G Sonkawade, **Satyendra Kumar,** Comparative Study of radon exhalation rate in soil samples from Kasimpur Thermal Power Plant, Aligarh, Uttar Pradesh, India, International Conference in Material Science and Ionizing Radiation Safety & Awareness, (ICMSIRSA-2016), University of Kolhapur, Kolhapur, January 28-30, 2015.

Radiation Physics and Chemistry 94 (2014) 49–53

Contents lists available at ScienceDirect

Radiation Physics and Chemistry

journal homepage: www.elsevier.com/locate/radphyschem

60 MeV Ni ion induced modifications in nano-CdS/polystyrene composite films

Satyendra Kumar [a], Paramjit Singh [b], R.G. Sonkawade [a], Kamlendra Awasthi [c], Rajesh Kumar [b,*]

[a] Department of Applied Physics, School of Physical Sciences, Babasaheb Bhimrao Ambedkar University, Lucknow 226025, India
[b] University School of Basics and Applied Sciences, Guru Gobind Singh Indraprastha University, New Delhi 110078, India
[c] Department of Physics, Malaviya National Institute of Technology, Jaipur 302017, India

HIGHLIGHTS

- Synthesis and irradiation of metal doped nano-composites with swift heavy ions (SHI) at different fluences.
- Structural, optical and chemical changes after irradiation were examined by XRD, UV–visible and FTIR spectroscopy respectively.
- Change in crystalline nature and decrease in band gap are observed with increase in fluence.
- The modifications caused by SHI in various chemical bonds are also discussed.

ARTICLE INFO

Article history:
Received 13 December 2012
Accepted 24 June 2013
Available online 1 July 2013

Keywords:
Nano-CdS/Polystyrene composite films
Ion beam irradiation
XRD
UV–vis
FTIR

ABSTRACT

The cadmium sulfide (CdS) nanoparticles of size in the range 50–60 nm were synthesized by micro-emulsion method. The polystyrene/CdS (PS/CdS) nanocomposites were doped with Ni and Cu metals. The pristine and doped samples were irradiated with 60 MeV Ni ions. The effect of doping of metals and ion irradiation was studied for modifications in structural, optical and chemical properties of PS/CdS nanocomposites. The decrease in peak width of XRD spectra of irradiated PS indicated the decrease in the amorphous nature at higher fluences. The optical absorption peaks of the irradiated and doped samples shifted towards visible region. The shift in case of metal doped samples was more pronounced than those of pure polystyrene and PS/CdS matrix samples. The increase in absorption was attributed to the generation of a conjugated system of bonds. The decrease in band gap energy value in case of Ni doped PS/CdS was greater than that of Cu doped PS/CdS and the ion irradiation further decreased the band gap energy value. The vibrational absorption peak of the Cd–S bond was observed at 405 cm^{-1} in FTIR spectra of metal doped PS/CdS composites. The intensity of styrene absorption lines decreased in all irradiated samples.

1. Introduction

Polymer nanocomposites represent a new field in nano-science. The smaller size of nano-particles than the wavelength of visible light makes the polymer nanocomposites a new perspective for optical materials. The optical properties of nano-composites can be modified by doping the polymer matrix with suitable dopant as well as by ion beam irradiation. The controlled swift heavy ions (SHI) irradiation may be used to modify the optical, structural, chemical, magnetic, electrical and other properties of the polymers and polymer nanocomposites (Tombrello, 1994; Steckenreiter et al., 1997; Kulshrestha et al., 2006; Kumar et al., 2006; Vijay et al., 2006; Awasthi et al., 2010). The incoming energetic ions interact with the target material by two ways; with nuclei of the target atoms (elastic collision) and with electrons of the target atoms (inelastic collision) depending upon the energy of the incoming ion. The inelastic collision dominates at high energies (greater than 10 MeV) and responsible for modifications of above said properties (Kanjilal, 2001). The most of the energy of SHI is lost in exciting electrons and ionizing atoms. Target ionization causes bond cleavages, free radical formation, degradation and cross-linking of polymeric chains and formation of unsaturated bonds (Fink et al., 1996; Picq et al., 1998). The extent of modifications (excitation, ionization etc.) by SHI depends upon mass, charge state, energy and fluence of the impinging ions. These parameters are defined by linear energy transfer (LET) value

* Corresponding author.
E-mail address: rajeshkumaripu@gmail.com (R. Kumar).

0969-806X/$ - see front matter © 2013 Elsevier Ltd. All rights reserved.
http://dx.doi.org/10.1016/j.radphyschem.2013.06.022

of incoming ion (Lee et al., 1999). The modifications also depend upon the nature (molecular structure and packing of polymeric chains etc.) of target polymers (Singh et al., 2013; Balanzat et al., 1994).

Polystyrene/CdS doped with metals followed by irradiated with SHI may give drastic modifications in its structural, optical and chemical properties. The unique size and quantum confinement properties make these polymer nanocomposites useful for applications such as light-emitting diodes (Tesster et al., 2002), lasers (Artemyev et al., 2001) and devices (Zhu et al., 2005). CdS nanocomposites have been highly studied because of their size dependent properties (Zhu et al., 2005). Their emission behavior varies with respect to the size, which can be controlled by the temperature and surface capping molecules during their synthesis (Alivisatos, 1996). Various reports on the synthesis of CdS nanocrystals have been presented using different methods (Peng and Peng, 2001; Gorelikov and Kumacheva, 2004; Peng et al., 1997). Micro-emulsion method used for the synthesis of nanocomposites is very effective for the size control of nano-particles among the other techniques present such as sol–gel template, chemical aerosol flow synthesis, ion beam synthesis, ultrasonic's irradiation in an aqueous solution, two phase approach and in situ micelle-template-interface reaction route. The literature has been reported to embed CdS nanoparticles in the polymer matrix (Farmer and Pattern, 2001; Wu et al., 2004; Han et al., 2005). In the literature some reports have been found on the use of varying concentration of nanoparticles in the polymer (Chen et al., 2007; Rong et al., 2003). However, a very limited data is available for the modification of optical, structural and chemical properties by ion beam irradiation.

The optical energy band gap and the crystallite size of polymer nanocomposites can be controlled by doping and ion beam treatment by controlling the doping concentration as well as beam parameters (current, energy, fluence etc.) respectively. The main objective of this work is to study the optical properties for the modification of band gap energy by the way of two modes: doping with metals (Ni and Cu) and ion beam treatment (irradiation). In addition to it the effects of ion beam on structural and chemical properties are also discussed.

2. Experimental

2.1. Materials

Polystyrene of average molecular weight 35,000 having density 1.06 g/mL and all other chemicals/solvents were purchased from Sigma Aldrich. All the chemicals were used as-received without any further treatment.

2.2. Prepration of CdS/PS nanocomposites film

CdS nanoparticles were synthesized by the reaction of sodium sulfide and cadmium nitrate in water-in-oil micro-emulsion system in which cyclohexane was used as a surfactant. The size of synthesized CdS nanoparticles was found to be in the range 50–60 nm. The SEM image of synthesized nanoparticles is shown in Fig. 1. For fabricating nanocomposite film with homogeneously dispersed cadmium sulfide CdS nanoparticles in polystyrene (PS) matrix, the polymer was firstly dissolved in chloroform and then 3 ml of synthesized CdS nanoparticles were added to the polymer solution and dispersed by ultrasonic agitation to ensure an even arrangement. After obtaining a uniform mixture, the mixture was poured on to a clean Petridish. The solvent was evaporated at room temperature (25 °C) to get thin films (thickness~20 μm) of

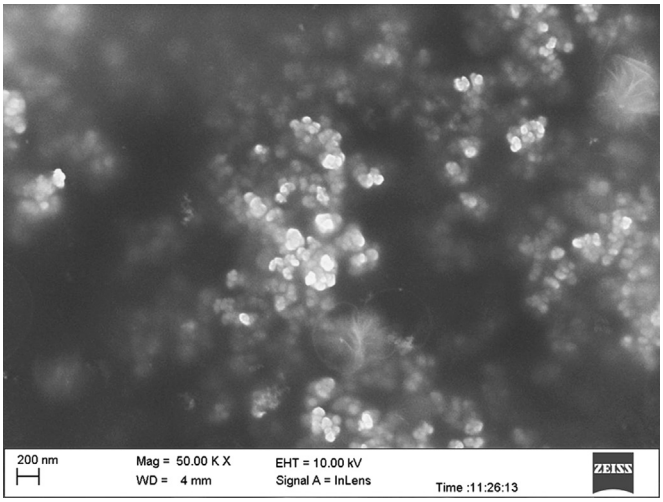

Fig. 1. SEM image of synthesized CdS nanoparticles.

polymer composites which were then dried in vacuum oven at 30 °C (Rong et al., 2003; Singh et al., 2011).

2.3. Irradiation

The specimens of the size (1.5 cm × 1.5 cm) were prepared for irradiation. Samples were mounted on a vertical vacuum shield ladder and irradiated in general purpose scattering chamber (GPSC) with 60 MeV Ni^{5+} ions beam from 15 UD pelletron accelerator at Inter University Accelerator Centre (IUAC), New Delhi, India to the fluences of 10^8 and 10^{11} ions/cm^2. The beam current was kept ~0.5 pnA to suppress thermal decomposition. The pristine and irradiated samples were characterized by UV–visible, FTIR and X-ray diffraction for the study of optical, chemical and structural properties. UV–visible spectroscopy was carried out in the wavelength range 250–800 nm using U-3300 Hitachi system. Preliminary structural studies were carried out by using Bruker AXS system with Cu-K_α radiation (1.54 Å) for a wide range of Bragg angles 2θ ($5 \leq 2\theta \leq 80$). Infrared measurements were performed in transmission mode using Nicolet Nexus 670 FTIR spectrometer.

2.4. SRIM (stopping and range of ions in materials) calculations

SRIM calculations were made to find electronic energy loss (S_e), nuclear energy loss (S_n) and projected range of Ni ions in target polymer and polymer nano-composites using SRIM-2008 code (Ziegler, 2010). The calculated values are given in Table 1. The S_e values for our target samples are 100 times larger than those of their S_n values ensuring nuclear energy loss to be nearly negligible. The projected range values are nearly equal to our sample thickness (20 μm), hence probability for ion implantation is quite low.

3. Results and discussion

3.1. X-ray diffraction

The XRD patterns of pristine and irradiated samples of polystyrene (PS) are shown in Fig. 2. The XRD pattern of pristine PS sample conforms to the XRD pattern reported by Singh and Samra, 2008. The main diffraction peaks of pristine sample of PS occurs at $2\theta = 19.76^\circ$. There is no phase change for the irradiated samples (Guzman et al., 1985) as their peak positions remain undisturbed. There is increase in peak width of the XRD spectra of pure PS at a

Table 1
SRIM calculated S_e, S_n values and projected range of 60 MeV Ni ion beams for target samples.

Target material	S_e (eV/Å)	S_n (eV/Å)	Projected range (μm)
Polystyrene (PS)	5.20×10^2	1.21	19.71
PS\CdS: Cu	5.94×10^2	1.67	17.56
PS\CdS: Ni	6.03×10^2	1.69	17.24

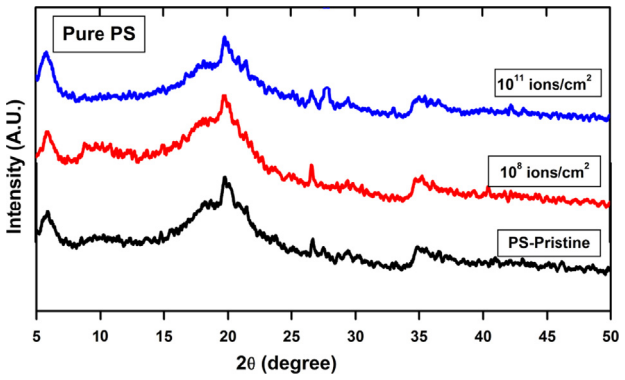

Fig. 2. X-ray diffraction patterns of pristine and Ni^{5+} irradiated polystyrene polymer films.

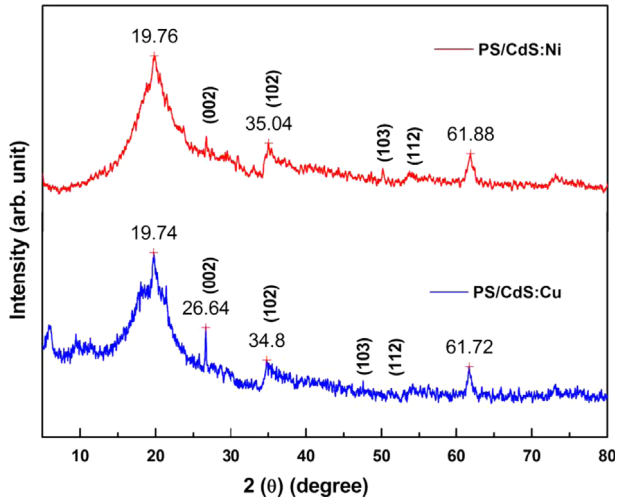

Fig. 3. X-ray diffraction patterns of PS/CdS: Cu and PS/CdS: Ni nanocomposites.

fluence of 10^8 ions/cm^2 whereas subsequent irradiation at still higher fluence (10^{11} ions/cm^2) causes decrease in peak width. This shows the alignment of the polymeric chains in a regular pattern and hence there is decrease in the amorphous nature at higher fluences. Fig. 3 shows the XRD patterns of as-prepared Cu doped PS/CdS and Ni doped PS/CdS films. All the diffraction peaks can be indexed as the cubic CdS crystals by comparing with the literature (Wu et al., 2004).

3.2. UV–visible spectroscopy

UV–visible spectra of pristine and irradiated samples of pure PS, Cu doped PS/CdS and Ni doped PS/CdS are shown in Figs. 4–6 respectively. The spectra of pure PS, Cu doped PS/CdS and Ni doped PS/CdS (Figs. 4–6) reveals the shift of absorption peak towards higher wavelength regime. This may be due to the formation of extended system of conjugated bonds Singh et al., 2007; El-Badry et al., 2009). The absorption bands are associated

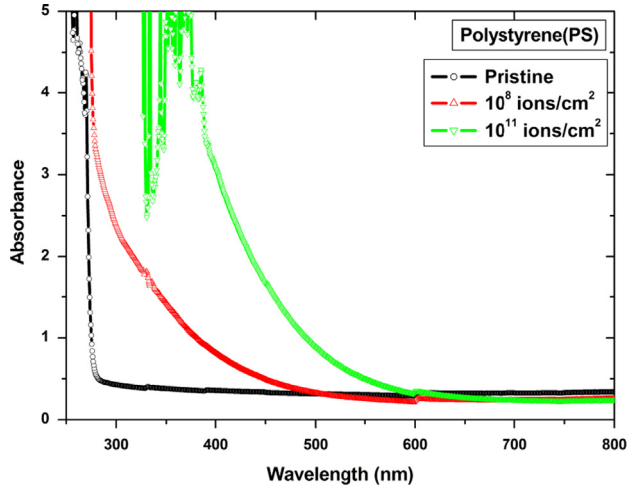

Fig. 4. UV–visible spectra of pristine and Ni^{5+} irradiated polystyrene (PS) polymer films.

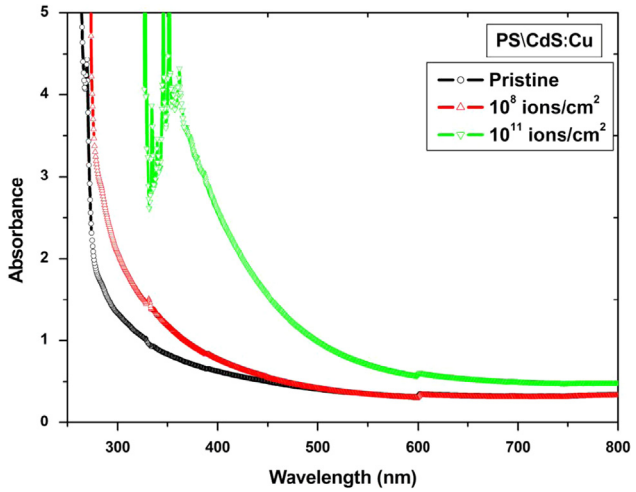

Fig. 5. UV–visible spectra of pristine and Ni^{5+} irradiated PS/CdS: Cu films.

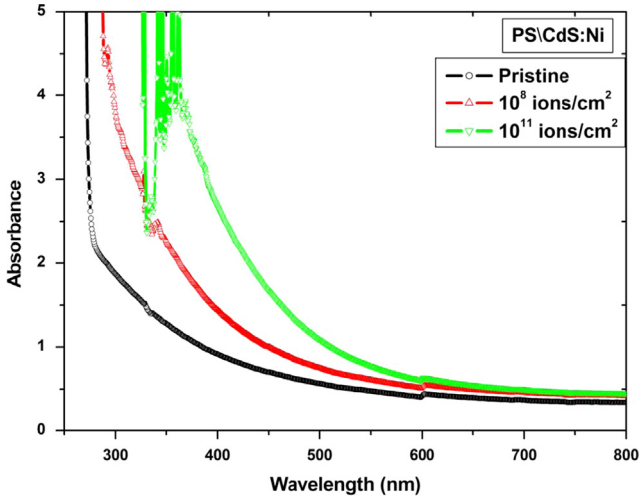

Fig. 6. UV–visible spectra of pristine and Ni^{5+} irradiated PS/CdS: Ni films.

with π–π^* electronic transitions (Singh et al., 2007). The energy band gap values of the pristine and irradiated sample films were calculated by using Tauc's expression (Tauc et al., 1996) as per

following equation:

$$(\alpha h\nu) = B(h\nu - E_g)^{1/2} \quad (1)$$

Here α is the absorption coefficient, $h\nu$ is the photon energy, B is band tailing parameter (Metwally, 1901) and E_g is the value of energy band gap. The E_g values of the films were calculated by the extrapolation of the plot of $(\alpha h\nu)^{1/2}$ versus $(h\nu)$ to the energy axis. The calculated values of E_g are tabulated in Table 2. The band gap value of pristine polystyrene is in close agreement with the value calculated by Singh and Samra, 2008; Singh et al., 2007. The table values clearly indicate the decrease in E_g value with doping of metal ion as well as with ion irradiation. The doping of Cu and Ni to PS/CdS decreases the band gap from pure polystyrene polymer from 4.35 eV to 3.95 and 3.42 eV respectively. Irradiation decreases the band gap further to quite a drastic level. There is 35%, 9% and 12% decrease in band gap from their pristine values for irradiated samples of PS, Cu doped PS/CdS and Ni doped PS/CdS films respectively at a fluence of 10^8 ions/cm^2. Whereas this decrease is 46%, 31% and 22% from their pristine values of PS, Cu doped PS/CdS and Ni doped PS/CdS films at a fluence of 10^{11} ions/cm^2. In the literature (Fink et al., 1996; Phukan et al., 2003) it has been shown that carbon enriched domains created in polymers during irradiations may be the reason for the decrease in band gap energy.

No. of carbon hexagon rings per conjugation length (N) were calculated from the modified Robertson relation (Kumar et al., 2011) using following equation:

$$E_g \approx (34.3/N^{1/2}) \quad (2)$$

The calculated values of N are tabulated in Table 2. The values are increasing with doping and ion irradiation as well as with increase of ion fluence.

3.3. FTIR spectroscopy

The FTIR spectrum of pristine polystyrene in Fig. 7 conforms to the spectrum reported by Evelyn et al., 1999. The spectrum shows the lines due to aromatic ring C–H stretching vibrations at 3081, 3060 and 3026 cm^{-1}, C–H stretch vibrations in CH_2 group at 2922 and 2851 cm^{-1}, the aromatic ring vibrations at 1602 and 1493 cm^{-1} and the lines due to the CH_2 deformation vibrations at 1452 cm^{-1} (Kondyurin et al., 2008; 2006). The intensity of all of these lines decreased after irradiation. In addition to it the C–H bending vibrations (675–950 cm^{-1} region) reduced in deeper layers at the fluence of 10^{11} ions/cm^2. The bands in the range 1755–2000 cm^{-1} disappeared completely at the fluence of 10^{11} ions/cm^2. No new absorption lines were observed in spectra of irradiated PS samples.

The FTIR spectra of pristine and irradiated samples of PS/CdS: Cu and PS/CdS: Ni nanocomposites are shown in Figs. 8 and 9 respectively. The vibrational absorption peak of the Cd–S bond can be observed at 405 cm^{-1} in both figures (Wu et al., 2004). The intensity of styrene absorption lines (3081, 3060, 3026, 2922, 2851, 1602, 1493 and 1452 cm^{-1}) decreased in irradiated samples of both the figures. No new peak could be observed in the spectra of irradiated samples of these figures also.

Table 2
Calculated values of band gap energy (E_g) and number of carbon hexagon rings per conjugation length (N) for PS, PS/CdS: Cu and PS/CdS: Ni nanocomposite films.

Sample	Fluence (ions/cm^2)	E_g (eV)	Value of N
PS	Pristine	4.35	62
	10^8	2.80	150
	10^{11}	2.34	215
PS\CdS: Cu	Pristine	3.95	75
	10^8	3.60	91
	10^{11}	2.73	158
PS\CdS: Ni	Pristine	3.42	100
	10^8	2.99	131
	10^{11}	2.66	166

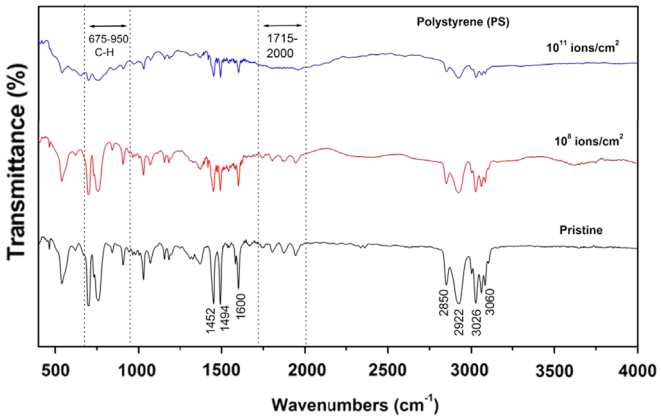

Fig. 7. FTIR spectra of pristine and Ni^{5+} irradiated polystyrene films.

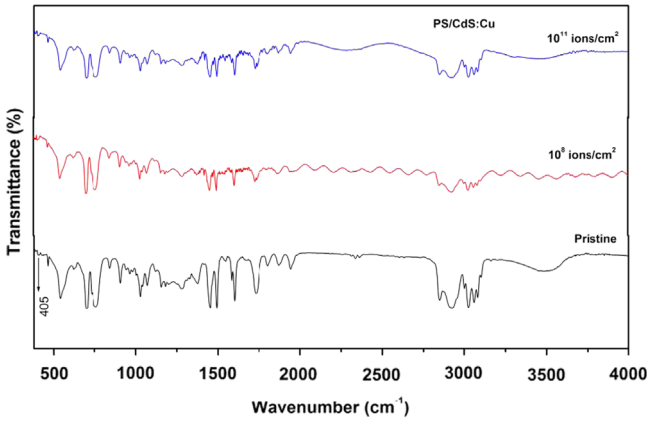

Fig. 8. FTIR spectra of pristine and Ni^{5+} irradiated PS/CdS: Cu films.

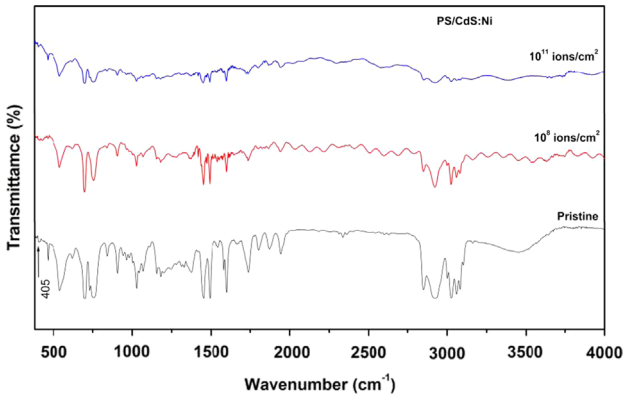

Fig. 9. FTIR spectra of pristine and Ni^{5+} irradiated PS/CdS: Ni films.

4. Conclusion

Ion beam irradiation is an effective tool to modify the material's properties. CdS nanoparticles of average size 50–60 nm were synthesized by micro-emulsion method. The polystyrene/CdS nanocomposites were doped with Ni and Cu metals followed by Ni ion irradiation. The effect of doping of metals and ion irradiation was studied for structural, optical and chemical modifications. The doping of metals decreased the optical energy band gap. The band

gap was further decreased when the doped samples of PS/CdS were irradiated with Ni ions. The decrease in band gap energy by ion irradiation was attributed to conjugated bonds formation. In addition to it, the amorphous nature of polystyrene decreased after ion irradiation at a fluence of 10^{11} ions/cm^2. The intensity of styrene absorption lines in FTIR spectra decreased in all irradiated samples. No new band formation was observed after ion beam irradiation in PS, PS/CdS: Ni and PS/CdS: Cu. The optical band gap energy of polymer nanocomposites can be controlled by irradiation with controlled ion beam. This can be engineered by controlling the ion beam parameters such as beam current, ion mass, charge and energy.

Acknowledgments

The authors are thankful to Dr. F. Singh, Dr. P. Kulriya, Dr. D. C. Agarwal and Inter University Accelerator Centre, New Delhi, India staff for providing help during irradiation and characterizations. The suggestions given by Prof. Rajendra Prasad, VCTM, Aligarh, India during data analysis and result discussions are gratefully acknowledged.

References

Alivisatos, A.P., 1996. Semiconductor clusters, nanocrystals, and quantum dots. Science 271 (5251), 933–937.
Artemyev, M.V., Woggon, U., Wannemacher, R., Jaschinski, H., Langbein, W., 2001. Light trapped in a photonic dot: microspheres act as a cavity for quantum dot emission. Nano Lett. 1, 309–314.
Awasthi, K., Kulshrestha, V., Avasthi, D.K., Vijay, Y.K., 2010. Optical, chemical and structural modification of oxygen irradiated PET. Radiat. Meas. 45, 850–855.
Balanzat, E., Bouffard, S., Cassani, A., Dooryhee, E., Protin, L., Grandin, J.P., Doualan, J.L., Margerie, J., 1994. Defect creation in alkali-halides under dense electronic excitations: experimental results on NaCl and KBr. Nucl. Instrum. Methods Phys. Res. Sect. B 91, 134–139.
Chen, L., Zhu, J., Li, Q., Chen, S., Wang, Y., 2007. Controllable synthesis of functionalized CdS nanocrystals and CdS/PMMA nanocomposite hybrids. Eur. Polym. J. 43, 4593–4601.
El-Badry, B.A., Zaki, M.F., Abdul-Kader, A.M., Hegazy, T.M., Morsey, A.A., 2009. Ion bombardment of poly-allyl-diglycol-carbonate (CR-39). Vacuum 83, 1138–1142.
Evelyn, A.L., Ila, D., Zimmerman, R.L., Bhat, K., Poker, D.B., Hensley, D.K., Klatt, C., Kalbitzer, S., Just, N., Drevet, C., 1999. Ion beam modification of PES, PS and PVC polymers. Nucl. Instrum. Methods Phys. Res. Sect. B 148, 1141–1145.
Farmer, S.C., Pattern, T.E., 2001. Photoluminescent polymer/quantum dot composite nanoparticles. Chem. Mater. 13, 3920–3926.
Fink, D., Klett, R., Chadderton, L.T., Cardosa, J.M., Montiel, R., Vezquez, H., Karanovich, A., 1996. Carbonaceous clusters in irradiated polymers as revealed by small angle X-ray scattering and ESR. Nucl. Instrum. Methods Phys. Res. Sect. B 111, 303–314.
Gorelikov, I., Kumacheva, E., 2004. Electrodeposition of polymer–semiconductor nanocomposite films. Chem. Mater. 16, 4122–4127.
Guzman, A.M., Carlson, J.D., Baras, J.E., Pronko, P.P., 1985. Chemical and physical changes induced in polyvinylidene fluoride by irradiation with high energy ions. Nucl. Instrum. Methods Phys. Res. Sect. B 7–8, 468–472.
Han, Z., Zhu, H., Bulcock, S.R., Ringer, S.P., 2005. One-step synthesis and structural features of CdS/montmorillonite nanocomposites. J. Phys. Chem. B 109, 2673–2678.
Kanjilal, D., 2001. Swift heavy ion-induced modification and track formation in materials. Curr. Sci. 80, 1560–1566.
Kondyurin, A., Gan, B.K., Bilek, M.M.M., McKenzie, D.R., Mizuno, K., Wuhrer, R., 2008. Argon plasma immersion ion implantation of polystyrene films. Nucl. Instrum. Methods Phys. Res. Sect. B 266, 1074–1084.
Kondyurin, A., Gan, B.K., Bilek, M.M.M., Mizuno, K., McKenzie, D.R., 2006. Etching and structural changes of polystyrene films during plasma immersion ion implantation from argon plasma. Nucl. Instrum. Methods Phys. Res. Sect. B 251, 413–418.
Kulshrestha, V., Awasthi, K., Acharya, N.K., Singh, M., Bhagwat, P.V., Vijay, Y.K., 2006. Structural, optical, thermo mechanical and transport property of ion irradiated polymer membranes. Polym. Bull. 56, 427–435.
Kumar, R., Ali, S.A., Singh, P., Prasad, R., 2011. Physical and chemical response of 145 MeV Ne^{6+} ion irradiated polymethylmethacrylate (PMMA) polymer. Nucl. Instrum. Methods Phys. Res. Sect. B 269, 1755–1759.
Kumar, R., De, U., Prasad, R., 2006. Physical and chemical response of 70 MeV carbon ion irradiated polyether sulphone polymer. Nucl. Instrum. Methods Phys. Res. Sect. B 248, 279–283.
Lee, E.H., Rao, G.R., Mansur, L.K., 1999. LET effect on cross-linking and scission mechanisms of PMMA during irradiation. Radiat. Phys. Chem. 55, 293–305.
Metwally, H.S., 1901. Electrical and optical studies in $Ge_{100-x}S_x$ chalcogenide thin films. Acta Phys. Pol. A 99, 683–690.
Peng, X., Schlamp, M.C., Kadavanich, A.V., Alivisatos, A.P., 1997. Epitaxial growth of highly luminescent CdSe/ CdS core/ shell nanocrystals with photostability and electronic accessibility. J. Am. Chem. Soc. 119, 7019–7029.
Peng, Z.A., Peng, X., 2001. Formation of high quality CdTe, CdSe and CdS nanocrystals using CdO as precursor. J. Am. Chem. Soc. 123, 183–184.
Phukan, T., Kanjilal, D., Goswami, T.D., Das, H.L., 2003. Study of optical properties of swift heavy ion irradiated PADC polymer. Radiat. Meas. 36, 611–614.
Picq, V., Ramillon, J.M., Balanzat, E., 1998. Swift heavy ions on polymers: hydrocarbon gas release. Nucl. Instrum. Methods Phys. Res. Sect. B 146, 496–503.
Rong, M.Z., Zhang, M.Q., Liang, H.C., Zeng, H.M., 2003. Surface modification and particle size distribution control in nano-CdS/polystyrene composite film. Chem. Phys. 286, 267–276.
Singh, L., Samra, K.S., 2008. Opto-structural characterization of proton (3 MeV) irradiated polycarbonate and polystyrene. Radiat. Phys. Chem. 77, 252–258.
Singh, L., Samra, K.S., Singh, R., 2007. Opto-chemical response of CR-39 and polystyrene to swift heavy ion irradiation. Nucl. Instrum. Methods Phys. Res. Sect. B 255, 350–356.
Singh, N.L., Shah, S., Qureshi, A., Tripathi, A., Singh, F., Avasthi, D.K., Raole, P.M., 2011. Effect of ion beam irradiation on metal particle doped polymer composites. Bull. Mater. Sci. 34 (1), 81–88.
Singh, P., Kumar, R., Prasad, R., 2013. Free volume evolution in 50 MeV Li^{3+} ion-irradiated polymers studied by positron annihilation lifetime spectroscopy. Radiat. Eff. Defects Solids 168, 97–105.
Steckenreiter, T., Balanzat, E., Fuess, H., Trautmann, C., 1997. Chemical modifications of PET induced by swift heavy ions. Nucl. Instrum. Methods Phys. Res. Sect. B 131, 159–166.
Tauc, J., Grigorovici, R., Vancu, A., 1996. Optical properties and electronic structure of amorphous germanium. Phys. Status Solidi 15, 627–637.
Tesster, N., Medvededev, V., Kazes, M., Kan, S., Banin, U., 2002. Efficient near-infrared polymer nanocrystal light-emitting diodes. Science 295, 1506–1508.
Tombrello, T.A., 1994. Predicting latent track dimensions. Nucl. Instrum. Methods Phys. Res. Sect. B 94, 424–428.
Vijay, Y.K., Kulshrestha, Vaibhav, Awasthi, Kamlendra, Acharya, N.K., Jain, A., Singh, M., Dolia, S.N., Khan, S.A., Avasthi, D.K., 2006. Characterization of nanocompsoite polymeric membrane. J. Polym. Res. 13, 357–360.
Wu, D., Ge, X., Zhang., Z., Wang, M., Zhang, S., 2004. Novel one-step route for synthesizing CdS/polystyrene nano-composite hollow spheres. Langmuir 20, 5192–5195.
Ziegler, J.F., 2010. SRIM—the stopping and range of ions in matter (2010). Nucl. Instrum. Methods Phys. Res. Sect. B 268, 1818–1823.
Zhu, L., Zhu, M.Q., Hurst, J.K., Li, A.D.Q., 2005. Spiropyran-based photochromic polymer nanoparticles with optically switchable luminescence. J. Am. Chem. Soc. 127, 8968–8970.

Nuclear Instruments and Methods in Physics Research B 358 (2015) 258–262

Contents lists available at ScienceDirect

Nuclear Instruments and Methods in Physics Research B

journal homepage: www.elsevier.com/locate/nimb

SHI irradiation of metal doped zinc sulfide polymer nanocomposites synthesized using micro emulsion method

Satyendra Kumar [a], Paramjit Singh [b], R.G. Sonkawade [c], Kamlendra Awasthi [d], Rajesh Kumar [b,*]

[a] Department of Applied Physics, School of Physical Sciences, Babasaheb Bhimrao Ambedkar University, Lucknow 226025, India
[b] University School of Basics and Applied Sciences, Guru Gobind Singh Indraprastha University, New Delhi 110078, India
[c] Inter University Accelerator Centre, New Delhi 110067, India
[d] Department of Physics, Malaviya National Institute of Technology, Jaipur 302017, India

ARTICLE INFO

Article history:
Received 23 March 2015
Received in revised form 2 July 2015
Accepted 3 July 2015

Keywords:
ZnS/polystyrene composite films
Ion beam irradiation
XRD
UV–Vis
FTIR

ABSTRACT

The metal doped ZnS nanoparticles dispersed in polystyrene were synthesized using micro emulsion method. The synthesized free standing nanocomposites films of 18 μm thickness were irradiated with 60 MeV nickel ions at two different fluences for the modification of structural, optical and chemical properties. The pristine and irradiated samples were characterized by X-ray diffraction, UV–visible and FTIR spectrophotometer. The SEM and XRD results confirmed the synthesis of nanoparticles. The ion irradiation shifted the optical absorption towards higher wavelength and decreased the band gap energy to significant levels. The infrared band at 465 cm^{-1} confirmed the Zn–S bonding. The intensity of other absorption bands was modified after ion irradiation.

1. Introduction

The polymer and nanoparticles intermixing to form nanocomposites has been widely practiced because of their large number of applications; such as those in optoelectronics, sensors, medical devices, drug delivery and membrane industry etc [1]. The control over the shape, size and functional properties of nanoparticles may be used to modify the mechanical, thermal, tribological, optical, electrical, magnetic, chemical and many other properties of the polymer nanocomposites [2]. There is wide range of literature available upon the different type of polymer nanocomposites, their synthesis and applications; but our focus is upon the ZnS nanoparticles intermixed with polystyrene polymer. ZnS is an important II–VI group semiconductor material. ZnS can have two different crystal structures (zinc blende and wurtzite), both of which have the same band gap energy (3.68 eV) and the direct band structure. It is widely used as phosphor in photoluminescence, electroluminescence and optical sensor [3,4]. The large amount of work has been carried out upon the Zn based polystyrene nanocomposites synthesized by different methods in the last decade [5–10]. In addition to it, some recent reports are published upon the Zn based polymer nanocomposites, other than polystyrene [10,11]. The above cited reports have been focused upon the studies of polymer nanocomposites by varying the concentration of the nanoparticles in the polymer matrix. The other idea to modify the material properties is by the way of controlled swift heavy ions (SHI) beam irradiation and ions implantation. There are some recent reports available on the ion beam modification of metal doped polymer nanocomposites [12–14]. There is no data available upon the ion beam treatment of ZnS doped polystyrene nanocomposites to the best of our knowledge. The present study is based upon the synthesis of ZnS nanoparticles by micro emulsion method; the synthesized ZnS nanoparticles were intermixed with polystyrene by solution cast method to form nano composite thin films. The synthesized films were irradiated with 60 MeV nickel ions for the study of structural, optical and chemical modifications.

2. Experimental

2.1. Materials and methods

Polystyrene (density 1.06 g/mL) of average molecular weight 35,000 and all other chemicals/solvents were purchased from Sigma Aldrich. All the chemicals were used as-received without any further treatment.

The structural, optical and chemical studies of pristine and irradiated samples were carried out at Inter University Accelerator

* Corresponding author.
E-mail address: rajeshkumaripu@gmail.com (R. Kumar).

http://dx.doi.org/10.1016/j.nimb.2015.07.010
0168-583X/

Centre (IUAC), New Delhi, India. X-ray diffraction studies were carried out by using Bruker AXS system with Cu-K_α radiation (1.54 Å) for a wide range of Bragg angles 2θ ($5 \leqslant 2\theta \leqslant 80$). UV–visible studies were carried out in the wavelength range 250–800 nm using U-3300 Hitachi system. Infrared measurements were performed in transmission mode using Nicolet Nexus 670 FTIR spectrometer.

2.2. Preparation of ZnS nanoparticles and nanocomposites films

The synthesis of ZnS nanoparticles was carried out by the reaction of zinc chloride ($ZnCl_2$) and sodium sulfide (Na_2S) in water-in-oil micro emulsion system [15]. Micro-emlusion of $ZnCl_2$ and Na_2S have 0.46 g of *n*-pentanol, 3.37 g of Triton X-100, 7.64 g of cyclohexane and 1 g of water. Molar ratio of water and surfactant was maintained at 1:1 while for sulfide and zinc ions was constant (=1). Concentration of sulfide and zinc were estimated per aqueous phase [16]. ZnS nanoparticles were successfully doped through chemical method reported in literature [17,18].

The 20–60 nm sized nanoparticles were obtained and confirmed in the SEM image (Fig. 1). The nanocomposites of ZnS and polystyrene were synthesized by solution cast method. The polystyrene (PS) polymer was dissolved in chloroform and ZnS nanoparticles were added to this solution followed by ultrasonic agitation for uniform arrangement. The obtained mixture was poured on to a clean glass petri disc floating on Hg to maintain uniform thickness of prepared sample. The solvent was allowed to evaporate at room temperature (25 °C) to get thin films of polymer composites and finally films were then dried in vacuum oven at 30 °C to remove the solvent content [19]. Average thickness of prepared thin films have been found 18 ± 2 μm and calculated as per weight, area and density relation.

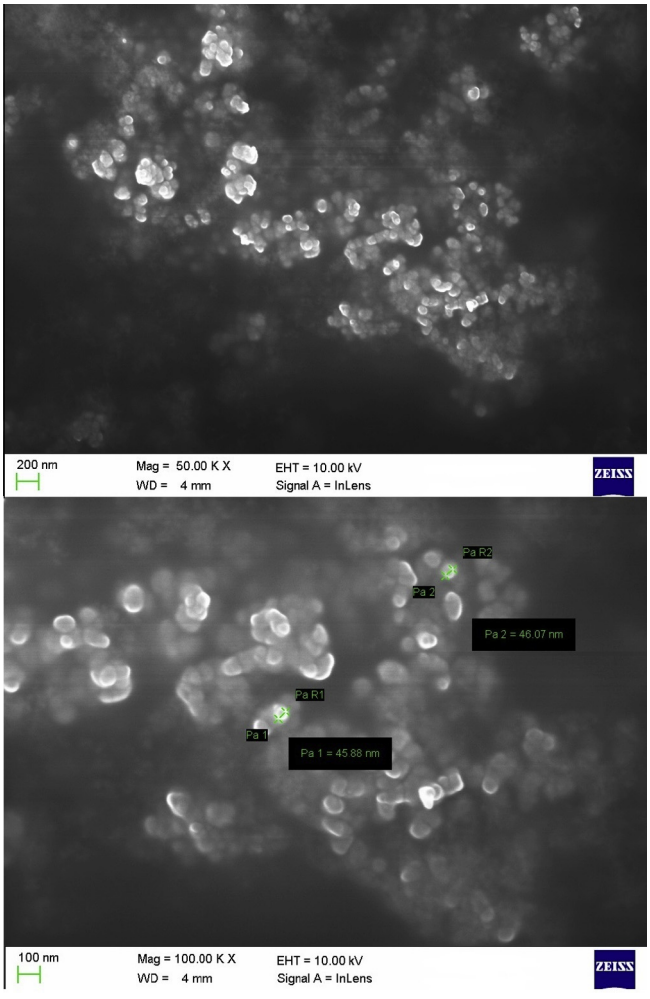

Fig. 1. SEM image of ZnS nanoparticles synthesized by micro emulsion method.

2.3. Preliminary calculations and ions irradiation

The preliminary calculations were carried out using SRIM-2010 code for ions range and energy loss inside the material [20]. The calculated values of electronic energy loss (S_e), nuclear energy loss (S_n) and projected range values are tabulated in Table 1. Our sample thickness of 18 μm is compatible with the SRIM calculated projected range for ions to pass through the sample; ensuring negligibly small ions implantation. The S_n values are also quite small, so the nuclear energy loss was least probable.

The irradiation experiment was carried out at Material Science chamber in IUAC, New Delhi, India. The composite samples of size 1.5 cm × 1.5 cm were mounted on the vertical ladder. The ladder was mounted in general purpose scattering chamber and the chamber was evacuated to $\sim 6 \times 10^{-6}$ Torr. The 60 MeV Ni^{5+} beam was selected for irradiation; the beam current was 0.5 pnA (particle nano-ampere). Two fluences, 10^{10} and 10^{11} ions/cm^2 were selected for irradiation.

3. Results and discussion

3.1. Structural studies by X-ray diffraction

The X-ray diffraction (XRD) was performed to determine the crystallographic orientation of ZnS nanoparticles. The Fig. 2 shows the diffraction patterns of Cu doped and Ni doped polystyrene ZnS (PS/ZnS) nanocomposites in 2θ mode. The polystyrene broad peak was observed at 19.38° in both cases. The intensity of this peak increased slightly after ion irradiation, which was insignificant for structural modifications. The prominent peaks observed at 35.35°, 39.44° and 53.73° are attributed to (002), (100) and (103) respectively, these peaks attribute the formation of ZnS nanoparticles and Zn blende structure [3,21].

3.2. Optical studies by UV–visible spectroscopy

Fig. 3(a)–(c) reveal the UV–visible absorption spectra of PS/ZnS, Cu doped PS/ZnS and Ni doped PS/ZnS nanocomposites respectively. The shift of the absorption peak towards longer wavelength was observed due to the formation of conjugated system of bonds after ion irradiation [22–24]. The shift became more pronounced as the ion fluence was increased. The band gap energy was observed to be decreased due to the formation of conjugated system of bonds. The band gap energy was calculated using Tauc's relation as following [25–27].

$$(\alpha h\nu) = B(h\nu - E_g)^2 \quad (1)$$

Table 1
SRIM calculated S_e, S_n values and projected range of 60 MeV Ni ion beams for target samples.

Target material	S_e (eV/Å)	S_n (eV/Å)	Projected range (μm)
PS	5.20×10^2	1.21	19.71
PS/ZnS	5.68×10^2	1.49	18.16
PS/ZnS: Cu	6.36×10^2	1.74	16.48
PS/ZnS: Ni	6.47×10^2	1.78	16.14

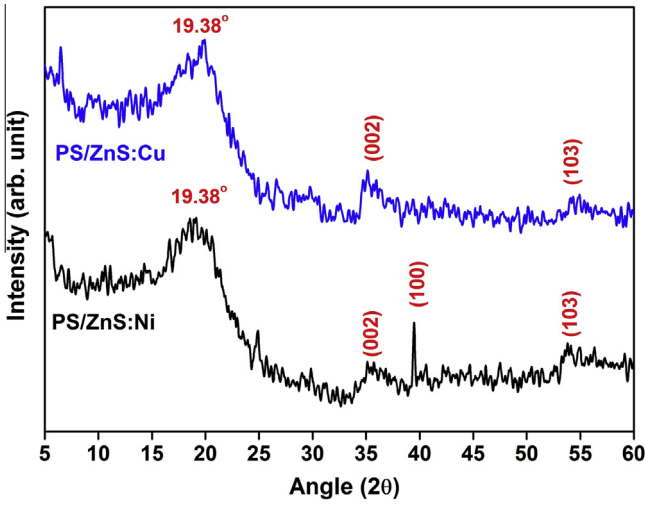

Fig. 2. X-ray diffraction patterns of PS/ZnS: Cu and PS/ZnS: Ni nanocomposites.

Here α is the absorption coefficient, $h\nu$ is the photon energy, B is band tailing parameter and E_g is the value of energy band gap for indirect transition [28]. The band gap of the nanocomposites films were calculated by the extrapolation of the plot of $(\alpha h\nu)^{1/2}$ versus $(h\nu)$ [29]. The calculated values are tabulated in Table 2. There is quite observable decrease in the value of E_g after ion exposure, also the band gap energy was decreased with the doping of Cu and Ni as compared to the pure polystyrene (4.35 eV) as per our previous reported data [30]. On the similar grounds, the number of carbon hexagon rings (N) was observed to be increased in number with the increase of ion fluence as per the values given in Table 2. The value of N was calculated using following equation [31,32].

$$E_g \approx (34.3/N^{1/2}) \quad (2)$$

3.3. Chemical studies via FTIR spectrophotometry

The FTIR spectra (in the wave number range of 400–4000 cm^{-1}) of pristine and irradiated samples of Cu doped PS/ZnS and Ni doped PS/ZnS are shown in Figs. 4 and 5 respectively. In FTIR spectra of Cu and Ni doped PS/ZnS sample, the peak at 465 cm^{-1} is due to Zn–S bonding and the band at 1734 cm^{-1} correspond to the C=O stretching [11]. The peak at 1495 cm^{-1} is responsible for aromatic stretches and the bands in the range 1700–1950 cm^{-1} are responsible for aromatic overtone [9]. The broad absorption band at 2915 cm^{-1} is assigned to C–H bond of PS [33]. The peaks of frequency range 2850–3000 cm^{-1} are observed which indicate the presence of CH stretch bonds which would confirm the functional group of alkanes.

The intensity of the bands changed after SHI irradiation. The intensity of some of the bands decreased very fast with increase of the ion fluence. The strong absorption band in the frequency range of 900–675 cm^{-1} showed the presence of aromatic group. FTIR spectra of Cu doped PS/ZnS in Fig. 4 show sharp fall in intensity of the bands at 1450 cm^{-1} and 1500 cm^{-1} representing C–H stretch attributed to chain scission which may be taking place at the carbonate site with the formation of new hydroxyl group. The intensity of the absorption band of C–C stretch at the frequency range of 1585–1600 cm^{-1} decreased after irradiation. It

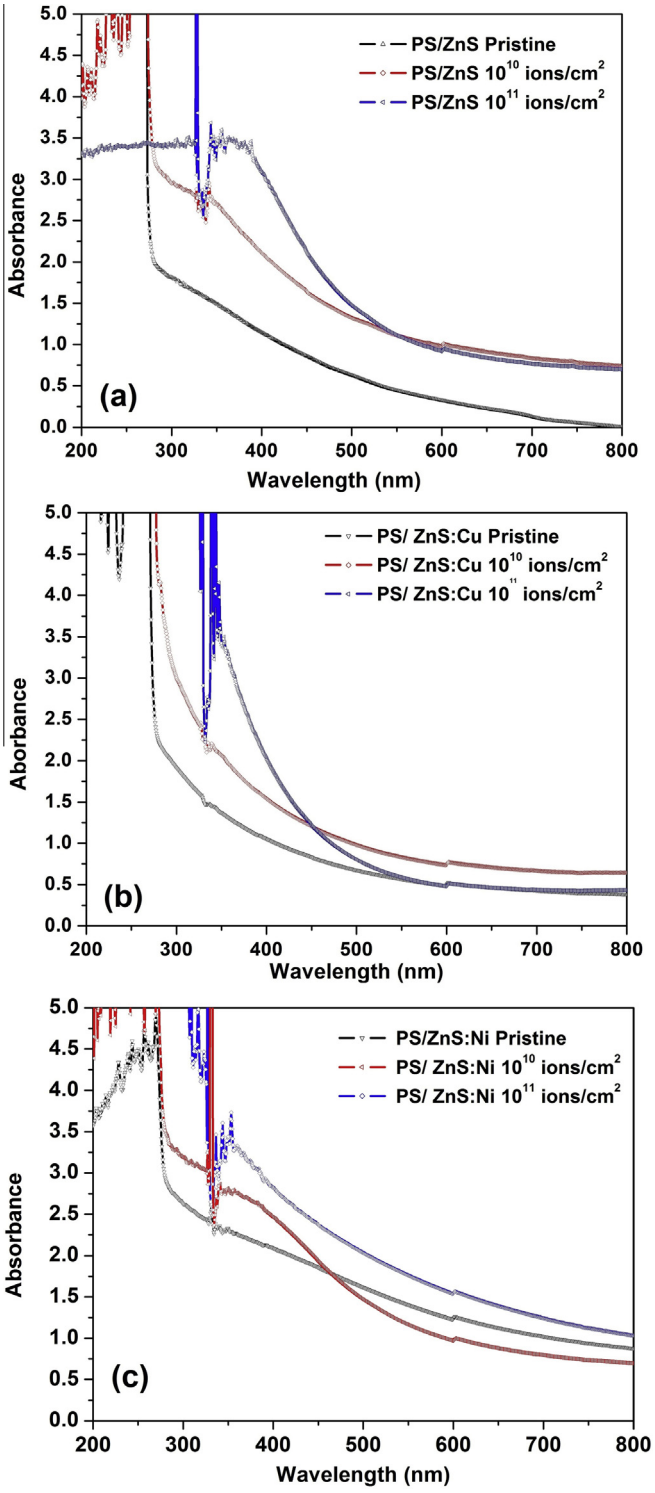

Fig. 3. UV–visible absorption spectra of (a) PS/ZnS, (b) Cu doped PS/ZnS and (c) Ni doped PS/ZnS nanocomposites.

Table 2
Variation of band gap energy (E_g) and number of carbon atoms per conjugation length (N) for Cu doped PS/Zn and Ni doped PS/ZnS nanocomposite films.

Sample	Fluence (ions/cm^2)	E_g (eV)	N
PS/ZnS:Cu	Pristine	4.20	67
	10^{10}	3.50	96
	10^{11}	3.06	126
PS/ZnS:Ni	Pristine	3.92	77
	10^{10}	2.81	149
	10^{11}	2.65	168

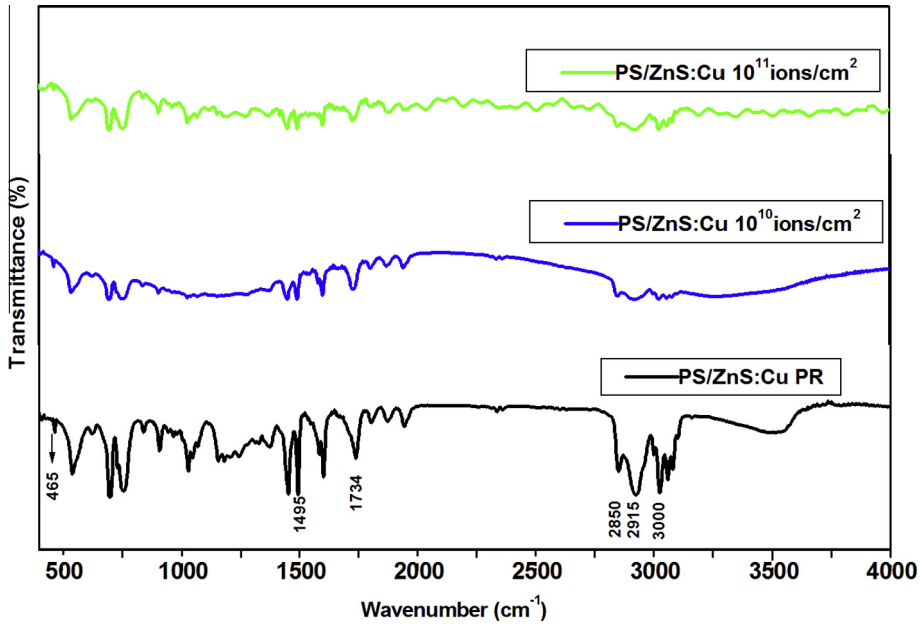

Fig. 4. FTIR spectra of PS/ZnS: Cu film irradiated with 60 MeV Ni ion beam.

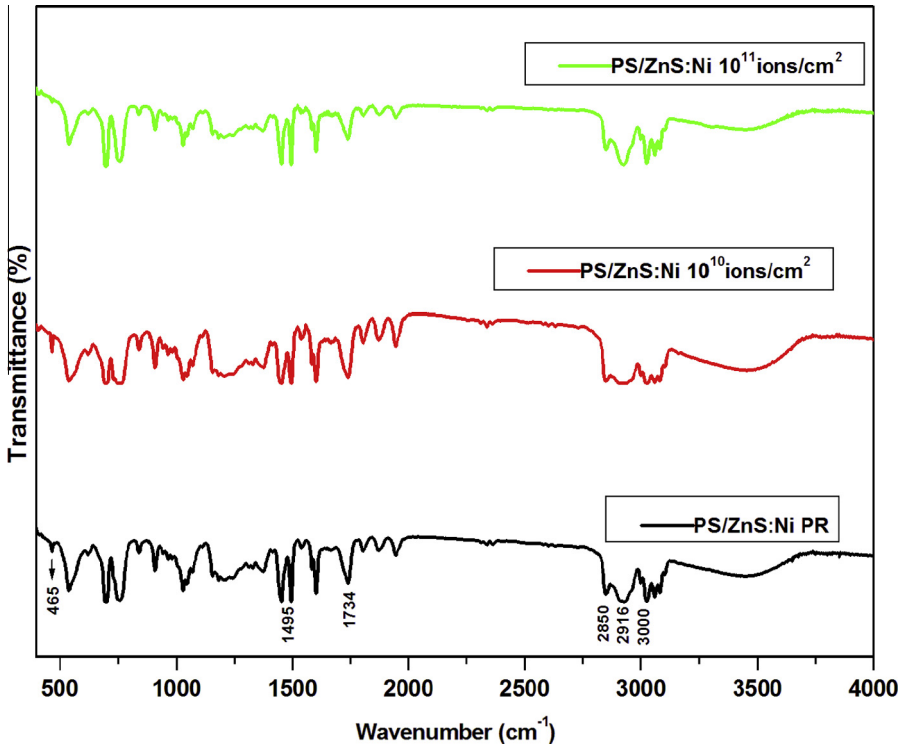

Fig. 5. FTIR spectra of PS/ZnS: Ni film irradiated with 60 MeV Ni ion beam.

explains that chain scissoring took place in metal doped nanocomposites after ion irradiation. There were significant decreases in absorption with ion irradiation for the Cu doped samples (Fig. 4), but this effect was not true for the Ni doped samples (Fig. 5). This may be attributed to reduction in particle size as a result of incorporation of Cu^{2+} ions with comparable radius to that of Zn^{2+} ions. Considering the Bohr exciton radius of ZnS (2.5 nm), our sample had a strong confinement regime and attributed to decrease in the absorbance shoulder.

4. Conclusion

The 20–60 nm sized ZnS nanoparticles were synthesized by micro emulsion method and dispersed in polystyrene polymer. The polymer nanocomposites were doped with Ni and Cu metals to obtain Ni doped and Cu doped PS/ZnS nanocomposites. The size of nanoparticles was verified by SEM results. The obtained Zn blende structure was confirmed by the (002), (100) and (103) peaks in the XRD results. The composites were irradiated with

60 MeV Ni^{5+} ions to further modify the structural, optical and chemical properties. There was minor increase in the polymer broad X-ray peak at 19.38° after ion irradiation. The shift of the absorption peak towards longer wavelength was observed due to the formation of conjugated system of bonds after ion irradiation in the UV–visible studies. The shift became more pronounced as the ion fluence was increased. The band gap energy was observed to be decreased due to the formation of conjugated system of bonds. There was 27% and 32% decrease in the band gap energy of the PS/ZnS:Cu and PS/ZnS:Ni composites after ion irradiation at fluence of 10^{11} ions/cm^2. The Zn–S bonding was confirmed in the FTIR band at 465 cm^{-1}.

Acknowledgments

The authors are thankful to staff of IUAC, New Delhi, India for providing the necessary facilities of ion irradiation and characterizations.

References

[1] A. Kumari, S.K. Yadav, S.C. Yadav, Colloids Surf. B 75 (2010) 1–18.
[2] F.J. Carrión, J. Sanes, M.D. Bermúdez, Mater. Lett. 61 (2007) 4531–4535.
[3] B. Bodo, R. Singha, S.C. Das, Int. J. Appl. Phys. Math. 02 (2012) 287–289.
[4] J.P. Borah, J. Barman, K.C. Sarma, Chalcogenide Lett. 5 (2008) 201–208.
[5] W. Chae, B.C. Kim, Polym. Adv. Technol. 16 (2005) 846–850.
[6] Chen-Chi M. Ma, Yi-Jie Chen, Hsu-Chiang Kuan, J. Appl. Polym. Sci. 100 (2006) 508–515.
[7] Manzi-Nshuti, D. Chen, S. Su, C.A. Wilkie, Polym. Degrad. Stab. 94 (2009) 1290–1297.
[8] Y. Tu, L. Zhou, Y.Z. Jin, C. Gao, Z.Z. Ye, Y.F. Yang, Q.L. Wang, J. Mater. Chem. 20 (2010) 1594–1599.
[9] X. Cheng, Q. Zhao, Y. Yang, S.C. Tjong, R.K.Y. Li, J. Mater. Sci. 45 (2010) 777–782.
[10] S. Awad, H. Chen, G. Chen, X. Gu, J.L. Lee, E.E. Abdel-Hady, Y.C. Jean, Macromolecules 44 (2011) 29–38.
[11] K. Kole, S. Gupta, P. Kumbhakar, P.C. Ramamurthy, Opt. Commun. 313 (2014) 231–237.
[12] M.G. de Julián Fernández, J. Manera, G. Spadavecchi, A. Maggioni, G. Quaranta, M. Mattei, E. Bazzan, M. Cattaruzza, E. Bonafini, A. Negro, S. Vomiero, C. Carturan, G. Della Mea, R. Rella, L. Vasanelli, P. Mazzoldi, Sens. Actuators B 111–112 (2005) 225–229.
[13] Y.K. Mishra, V.S.K. Chakravadhanula, U. Schürmann, H. Kumar, D. Kabiraj, S. Ghosh, V. Zaporojtchenko, D.K. Avasthi, F. Faupel, Nucl. Instr. Meth. Phys. Res. Sect. B 266 (2008) 1804–1809.
[14] S.S. Ray, Polymer 51 (2010) 3966–3970.
[15] S.K. Kulkarni, U. Winkler, N. Deshmukh, P.H. Borse, R. Fink, E. Umbach, Appl. Surf. Sci. 169–170 (2001) 438–446.
[16] D.J. Jovanović, Ivana Lj. Validžić, I.A. Janković, N. Bibić, J.M. Nedeljković, Mater. Lett. 61 (2007) 4396–4399.
[17] V. Ramasamy, K. Praba, G. Murugadoss, Spectrochim. Acta A 96 (2012) 963–971.
[18] G. Murugadoss, J. Lumin. 132 (2012) 2043–2048.
[19] N.L. Singh, S. Shah, A. Qureshi, A. Tripath, F. Singh, D.K. Avasthi, P.M. Raole, Bull. Mater. Sci. 34 (1) (2011) 81–88.
[20] J.F. Ziegler, M.D. Ziegler, J.P. Biersack, Nucl. Instr. Meth. Phys. Res. Sect. B 268 (2010) 1818–1823.
[21] H.A. Ali, A.A. Iliadis, L.J. Martinez-Miranda, U. Lee, Solid-State Electron. 50 (2006) 1105–1112.
[22] P. Singh, R. Kumar, Adv. Polym. Technol. 33 (3) (2014) 09.
[23] R.K. Dhillon, P. Singh, S.K. Gupta, S. Singh, R. Kumar, Nucl. Instr. Meth. Phys. Res. Sect. B 301 (2013) 12–16.
[24] P. Singh, R. Kumar, H.S. Virk, R. Prasad, Indian J. Pure Appl. Phys. 48 (2010) 321–325.
[25] N. Reddeppa, A.K. Sharma, V.V.R. Narasimha Rao, W. Chen, Measurement 47 (2014) 33–41.
[26] P. Singh, R. Kumar, J. Cyriac, M.T. Rahul, P.M.G. Nambissan, R. Prasad, Nucl. Instr. Meth. Phys. Res. Sect. B 320 (2014) 64–69.
[27] R. Kumar, P. Singh, Appl. Surf. Sci. 328 (2015) 482–490.
[28] P. Singh, R. Kumar, P.M.G. Nambissan, Vacuum 115 (2015) 31–38.
[29] P. Singh, R. Kumar, R. Singh, A. Roychowdhury, D. Das, Appl. Surf. Sci. 328 (2015) 482–490.
[30] S. Kumar, P. Singh, R.G. Sonkawade, K. Awasthi, R. Kumar, Radiat. Phys. Chem. 94 (2014) 49–53.
[31] P. Singh, S.A. Ali, R. Kumar, Radiat. Phys. Chem. 96 (2014) 181–185.
[32] R. Kumar, P. Singh, Results Phys. 3 (2013) 122–128.
[33] A.M. Arabi, T. Ebadzadeh, A.A. Yousefi, M. Pishvaei, E.M. Rad, C. Zamani, Micro Nano Lett. 6 (2011) 844–847.

Radiation Physics and Chemistry 94 (2014) 54–57

Contents lists available at ScienceDirect

Radiation Physics and Chemistry

journal homepage: www.elsevier.com/locate/radphyschem

Study of physical and chemical modifications induced by 50 MeV Li^{3+} ion beam in polymers

Paramjit Singh [a], Satyendra Kumar [b], Rajendra Prasad [c], Rajesh Kumar [a,*]

[a] University School of Basic & Applied Sciences, Guru Gobind Singh Indraprastha University, New Delhi 110078, India
[b] Baba Saheb Bhimrao Amedkar University, Lucknow 226025, India
[c] Vivekananda College of Technology & Management, Aligarh 202002, India

HIGHLIGHTS

- We irradiated the industrial polymers with Swift Heavy Ions at different fluences.
- Structural effects, optical and chemical changes after irradiation were examined by XRD, UV–Visible and FTIR spectroscopy respectively.
- Increase in crystalline nature and decrease in band gap is observed with increase in fluence.
- Increase in particle size and variation in the Urback's energy is observed with increase of fluence.
- The modifications caused by SHI in various chemical bonds are also discussed.

ARTICLE INFO

Article history:
Received 13 December 2012
Accepted 5 July 2013
Available online 16 July 2013

Keywords:
Polymers
Ion irradiation
XRD
UV–vis
Urbach's energy

ABSTRACT

Polyether-sulphone and polyamide-nylone-6 polymers were irradiated by 50 MeV Li^{3+} ions for modifications in structural, optical and chemical properties. The decrease in peak width and increase in peak intensity of XRD spectra indicated alignment of polymeric chains in a regular pattern and hence there was decrease in the amorphous character of the irradiated polymers. The gradual increase in the optical absorption and shift towards visible region was observed in optical absorption spectra of irradiated polymers. The increase in absorption was attributed to the generation of a conjugated system of bonds which lowered the band gap of irradiated polymers to significant values. The thermal fluctuations in the band gap energy due to temperature dependent self energies of the electrons were observed from the calculated values of the Urbach's energy. The FTIR spectra obtained after irradiation exhibited decrease in absorbance for various bands in case of PN-6 whereas opposite behavior was observed in case of PES polymer.

1. Introduction

The polymer modifications by ion beam irradiation has been established for industrial and research applications. The polymers under study are polyether-sulphone (PES) and polyamide-nylone-6 (PN-6). Some important results of ion beam modifications on these polymers during last decade are summarized below.

The effect of 150 keV argon ions on PES had been studied by Kurmaev et al., (1999) with fluorescent X-ray emission spectroscopy. They studied the electronic structure and chemical bonding of pristine and irradiated samples using deMon density function theory (DFT) and compared the calculated results with experimentally obtained X-ray fluorescence spectra. The change in polymer structure induced by 6 MeV electrons irradiation on PES was studied by Dudra and Wysocki, (2005). They predicted that the probabilities of cross-linking and chain-scission depend on irradiation dose and obtained the correlation between degree of cross-linking and fluorescence. The PN-6 sheets irradiated with electron beam were investigated in relation to their thermal stability in various environments (air, distilled water and NaCl solution) at 70 °C by Zaharescu et al., (2010). They predicted that the durability of irradiated samples in air is longer than in water and salt solutions. The grafting of monomers (acrylic, methacrylic acids and acrylamide) onto PN-6 was studied by Timus et al., (2000). They predicted the dependence of degree of grafting upon radiation dose and extent of monomer dilution. The early work on the above discussed polymers was mainly related to chemical and compositional study by low energy ions and electrons irradiation. Very limited data (Samra et al., 2011; Kulshrestha et al., 2010) is available on the study of optical and structural properties of these polymers by high energy ions irradiation.

The objective of this work is to study the structural and optical properties for the modifications of average crystallite size and

* Corresponding author. Mobile: +91 9718876101.
E-mail address: rajeshkumaripu@gmail.com (R. Kumar).

0969-806X/$ - see front matter © 2013 Elsevier Ltd. All rights reserved.
http://dx.doi.org/10.1016/j.radphyschem.2013.07.008

band gap energy by 50 MeV Li^{3+} ions irradiation. In addition to it, ion induced chemical modifications are also discussed.

2. Experimental methods

250 μm thick PES and PN-6 polymer flat sheets were procured from Goodfellow, Cambridge Ltd. (UK). The samples of size (1.5 cm × 1.5 cm) were cut from the sheets and used as-received form without any further treatment. The samples were exposed to 50 MeV Li^{3+} beam in material science beam line at inter university accelerator center (IUAC), New Delhi, India under high vacuum ($\sim 7 \times 10^{-6}$ Torr). Fluences were taken ranging from 10^{10} to 10^{13} ions/cm^2. The beam was scanned in the x–y plane to irradiate the whole target sample area. The beam current (~1 pnA) was kept low to suppress thermal decomposition. X-ray diffraction (XRD) studies were carried out using Bruker AXS system by Cu-K_α radiation (1.54 Å). UV–visible (UV–vis) studies were carried out using U-3300, Hitachi system. The chemical modifications were studied by a Fourier transform infrared spectrometer using Thermo Nicolet Nexus 670 FTIR.

The projected range and electronic energy loss (S_e) of 50 MeV Li ions in both polymers were calculated by SRIM code (Ziegler, 2010). The S_e values are 6.81 and 6.29 eV/Å and the projected range values are 418.8 and 449.2 μm for PES and PN-6 respectively. Since projected range values are more than the thicknesses of our polymers so the probability of ion implantation was almost negligible.

3. Results and discussion

3.1. XRD studies

The diffraction patterns of pristine and irradiated PES and PN-6 films are shown in Figs. 1 and 2 respectively. The broad peaks occur at 2θ ~19.09° for PES, whereas two broad peaks occur at 2θ ~20.2° and 23.3° in case of PN-6 polymer. No significance shift of peak position is observed in any diffraction pattern indicating that there is no change in lattice parameters. It is observed that the peak intensity increases and peak width decreases with increase of ion fluence; which suggests the alignment of polymeric chains in a regular pattern and decrease in amorphouse character of irradiated polymers. Samra et al., (2011) had mentioned in their study on oxygen ion irradiated PES polymer that increase in peak intensity was related to cross-linking in polymeric chains. Cross-linking or alignment of polymeric chains depends upon chemical nature and geometrical structure of the polymer (Gowariker et al., 2002) as well as ion beam parameters (mass, charge, energy etc.). However, in case of solid polymeric materials, the exact nature of the interrelation between spacing, crystallite size and the degree of disorder is yet to the ascertained in proper perspective (Virk et al., 2001).

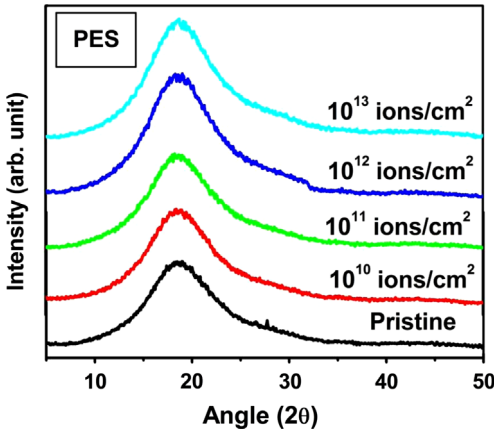

Fig. 1. XRD spectra of pristine and Li^{3+} ion irradiated PES polymer.

The average crystallite size (L) was calculated by using the Scherrer formula reported in literature (Sharma et al., 2007). The calculated values are given in Table 1. The values are increasing at higher fluences.

3.2. UV–vis studies

UV–vis spectra of pristine and irradiated samples of PES and PN-6 are shown in Figs. 3 and 4 respectively. The optical absorption edges of the irradiated polymer samples shift towards the visible region of the spectrum with the increase of ion fluence. This shift may be attributed to formation of conjugated system of bonds (Mackova et al., 2005) and increase in conjugation length (Mackova et al., 2009). Similar results were observed by Kulshrestha et al., (2010) and Samra et al., (2011) in ion irradiated PES. Kumar et al., (2006b) reported the shift in absorbance spectra of proton and carbon ion irradiated PES polymer to the formation of carbonaceous clusters.

Few absorption peaks at ~260 nm and ~330 nm are seen in case of irradiated samples of PN-6. These peaks are assigned for $\pi \rightarrow \pi^*$ inter band transition (Kumar et al., 2008). The optical band gap energy (E_g) was calculated from the absorption spectra by extra plotting the linear portion of the graph between $(\alpha h\nu)^{1/2}$ and $(h\nu)$ to the energy axis using the Tauc's relation (Tauc et al., 1966) and values are calculated using following equation:

$$(\alpha h\nu) = B(h\nu - E_g)^n \quad (1)$$

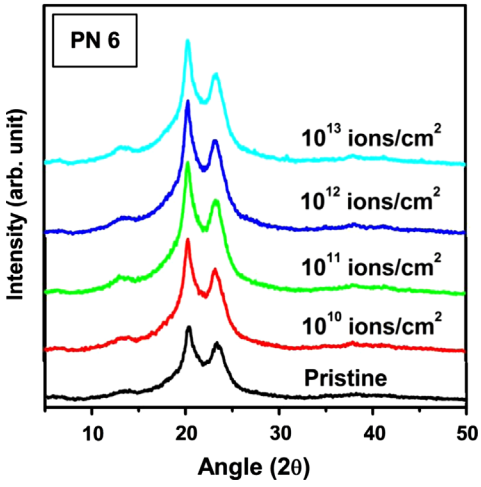

Fig. 2. XRD spectra of pristine and Li^{3+} ion irradiated PN-6 polymer.

Table 1
Calculated values of average crystallite size (L), indirect band gap (E_g) and the Urback's energy (E_u) for pristine and irradiated samples of PES and PN-6 polymers.

Fluence (ions/cm^2)	PES			PN-6		
	L (Å)	E_g (eV)	E_u (eV)	*L* (Å)	E_g (eV)	E_u (eV)
Pristine	10.53	3.03	0.13	15.72	3.62	0.52
10^{10}	10.91	3.01	0.11	15.73	3.25	0.51
10^{11}	10.92	2.99	0.11	15.89	2.87	0.53
10^{12}	11.01	2.95	0.11	15.93	2.77	0.52
10^{13}	11.01	2.92	0.10	15.98	2.65	0.50

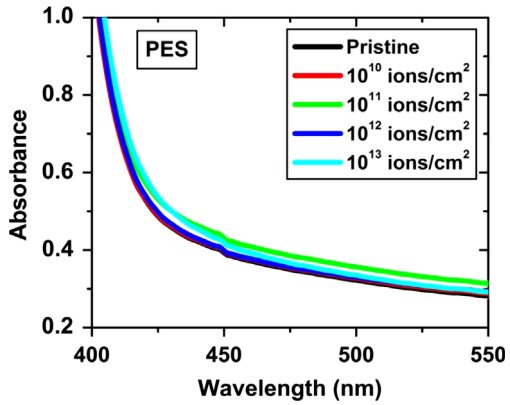

Fig. 3. UV–vis spectra of pristine and Li^{3+} ion irradiated PES polymer.

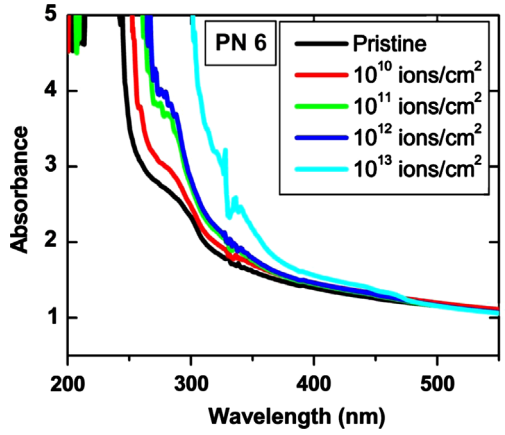

Fig. 4. UV–vis spectra of pristine and Li^{3+} ion irradiated PN-6 polymer.

here B is band tailing parameter (Metwally, 1901). Its value depends on transition probability and can be assumed to be constant within the optical frequency range. α is optical absorption coefficient, its value is calculated from the absorbance (A) after correction for reflection losses using following equation:

$$\alpha(\nu) = 2.303\ A/l \tag{2}$$

here l is the sample thickness in centimeters. The value of n characterizes the transition processes in K-space. Its value is 1/2, 3/2, 2 and 3 for direct allowed, direct forbidden, indirect allowed and indirect forbidden transitions respectively (Migahed and Zidan, 2006). The value of n is taken to be equal to 2 for indirect allowed transitions (indirect band gap calculation). For amorphous materials the Bloch functions can be described by a linear combination of the crystalline wave functions of the respective bands and hence the momentum ($\hbar k$) is not conserved even in a direct transition. Therefore in amorphous materials, a plot of $(\alpha h\nu)^{1/2}$ vs $h\nu$ could be used to determine the band gap even for a direct transition (Buchholz et al., 2009). The values of indirect band gap are tabulated in Table 1. The calculated values show that the band gap of polymers is decreasing with increase of ion fluence. There are 3.63% and 26.79% decrease in band gap value of PES and PN-6 respectively. The decrease in band gap is attributed to the formation of lower energy states due high electronic LET (linear energy transfer) by ion in polymer which results in carbon-enriched cluster formation (Gupta et al., 2000), free radical (Sinha et al., 2001) and conjugated bond formation (Farenzena et al., 1995). The main reason for decrease in band gap energy is attributed to formation of conjugated system of bonds.

The thermal fluctuations in the band gap energy were estimated by calculating the Urbach's energy (E_u) (Skettrup, 1978) using following equation:

$$\alpha(\nu) = \alpha_o exp(h\nu/E_u) \tag{3}$$

The reciprocal of the slopes of the linear portion in the lower photon energy region of the plot of ln (α) as a function of photon energy ($h\nu$) gives the value of E_u (Migahed and Zidan, 2006). The calculated values of E_u for pristine and irradiated samples of PES and PN-6 are given in Table 1. The value decreases at higher fluences in both cases. The main reason for the change in value of E_u at higher fluences is shift of the band gap energy which is due to temperature-dependent self energies of the electrons and holes interacting with the phonons (Dow and Redfield, 1978).

3.3. FTIR studies

The infrared spectra corresponding to pristin and irradiated samples of PES and PN- 6 are shown in Figs. 5 and 6 respectively. FTIR spectra of pristine sample of PES conforms with the spectra

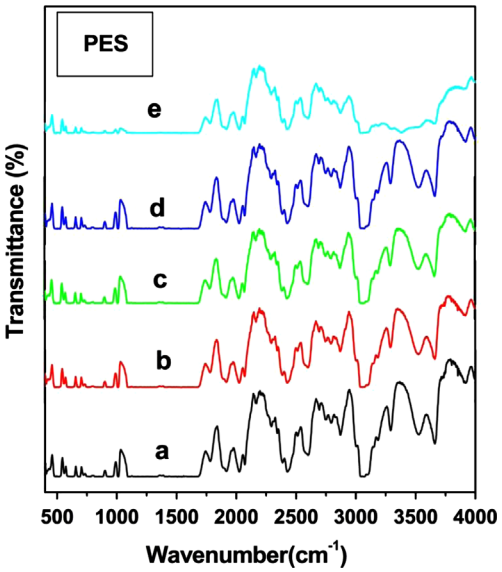

Fig. 5. FTIR spectra of pristine and Li^{3+} ion irradiated PES polymer. Here a, b, c, d and e stand for pristine, 10^{10}, 10^{11}, 10^{12} and 10^{13} ions/cm^2 respectively.

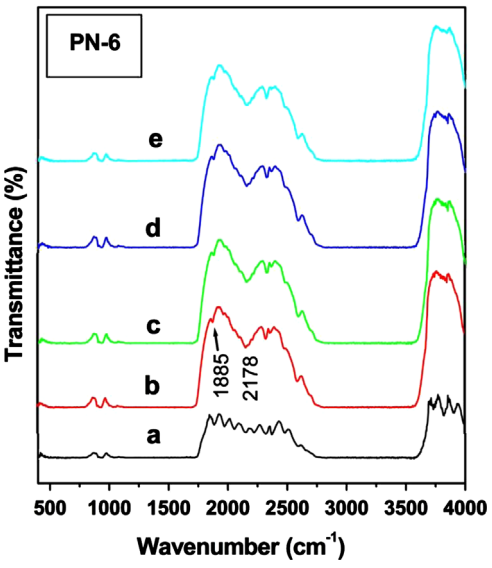

Fig. 6. FTIR spectra of pristine and Li^{3+} ion irradiated PN-6 polymer. Here a, b, c, d and e stand for pristine, 10^{10}, 10^{11}, 10^{12} and 10^{13} ions/cm^2 respectively.

reported by Samra et al., 2011. The spectra show increase in absorbance (decrease in percentage transmittance) for irradiated samples. Similar effects are seen in our previous measurement on carbon ion irradiated PES polymer (Kumar et al., 2006a). The FTIR spectra of PN-6 show decrease in absorbance bands for irradiated samples. The intensity of characteristic peak at position 945 cm^{-1} corresponding to C–N stretching vibration of $–CH_2–N–$ group (Vasanthan and Salem, 2001) is increased towards larger values of percentage transmittance. No new band formation was observed in irradiated samples of both the polymers.

4. Conclusions

The structural, optical and chemical properties of polyethersulphone (PES) and polyamide nylone-6 (PN-6) polymers were modified by 50 MeV Li^{3+} ion beam irradiation. The increase in intensity of XRD peaks confirmed the alignment of polymeric chains in a regular pattern as a result of which there was decrease in the amorphouse character of irradiated polymers. The shift of the UV–vis spectra towards higher wavelength decreased the band gap energy of irradiated polymers. There was 3.63% and 26.79% decrease of band gap in PES and PN-6 polymers respectively. The FTIR spectra showed decrease in absorbance (increase in percentage transmittance) for irradiated samples of PN-6, whereas PES polymer samples showed opposite behavior.

Acknowledgments

The authors are thankful to staff of Inter University Accelerator Center, New Delhi, India for providing help during irradiation and characterizations. Financial assistance provided by the Council of Scientific & Industrial Research (CSIR), Government of India to Mr. Paramjit Singh for the research work as Senior Research Fellow (SRF) [Sanction no. 09/806(0026)/2012-EMR-I] is gratefully acknowledged.

References

Buchholz, D.B., Liu, J., Marks, T.J., Zhang, M., Chang, R.P.H., 2009. Control and characterization of the structural, electrical, and optical properties of amorphous zinc–indium–tin oxide thin films. ACS Appl. Mater. Interfaces 1 (10), 2147–2153.

Dow, J.D., Redfield, D., 1978. Towards a unified theory of Urbach's rule and exponential absorption edges. Phys. Rev. B 05, 594–610.

Dudra, A., Wysocki, S., 2005. The influence of degree of crosslinking on the distribution of fluorescence lifetimes in poly(ether sulphone) (PES). Polym. Degrad. Stab. 89, 300–311.

Farenzena, L.S., Papaleo, R.M., Hallen, A., de Araujo, M.A., Livi, R.P., Sundqvist, B.U.R., 1995. Modifications in the chemical bonding and optical absorption of PPS by ion bombardment. Nucl. Instrum. Methods Phys. Res., Sect. B 105, 134–138.

Gowariker, V.R., Viswanathan, N.V., Sreedhar, J., 2002. Polymer Science. New Age International, India.

Gupta, S., Choudhary, D., Sarma, A., 2000. Study of carbonaceous clusters in irradiated polycarbonate with UV–vis spectroscopy. J. Polym. Sci., Part B: Polym. Phys 38, 1589–1594.

Kulshrestha, V., Agarwal, G., Awasthi, K., Tripathi, B., Acharya, N.K., Vyas, D., Saraswat, V.K., Vijay, Y.K., Jain, I.P., 2010. Microstructure change in poly (ethersulfone) films by swift heavy ions. Micron 41, 390–394.

Kumar, R., Ali, S.A., Mahur, A.K., Virk, H.S., Singh, F., Khan, S.A., Avasthi, D.K, Prasad, R., 2008. Study of optical band gap and carbonaceous clusters in swift heavy ion irradiated polymers with UV–vis spectroscopy. Nucl. Instrum. Methods Phys. Res., Sect. B 266, 1788–1792.

Kumar, R., De, U., Prasad, R., 2006a. Physical and chemical response of 70 MeV carbon ion irradiated polyether sulphone polymer. Nucl. Instrum. Methods Phys. Res., Sect. B 248, 279–283.

Kumar, S.V., Ghadei, B., Jal, P.K., Dey, K., Krishna, J.B.M., Saha, A., 2006b. Modification of polyethersulphone induced by high energy proton, C^{+}, and Ne^{6+} ions: a spectroscopic study. J. Appl. Polym. Sci. 101, 1591–1597.

Kurmaev, E.Z., Winarski, R.P., Endo, K., Ida, T., Moewes, A., Ederer, D.L., Pivin, J.-C., Shamin, S.N., Trofimova, V.A., Yarmoshenko, Yu.M., 1999. Radiation-induced degradation of polyethersulphone films studied by fluorescent X-ray emission spectroscopy. Nucl. Instrum. Methods Phys. Res., Sect. B 155, 431–439.

Mackova, A., Bocan, J., Khaibullin, R.I., Valeev, V.F., Slepicka, P., Sajdl, P., Svorcik, V., 2009. Characterisation of Ni^{+} implanted PEEK, PET and PI. Nucl. Instrum. Methods Phys. Res., Sect. B 267, 1549–1552.

Mackova, A., Havranek, V., Svorcik, V., Djourelov, N., Suzuki, T., 2005. Degradation of PET, PEEK and PI induced by irradiation with 150 keV Ar^{+} and 1.76 MeV He^{+} ions. Nucl. Instrum. Methods Phys. Res., Sect. B 240, 245–249.

Metwally, H.S., 1901. Electrical and optical studies in Ge100-xSx chalcogenide thin films. Acta Phys. Pol., A 99, 683–690.

Migahed, M.D., Zidan, H.M., 2006. Influence of UV-irradiation on the structure and optical properties of polycarbonate films. Curr. Appl Phys. 6, 91–96.

Samra, K.S., Thakur, S., Singh, L., 2011. Structural, thermal and optical behavior of 84 MeV oxygen and 120 MeV silicon ions irradiated PES. Nucl. Instrum. Methods Phys. Res., Sect. B 269, 550–554.

Sharma, T., Aggarwal, S., Sharma, A., Kumar, S., 2007. Effect of nitrogen ion implantation on the optical and structural characteristics of CR-39 polymer. J. Appl. Phys. 102, 063527.

Sinha, D., Phukan, T., Tripathy, S.P., Mishra, V., Dwivedi, K.K., 2001. Optical and electrical properties of gamma irradiated PADC detector. Radiat. Meas. 34, 109–111.

Skettrup, T., 1978. Urbach's rule derived from thermal fluctuations in the band-gap energy. Phys. Rev. B: Condens. Matter Mater. Phys 18, 2622–2631.

Tauc, J., Grigorovici, R., Vancu, A., 1966. Optical properties and electronic structure of amorphous Germanium. Phys. Status Solidi 15, 627–637.

Timus, D.M., Cincu, C., Bradley, D.A., Craciun, G., Mateescu, E., 2000. Modification of some properties of polyamide-6 by electron beam induced grafting. Appl. Radiat. Isot. 53, 937–944.

Vasanthan, N., Salem, D.R., 2001. FTIR spectroscopic characterization of structural changes in polyamide-6 fibers during annealing and drawing. J. Polym. Sci., Part B: Polym. Phys. 39, 536–547.

Virk, H.S., Chandi, P.S., Srivastava, A.K., 2001. Physical and chemical changes induced by 70 MeV carbon ions in polyvinylidene difluoride (PVDF) polymer. Nucl. Instrum. Methods Phys. Res., Sect. B 183, 329–336.

Zaharescu, T., Silva, L.G.A., Jipa, S., Kappel, W., 2010. Post-irradiation thermal degradation of PA6 and PA6,6. Radiat. Phys. Chem. 79, 388–391.

Ziegler, J.F., 2010. SRIM–The stopping and range of ions in matter. Nucl. Instrum. Methods Phys. Res., Sect. B 268, 1818–1823.

Gamma Radiation Induced Modifications on Physicochemical Properties of Makrofol (KG and N) Polycarbonate

SANJEEV KUMAR GUPTA, PARAMJIT SINGH, RAJESH KUMAR

University School of Basic and Applied Sciences, Guru Gobind Singh Indraprastha University, New Delhi 110 078, India

SATYENDRA KUMAR

Department of AS and HU, ABES Engineering College, Ghaziabad 201 009, India

Correspondence to: Rajesh Kumar; e-mail: rajeshkumaripu@gmail.com.

Received: September 22, 2014
Accepted: December 22, 2014

ABSTRACT: Makrofol (KG and N) polycarbonates (PCs) are the most versatile solid-state nuclear track detectors. These polymers were exposed to gamma radiation of doses ranging from 250 to 1000 kGy. The pristine and exposed samples were characterized by X-ray diffraction (XRD), UV–vis spectrophotometry, and Fourier transform infrared spectrophotometry for the structural, optical, and chemical studies, respectively. The XRD studies showed that crystallite size for exposed samples of makrofol-KG PC decreased from 64.7 to 57.9 Å and for makrofol-N PC it increased from 19.1 to 21.1 Å. The band gap energy decreased from 4.40 to 4.07 eV for makrofol-KG and from 4.26 to 3.83 eV for makrofol-N after the gamma exposure. The number of carbon atoms per conjugation length as obtained from UV–vis studies was increased in both cases. The activation energy showed fluctuations for exposed samples of both polymers. The intensity of various absorption bands of the infrared spectra decreased at some doses for both the PCs, indicating the change in the chemical properties of the exposed samples. Adv Polym Technol 2015, 0, 21510; View this article online at wileyonlinelibrary.com. DOI 10.1002/adv.21510

KEY WORDS: Gamma exposure, FT-IR, Polycarbonates, UV–Vis spectroscopy, X-ray diffraction

Introduction

Polycarbonates (PCs) made from bisphenol-A are crystal clear and colorless amorphous engineering thermoplastics notable for their high impact resistance. PC, being a versatile material with attractive processing and physical properties, finds many applications that include glazing, safety shields, lenses, casings and housings, light fittings, kitchenware (microwaveable), medical apparatus (sterilizable), CDs, and many more. Irradiation of PCs by ionizing radiations modifies their structural, optical, and chemical properties. Effects of neutron doses on the structural properties of makrofol PC were studied by Nouh et al.[1] They found an increase in the amorphous phase and average molecular mass due to cross-linking, which enhanced the quality of the polymer. Jaleh et al.[2] evaluated the physicochemical properties of electron beam (25–250 kGy) irradiated PC film showing the degradation of the polymer at higher doses. Similarly, physicochemical properties of various polymers can also be modified by gamma exposure. This technique is widely used in medical device sterilization.[3] Effects of gamma irradiation on different polymers have been reported in the literature.[4–6] In the present study, we have taken two polymers makrofol-KG and makrofol-N. Both are PCs having same chemical composition ($C_{16}H_{14}O_3$), but makrofol-KG (MF-KG) is colorless, monoaxially oriented, and crystallized, whereas makrofol-N is cast isotropic and is of light yellow color.

Being the most versatile solid-state nuclear track detectors many researchers have studied the modifications in various properties of makrofol (KG and N) polymers by the irradiation with gamma radiations and ions. In the literature, the structural changes in makrofol-KG PC by irradiation with O^{5+} ions were studied by way of dielectric constant and loss factor measurements by Mujahid et al.[7] Soares et al.[8] reported the possibility of using makrofol as an Alpha spectrometer by measuring their alpha track-etch pit diameters. It has been shown by Tayel et al.[9] that the properties of makrofol DE 7-2 polymer can be effectively modified by gamma irradiation so as to use the polymer as a sensor and for bioengineering applications. Thermal and optical behaviors of makrofol-N due to irradiation by a proton beam of different doses from 10 to 80 kGy were studied[10] and reported the 19% decrease in thermal stability of makrofol-N. The etching and structural response of makrofol (KG and N) from low dose (0.5 kGy) to high dose (1000 kGy) of gamma irradiation

was studied by Singh and Prasher[11] and it was predicted that both polymers remain insensitive to low doses, but they were influenced at higher doses. It has been shown by Delgado et al.[12] that the probability for the single-bond scissoring was higher than that for double-bond scissoring when makrofol-KG was irradiated with 350 MeV Au^{26+} ions. The modifications induced by 100 MeV silicon ions in makrofol-KG were studied and it was found that the carbonization of the polymer takes place at higher fluence and there is an improvement in the orientational behavior of the molecules.[13] There is no new literature available on the effects of gamma radiations on physicochemical properties of makrofol-KG and makrofol-N at higher doses to the best of our knowledge. The present work provides an opportunity to probe inside the polymer material by modifying its various physico-chemical properties by exposing it with gamma radiation and applying it to produce new polymers with enhanced structural and optical properties. The objective of the present study is to find the modification induced in the structural, optical, and chemical properties of makrofol-KG and makrofol-N PCs due to gamma irradiations in the range of 250–1000 kGy dose. The parameters such as band gap energy (E_g), number of carbon atoms per conjugated length (N), activation energy (E_u), and crystallite size (L) are calculated from the data obtained from UV–vis and X-ray diffraction (XRD) results. The chemical modifications have been studied by Fourier transform infrared (FTIR) spectrophotometry.

Experimental

MATERIALS

Thin sheets of makrofol (KG and N) PCs of thickness 20 μm each having density in the range of 1.20–1.22 g/cm^3 were commercially purchased from Goodfellow, UK. The melting temperature (T_m) of both the polymers is 155°C and their glass transition temperature (T_g) is 147°C.

METHODS

The samples of size 1 cm × 1 cm were cut from the sheets and irradiated by gamma radiation emitted from Co^{60} source of dose rate varying from 5.416 to 5.409 kGy/h at Inter University Accelerator Centre (IUAC), New Delhi, India. The different samples were exposed at the doses of 250, 500, 750, and 1000 kGy. XRD studies were carried out using a Bruker AXS system (Cu-K_α radiation, 1.54 Å) for a wide range of Bragg's angle 2θ ($5° < \theta < 50°$). The chemical modifications were studied by using a Thermo Nicolet Nexus 670 FTIR spectrophotometer in the range of 4000–400 cm^{-1}. XRD and FTIR facilities were availed from National Physical Laboratory, New Delhi, India. UV–vis studies (in 200–800 nm range using a U-3300 Hitachi system) were carried out at IUAC, New Delhi, India.

Results and Discussion

UV–VIS STUDIES

The optical properties of the polymers are studied by UV–vis spectroscopy. The UV–vis spectra of pristine- and gamma-irradiated makrofol-KG and makrofol-N PC samples are shown in Figs. 1a and 2a, respectively. The spectra shows a shift in the optical absorption edge of irradiated samples toward red end of the spectrum, which increases with the increase in gamma dose, indicating a growing concentration of conjugated system of bonds.[6] Owing to this shift, the optical band gap energy (E_g) of the polymers decreased, which was calculated by applying Tauc's relation[14,15] for direct transitions as per the following equation:

$$(\alpha h\nu) = B\left(h\nu - E_g\right)^n \tag{1}$$

where α is the optical absorption coefficient and B is the band tailing parameter and its value depends on the transition

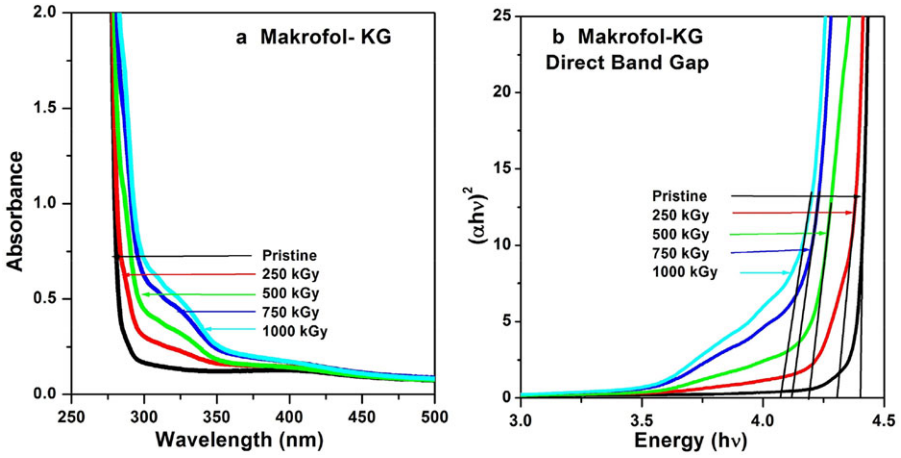

FIGURE 1. (a) UV–vis spectra of pristine and gamma rays irradiated makrofol-KG polycarbonate. (b) The dependence of $(\alpha h\nu)^2$ on photon energy $(h\nu)$ for pristine and gamma rays irradiated makrofol-KG polycarbonate.

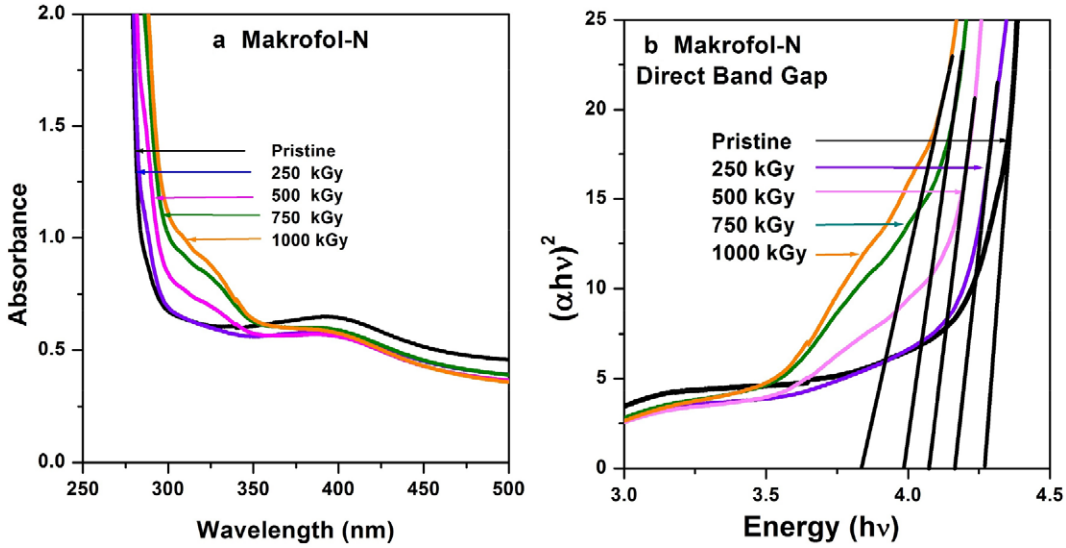

FIGURE 2. (a) UV–vis spectra of pristine and gamma rays irradiated makrofol-N polycarbonate. (b) The dependence of $(\alpha h\nu)^2$ on photon energy $(h\nu)$ for pristine and gamma rays irradiated makrofol-N polycarbonate.

probability. The value of n is taken to be equal to 1/2 for direct allowed transition (direct band gap calculation). The plots for band gap energy calculation are shown in Figs. 1b and 2b for makrofol-KG and makrofol-N PCs, respectively, and the values of direct band gap energy are presented in Tables I and II. The table values clearly indicate that with the increase in gamma dose, the band gap energy decreased from 4.40 to 4.07 eV for makrofol-KG and from 4.26 to 3.83 eV for makrofol-N PC. The decrease in the band gap energy is quite significant within the calculated errors (~2%). The interaction of gamma radiations with polymers results in the formation of free radicals, which may further induce chain scissoring, unsaturated bond formation, and conjugated bond formation. With the increase in gamma dose, the rate of formation and concentration of free radicals increase, which results in the increase in unsaturated and conjugated bonds and hence a decrease in the band gap energy takes place.

TABLE I
Calculated Values of Band Gap Energy (E_g), Number of Carbon Atoms per Conjugation Length (N), and Activation Energy (E_u) for Pristine and Gamma Rays Irradiated Samples of Makrofol-KG Polycarbonate

Dose (kGy)	E_g(eV)	N	E_u
Pristine	4.40	~61	0.09
250	4.30	~64	0.24
500	4.19	~67	0.22
750	4.11	~69	0.22
1000	4.07	~71	0.20

The typical error in the band gap energy is ±2%.

TABLE II
Calculated Values of Band Gap Energy (E_g), Number of Carbon Atoms per Conjugation Length (N), and Activation Energy (E_u) for Pristine and Gamma Rays Irradiated Samples of Makrofol-N Polycarbonate

Dose (kGy)	E_g(eV)	N	E_u
Pristine	4.26	~65	0.17
250	4.15	~68	0.30
500	4.07	~71	0.26
750	3.99	~74	0.24
1000	3.83	~93	0.23

The typical error in the band gap energy is ±2%.

Another effect of shift of absorption edge toward longer wavelength is the increase in number of carbon atoms per conjugation length (N) and is calculated with the help of following equation given by Fink et al.[16,17]:

$$N \approx (34.3/E_g)^2 \tag{2}$$

The calculated values of N for makrofol-KG and makrofol-N are shown in Tables I and II, respectively, which shows that with the increase in gamma dose, the value of N increased from 61 to 71 for makrofol-KG polymer and from 65 to 93 for makrofol-N.

Another parameter that defines the irregularities in the chemical structure of a polymer is called activation energy or Urbach's energy (E_u) defined by the following equation as:

$$E_u \approx \frac{h\nu}{\ln(\alpha/\beta)} \tag{3}$$

where $h\nu$ is the energy of photon, β is a constant, and α is the absorption coefficient. The value of activation energy (E_u) is determined by taking the reciprocal of the slope of the linear portion of the curves between the ln (α) and $h\nu$. The calculated values of E_u for pristine and gamma irradiated samples of makrofol-KG and makrofol-N PCs for various doses are shown in Tables I and II, respectively. The value of E_u increased from 0.09 to 0.24 and from 0.17 to 0.30 for the irradiated polymer samples of makrofol-KG and makrofol-N, respectively. This increase in values of E_u for both polymers shows a degradation

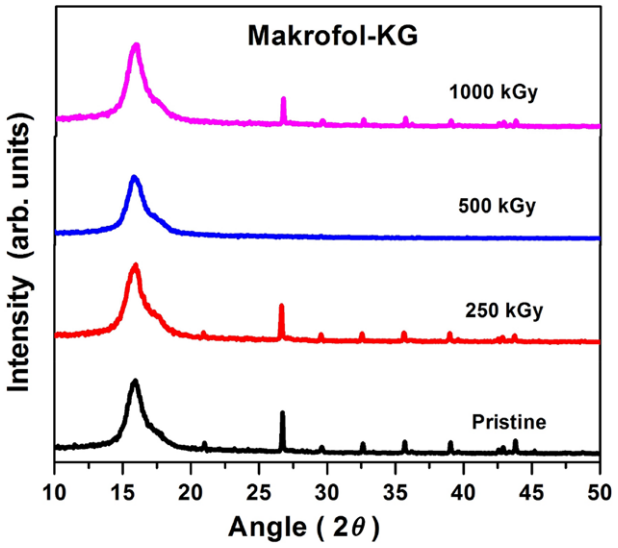

FIGURE 3. X-ray diffraction patterns of pristine and gamma rays irradiated makrofol-KG polycarbonate.

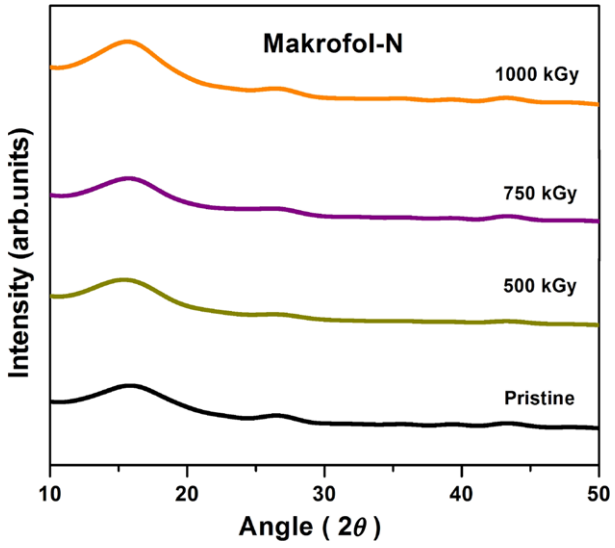

FIGURE 4. X-ray diffraction patterns of pristine and gamma rays irradiated makrofol-N polycarbonate.

of the optical and structural properties of the polymers,[18] which may be either due to the formation of carbon-rich clusters or due to the increase in defects in the polymer samples after gamma exposure.

X-RAY DIFFRACTION STUDIES

X-ray diffraction patterns of pristine and gamma radiation irradiated samples of makrofol-KG and makrofol-N PCs are shown in Figs. 3 and 4, respectively. XRD pattern of pristine makrofol-KG and makrofol-N sample conforms to the XRD pattern reported by Kumar et al.[19] The diffraction peaks occurred at 15.83° and 15.68° for makrofol-KG and makrofol-N, respectively, and their positions remained unchanged after the polymer samples were irradiated with gamma rays; it indicates that the lattice parameters of the polymers remain intact. The peak width (in the form of full width at half maximum, FWHM) increased and the peak intensity decreased in the case of makrofol-KG PC with the increase in gamma dose, indicating the increase in amorphous nature; but the opposite effect (a decrease in the value of FWHM and an increase in peak intensity) was observed in the case of makrofol-N polymer.

The variation in peak width due to gamma irradiation indicates the modification in the crystallite size (L) of the polymers, which is calculated by using the following equation given by Scherrer[20,21]:

$$L = K\lambda/(b\cos\theta) \tag{4}$$

where K is a constant of proportionality (called the Scherrer constant), b is the FWHM of the peak (in radian), λ is the wavelength of the X-rays used (1.54 Å), and θ is the angle, which is calculated by taking ½ of 2θ value. The calculated values are shown in Tables III and IV. The variation in the values of "L" may be attributed to the processes such as free radical formation, chain scission, and cross-linking of polymeric chains in the polymers upon irradiation followed by the modifications in the properties. The variation of crystallite size with respect to gamma dose is shown in Figs. 5a and 5b for makrofol-KG and makrofol-N PCs, respectively.

FTIR STUDIES

The chemical modifications in the gamma rays irradiated samples of makrofol (KG and N) PCs were studied by FTIR spectroscopy in the range of 4000–400 cm^{-1}, and the corresponding spectra of pristine and gamma rays irradiated samples are shown in Figs. 6 and 7, respectively. By the analyses of FTIR spectra, the absorption bands for makrofol-KG corresponding to following groups are identified: CH (765, 1408, 2865–2968 cm^{-1}),

TABLE III
Calculated Values of Crystallite Size (L) for Pristine and Gamma Rays Irradiated Samples of Makrofol-KG Polycarbonate

Dose (kGy)	L (Å)
Pristine	64.7
250	57.5
500	57.9
1000	57.9

The typical errors in the quantities are ±2%.

TABLE IV
Calculated Values of Crystallite Size (L) for Pristine and Gamma Rays Irradiated Samples of Makrofol-N Polycarbonate

Dose (kGy)	L (Å)
Pristine	19.1
500	19.2
750	21.2
1000	21.1

The typical errors in the quantities are ±2%.

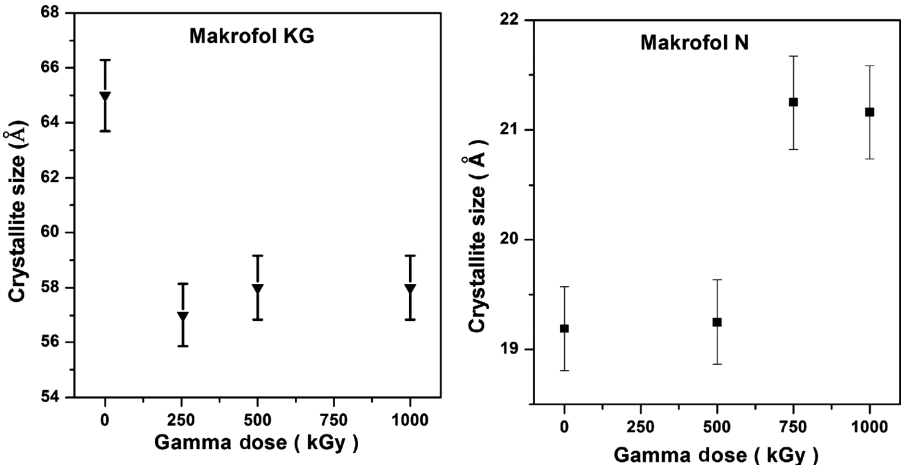

FIGURE 5. Variation of crystallite size with respect to gamma dose for (a) makrofol -KG and (b) makrofol-N polycarbonate. The typical errors in both the plotted graphs are ±2%.

C≡C (2030–2165 cm^{-1}), C=O (1763 cm^{-1}), CO (885 cm^{-1}), C=C (553, 1010, 1078, 1502, 1596 cm^{-1}), C–O (1220 cm^{-1}), CC (1361 cm^{-1}), CH (1408 cm^{-1}), and C=CH (830 cm^{-1}).[12,22] Similarly for makrofol-N, the absorption bands corresponding to the same groups as in makrofol-KG are identified but with a slight difference in wave numbers. The position of the bands for the irradiated samples is same as that of pristine sample for both polymers, but the intensity of the bands is decreased in the irradiated samples of makrofol-KG polymer at all doses; whereas for makrofol-N polymer samples, the intensity of band decreased at doses 250 and 750 kGy and showed no change at doses of 500 and 1000 kGy as compared with the pristine. Also, no new bands are noticed in the irradiated samples of both polymers.

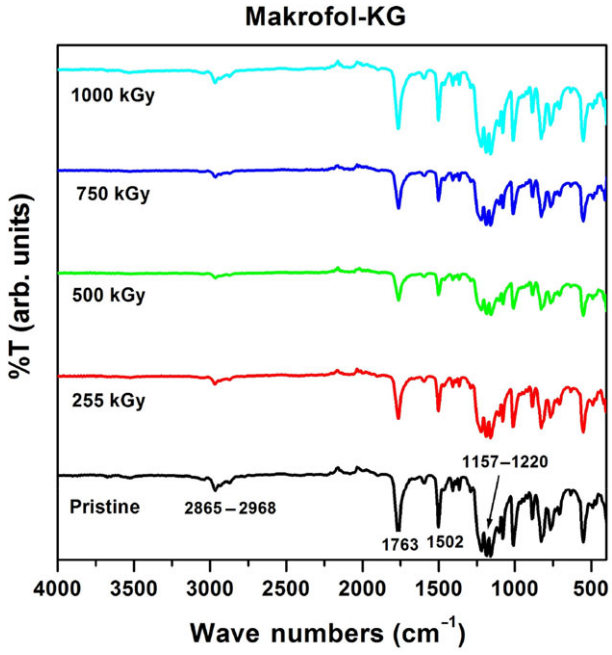

FIGURE 6. FTIR spectra of pristine and gamma rays irradiated makrofol-KG polycarbonate.

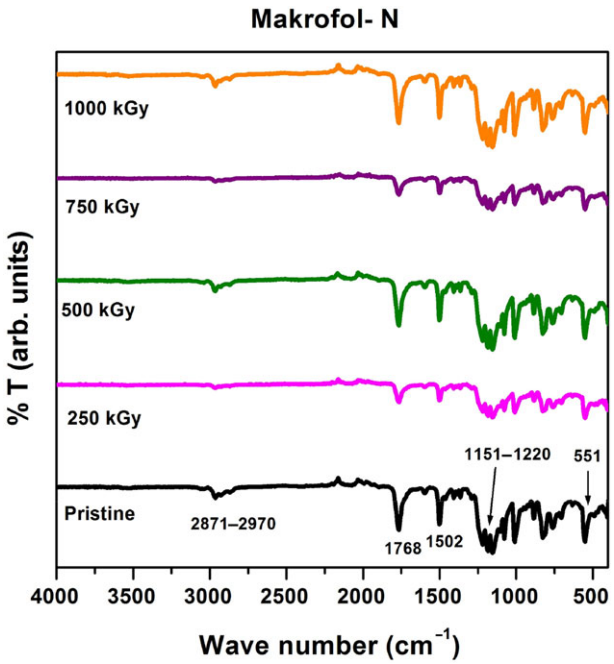

FIGURE 7. FTIR spectra of pristine and gamma rays irradiated makrofol-N polycarbonate.

Conclusions

Modifications in physicochemical properties of makrofol (KG and N) PCs due to gamma radiation exposure have been studied with the help of XRD, UV–vis, and FTIR spectroscopy. The XRD spectra of exposed samples showed amorphization of makrofol-KG PC with an increase in the gamma doses, whereas in makrofol-N PC, a decrease in the amorphization of the exposed samples was observed. The absorption edges of UV–vis shifted toward a visible region gradually, thereby decreasing the band gap energy for both the polymers. The carbon-enriched

cluster formation, free radicals formation, and formation of conjugated system of bonds caused shift of the spectrum toward visible region and hence the band gap energy decreased. The increase in activation energy showed an overall degradation of both polymers. The FTIR studies showed a decrease in intensity of the infrared absorption bands for almost all irradiated samples of makrofol-KG, whereas for makrofol-N the intensity of the bands decreased for some doses of gamma radiations. The modification observed in optical properties of both polymers particularly in makrofol-N opens up new prospects of developing new material with enhanced conductivity.

Acknowledgments

The authors are thankful to Dr. S. P. Lochab (Sr. Scientist) and the staff at Inter University Accelerator Centre (IUAC), New Delhi, India, for providing gamma irradiation facilities and UV–vis characterization technique. The authors are also thankful to Dr. N. Vijayan (Scientist) at National Physical Laboratory (NPL), New Delhi, India, for providing characterization techniques of XRD and FTIR.

References

1. Nouh, S. A.; Amer, H.; Remon, S. W. Nucl Instrum Methods Phys Res, Sect B 2009, 267, 1129–1134.
2. Jaleh, B.; Parvin, P.; Sheikh, N.; Ziaie, F.; Haghshenas, M.; Bozorg, L. Radiat Phys Chem 2007, 76, 1715–1719.
3. Murray, K. A.; Kennedy, J. E.; McEvoy, B.; Vrain, O.; Ryan, D.; Cowman, R.; Higginbotham, C. L. J Mech Behav Biomed Mater 2013, 17, 252–268.
4. Cardoso, E. C. L.; Scagliusi, S. R.; Lima, L. F. C. P.; Bueno, N. R.; Brant, A. J. C.; Parra, D. F.; Lugão, A. B. Radiat Phys Chem 2014, 94, 249–252.
5. Said, H. M. J Radiat Res Appl Sci 2013, 6, 11–20.
6. Raghuvanshi, S. K.; Ahmad, B.; Siddhartha; Srivastava, A. K.; Krishna, J. B. M.; Wahab, M. A. Nucl Instrum Methods Phys Res, Sect B 2012, 271, 44–47.
7. Mujahid, M.; Srivastava, D. S.; Avasthi, D. K. Radiat Phys Chem 2011, 80, 582–586.
8. Soares, C. J.; Alencar, I.; Guedes, S.; Takizawa, R. H.; Smilgys, B.; Hadler, J. C. Radiat Meas 2013, 50, 246–248.
9. Tayel, A.; Zaki, M. F.; El Basaty, A. B.; Hegazy, T. M. J Adv Res (in press).
10. Mishra, R.; Tripathy, S. P.; Dwivedi, K. K.; Khathing, D. T.; Ghosh, S.; Müller, M.; Fink, D. Radiat Meas 2003, 36, 639.
11. Singh, S.; Prasher, S. Radiat Eff Defects Solids 2004, 159, 359–367.
12. Delgado, A. O.; Rizzutto, M. A.; Tabacniks, M. H.; Added, N.; Fink, D. Nucl Instrum Methods Phys Res, Sect B 2009, 267, 1546–1548.
13. Kumar, R.; Singh, P.; Ali, S. A.; Sharma, A.; Khan, S. A.; Sonkawade, R. G.; Prasad, R. Indian J Pure Appl Phys 2010, 48, 166–171.
14. Singh, P.; Kumar, R.; Cyriac, J.; Rahul, M. T.; Nambissan, P. M. G.; Prasad, R. Nucl Instrum Methods Phys Res, Sect B 2014, 320, 64–69.
15. Singh, P.; Ali, S. A.; Kumar, R. Radiat Phys Chem 2014, 96, 181–185.
16. Fink, D.; Chung, W. H.; Klett, R.; Schmoidt, A.; Cardosa, J.; Montiel, R.; Vazqez, M. H.; Wang, L.; Hosoi, F.; Omichi, H.; Goppelt-Langer, P. Radiat Eff Defects Solids 1995, 133, 193–208.
17. Kumar, R.; Singh, P. Results Phys 2013, 3, 122–128.
18. Devgan, K.; Singh, L.; Samra, K. S. Radiat Phys Chem 2013, 88, 49–55.
19. Kumar, V.; Sonkawade, R. G.; Dhaliwal, A. S. Nucl Instrum Methods Phys Res, Sect B 2012, 287, 4–9.
20. Mujahid, M.; Srivastava, D. S.; Gupta, S.; Avasthi, D. K. Radiat Phys Chem 2005, 74, 118–122.
21. Singh, P.; Kumar, R. Vacuum 2013, 96, 46–51.
22. Singh, L.; Samra, K. S. Nucl Instrum Methods Phys Res, Sect B 2007, 263, 458–462.